Actinomycetes from neglected areas, Iranian soil, their taxonomy, and secondary metabolites

Von der Fakultät für Lebenswissenschaften

der Technischen Universität Carolo-Wilhelmina zu Braunschweig

zur Erlangung des Grades einer

Doktorin der Naturwissenschaften

(Dr. rer. nat.)

genehmigte

D i s s e r t a t i o n

von Shadi Khodamoradi
aus Tabriz / Iran

1. Referent: Professor Dr. Michael Steinert

2. Referent: Privatdozent Dr. Joachim Wink

eingereicht am: 09.02.2021

mündliche Prüfung (Disputation) am: 16.04.2021

Druckjahr 2021

Vorveröffentlichungen der Dissertation

Teilergebnisse aus dieser Arbeit wurden mit Genehmigung der Fakultät für Lebenswissenschaften, vertreten durch den Mentor der Arbeit, in folgenden Beiträgen vorab veröffentlicht:

Publikationen

Khodamoradi S, Stadler M, Wink J, Surup F. Litoralimycins A and B, New Cytotoxic Thiopeptides from Streptomonospora sp. M2. Marine Drugs. 2020 Jun;18(6):280.

Conference Talk

Shadi Khodamoradi. *Streptomonospora litoralis* sp. nov., a halophilic actinomycetes with antibacterial activity from beach sands. *11th International PhD Symposium,* Braunschweig, Germany (2018)

Posterbeiträge

Shadi Khodamoradi, Richard L. Hahnke, Frank Surup, Manfred Rohde, Michael Steinert, Marc Stadler, Joachim Wink. Isolation of a new *Streptomonospora*-species producing a new peptide antibiotic. The HIPS Symposium, Saarbrücken, Germany (2019).

Shadi Khodamoradi. Isolation of new *Streptomyces* sp. producing the new antibacterial compound from the soil sample collected from Iran/ Tehran/ Alborz Mountain HZI. *12th International PhD Symposium,* Braunschweig, Germany (2019)

Shadi Khodamoradi. Isolation, characterization, and Antagonistic Properties of novel species of halophilic *Streptomonospora.10th International PhD Symposium,* Braunschweig, Germany (2017)

Acknowledgements

First of all, I want to give my sincere gratitude to my principal supervisor PD Dr. Joachim Wink for giving me the chance to explore the wonderful science and sharing his knowledge with me. I appreciate his patience and constant support throughout my PhD journey.

I would also like to thank Prof. Dr. Marc Stadler for his great support and giving the opportunity to work in his group. Your guidance and teaching have developed my skill in many ways, especially in academic writing. I thank my associated supervisor Prof. Dr. Michael Steinert for his scientific advice and support. I would like to thank Dr. Stephan Hüttel for his kind support, continuous help and encourage during my PhD study.

I would like to give special thanks to my collaboration partners Dr. Frank Surup, Dr. Kathrin Mohr, Dr. Kathrin Wittstein, Dr. Steffen Bernecker, Dr Manfred Rohde, Prof. Dr. Peter Kämpfer, Dr. Eike Steinmann, Dr. Christian Rückert, and Christel Kakoschke.

My sincere thanks to my coauthors Prof. Dr. Yvonne Mast for her kind help and advices, Dr. Peter Schumann, Dr. Richard Hahnke, and other members of DSMZ, Dr. Meina Neumann-Schaal and Gabriele Pötter.

I would like to further acknowledge to our graduate school in the HZI for their astonishing support and organization during my study especially Dr. Sabine Kirchhoff.

I am much grateful to Prof. Dr. Ludger Beerhues for taking over the chair during my defense. My deepest thank to Romy Schade and Silke Reinecke for their great technical support. I would like to mention my appreciation to all members of the MWIS group, especially to Kerstin Schober, Esther Surges, Axel Schulz, Kevin Becker, and Sebastian Pfütze for helping me with chemistry part. I extend my

special thanks to my colleague Dr. Chandra Risdian for sharing his knowledge and so many advices in the last years.

I would also like to express my gratitude to my group members, Stephanie Schulz, Klaus Peter Conrad, Aileen Gollasch, Birte Trunkwalter, Wera Collisi and Jolanta Lulla for the professional technical support. I thank all of my other colleagues, Nasim Safaei, Senlie Octaviana, Rina Andriyani, Hani Pira, Sana Ullah Tareen for the warm environment in our group. Also I thank previous students Dr. Lucky Mulwa and Dr. Omar Messaoudi for their kind scientific advices during my PhD study.

Many thanks to all friends for their support and all the happy time we spent together during this journey. Finally, I would like to thank my kind family for their love and support throughout the years, which enabled me to follow my dreams.

Table of Contents

List of Figures

List of Tables

List of Supplementary Figures

List of Supplementary Tables

List of Abbreviations

16S rRNA	Component of the 30S small ribosomal subunit of a prokaryotic
5S rRNA	Component of the 30S large ribosomal subunit of a prokaryotic
23S rRNA	Component of the 30S large ribosomal subunit of a prokaryotic
[M+H]+	Protonated molecular ion
ASW	Artificial sea water
BGCs	biosynthetic gene clusters
BLAST	Basic local alignment search tool
Bp	Base pair
°C	Degree Celsius
DAD	Diode array detector
DAP	2, 6-Diaminopimelic acid
DDH	DNA-DNA hybridization
DNP	Dictionary of natural products
DW	Distilled water
EDTA	Ethylene diamine tetraacetic acid
G+C	Guanine and cytosine (content)
HEPES	(4-(2-Hydroxyethyl)-1-piperazineethanesulfonic acid
HPLC	High performance liquid chromatography
HR-ESI-MS	High resolution electrospray ionization mass spectrometry
JSRM	Jump start ready mix
MALDI-TOF	Matrix-assisted laser desorption/ionization-time of flight
NMR	Nuclear magnetic resonance
MIC	Minimum inhibition concentration
MLSA	MLSA Multilocus sequence analysis
PCR	Polymerase chain reaction
rpm	Revolutions per minute
TLC	Thin layer chromatography

Abstract

Actinobacteria constitute the largest among 30 major phyla of Eubacteria. Actinobacteria are Gram-positive and are well known as producers of bioactive secondary metabolites, which have been utilized in medical, industrial, and agricultural applications. More than 50% of the currently described antibiotics are produced by Actinobacteria. In search of new bioactive compounds, researchers are now having to search neglected or yet undiscovered habitats. In this work, novel Actinobacteria have been isolated from various locations in Iran and neglected environments in Germany. Among those, two strains ($M2^T$ and M3) were examined for polyphasic taxonomy. Strain $M2^T$ was identified as a novel species within the genus *Streptomonospora*. Analysis and isolation of compounds from its extract revealed two novel thiopeptide derivatives (litoralimycins A and B). Another study identified strain 86D, isolated from Lavasan/Iran, with moderate activity against *Bacillus subtilis* DSM 10 and *Staphylococcus aureus* Newman. The polyphasic findings support that strain 86D represents a novel species in the genus *Streptomyces*. From the non-*Streptomyces* strains isolated from the soil of Iran, strain 31sw was selected for polyphasic taxonomy. The chemotaxonomy evaluation and whole-genome sequencing data supported the notion that 31sw belongs to the genus *Saccharomonospora*. Strain 31sw represents a potential subspecies of species *Saccharomonospora xinjiangensis* DSM 44391^T.

Keywords*:* Actinobacteria, *Streptomyces,* drug discovery, antibiotics, *Streptomonospora,* thiopeptide, *Saccharomonospora,* Iran, neglected habitat.

Abstrakt

Actinobakterien bilden das größte der 30 Hauptphyla der Eubakterien. Actinobakterien sind Gram-positiv und bekannt als Produzenten von bioaktiven Sekundärmetaboliten, die in der Medizin, Industrie und Landwirtschaft eingesetzt werden. Mehr als 50% der derzeit beschriebenen Antibiotika werden von Actinobakterien produziert. Auf der Suche nach neuen bioaktiven Verbindungen durchsuchen Forscher vernachlässigte oder noch unerforschte Lebensräume. In dieser Arbeit wurden neue Actinobakterien von verschiedenen Standorten im Iran und aus vernachlässigten Lebensräumen in Deutschland isoliert. Davon wurden zwei Stämme (M2^T und M3) mittels der polyphasische Taxonomie untersucht. Der Stamm M2^T wurde als eine neue Spezies innerhalb der Gattung *Streptomonospora* identifiziert. Die Analyse und Isolierung von Verbindungen aus seinem Extrakt ergab zwei neue Thiopeptidderivate (Litoralimycine A und B). Eine weitere Studie identifizierte den Stamm 86D, isoliert aus einer prober aus Lavasan/Iran, mit moderater Aktivität gegen *Bacillus subtilis* DSM 10^T und *Staphylococcus aureus* Newman. Die polyphasischen Befunde unterstützen, dass Stamm 86D eine neue Spezies in der Gattung *Streptomyces* darstellt. Von den Nicht-Streptomyces-Stämmen, die aus dem Boden des Iran isoliert wurden, wurde der Stamm 31sw für die polyphasische Taxonomie ausgewählt. Die chemotaxonomische Auswertung und die Daten der Ganzgenomsequenzierung unterstützten die Annahme, dass 31sw zur Gattung *Saccharomonospora* gehört. Der Stamm 31sw repräsentiert eine potentielle Unterart der Spezies *Saccharomonospora xinjiangensis* DSM 44391^T.

Schlüsselwörter: Actinobakterien, *Streptomyces,* Wirkstoffforschung, Antibiotika, *Streptomonospora*, Thiopeptid, *Saccharomonospora*, Iran, vernachlässigter Lebensraum.

1 Introduction

1.1 Natural products

Natural products (NPs) are chemical compounds of biological origin that show various bioactivities and, thus, serve as important sources for novel drugs. The chemical structures of NPs can be highly diverse, ranging from simple to very complex molecules. Primary metabolites are those metabolites that are directly involved in the metabolic pathways of an organism and necessary for its growth, development, and reproduction. Secondary metabolites are normally not essential for the reproduction, growth, or development of the organism. Their production is a consequence of cell communications, adaptation to the environment, or as a defence mechanism against predators, prey, and competing organisms[1]. Countless secondary metabolites have been applied as natural products in medicine, agriculture, and manufacturing. More than 2,140,000 secondary metabolites are known, which are classified based on their mode of biosynthesis. In total, secondary metabolites are divided into five main classes, including terpenoids, fatty acid-derived substances, polyketides, alkaloids, nonribosomal and ribosomal polypeptides, and enzyme cofactors[2]. In 1896, the first antibiotic was discovered from the fungus *Penicillium glaucum* by Bartolomeo Gosio, which he demonstrated as the active antibacterial compound against anthrax bacterium. Nevertheless, the discovery was forgotten and, later, with the introduction of penicillin in 1929 by Alexander Fleming, the era of antibiotics began, saving an uncountable number of lives since[3]. Many of the currently used antibiotic classes were discovered in the "golden age" of antibiotics by systematic screening methods of *Streptomyces* that were introduced by Selman Waksman in the1940s[4]. This discovery during 1940–1960 was a turning peak in human history. However, in the case of streptomycin, presented in 1944 for the treatment of tuberculosis (TB; "The Great White Plague"), after a while, some *Mycobacterium tuberculosis* strains appeared resistant to medicinal doses of the antibiotics. As other antibiotics have been discovered and launched, similar styles of resistance have[5]. The time course of discovery and resistance expansion for the main classes of antibiotics is presented in Figure 1. From 1970 to 2010, pharmaceutical companies have reduced their drug discovery programs[6,7]. This issue has arisen from the complicated

process and high cost of compound isolation besides of isolating known compounds frequently. However, the advent of new technologies, such as molecular networking techniques, which simplified the analysis of compounds, made the process of substance identification more rapid and precise, which is one reason why the field of antibiotic discovery has been revived in recent years[7]. Bacteria have long been known as a remarkably useful source for antibiotics[8]. The Actinobacteria, myxobacteria, cyanobacteria, pseudomonads, and *Bacillus* species (within the prokaryotic domain), and the filamentous fungi (among eukaryotic microorganisms) have a high potential to produce a large number of various chemical and biological active compounds[9]. Scientists believe that many natural products are still undiscovered. About 23 000 bioactive secondary metabolites produced by microorganisms, which over 10 000 of them are produced by *Actinomycetes*, regarding 45% of all bioactive microbial metabolites discovered[10]. However, isolating compounds from Actinobacteria these days often lead to the rediscovery of known substances when applying conventional approaches. Thus, it is important to focus on novel strategies to exploit Actinobacteria for their biosynthetic potential[11]. Therefore, several methods for drug discovery have been conducted in recent years. These include genome mining, modification of cultivation conditions, and biodiversity mining[12]. Mining genomics data has suggested a large number of novel antibiotics encoded in the genomes of both cultivable and uncultivable organisms that remain to be discovered[13]. Several previous studies revealed that Actinobacteria, with their huge genomes, are notable for SMs (secondary metabolites) production. Many observations have been done in *Streptomyces* species and other actinomycetes genera, showing that the number of likely SMs is ~10-times greater than the number of secondary metabolites so far isolated[14]. Therefore, it was determined that only a relatively small proportion of SM gene clusters (SMGCs) encoded by microbes are expressed at significant levels during fermentations[15–17]. It remains problematic express (in the fermentation stage) those genes responsible for new antibiotics from Actinobacteria. However, several approaches have been used to stimulate the expression of such genes to identify novel constructions[18–20,35]. Some of the new bioactive compounds retrieved by genome mining methods and produced under laboratory conditions include the fungicidal orfamide, from

Pseudomonas fluorescens[21], stambomycin, from *Streptomyces*[22], and the siderophore coelichelin from *Streptomyces coelicolor*[23].

Numerous experiments have indicated that modifying the culture condition can also stimulate the production of antibiotics. For instance, changing of particular nutrients (such as carbon, phosphate, and nitrogen source), oxidative and nitrosative stress, and higher temperature can influence the production of secondary metabolites[24,25]. Co-cultivation of the target organism with two or more different microbes is a strategy to mimic the ecological condition on a laboratory scale. Competition among these microbes is purposely provoked in the hope that biosynthetic genes that remain silent under conventional culture conditions are activated and transcribed under pressure conditions. This method has been used for enhancing the production of particular compounds or the induction of different new bioactive SMs that are not express under conventional laboratory conditions produced[26]. Two *Streptomyces leeuwenhoekii*, strains C34 and C58, in co-cultivation with *Aspergillus fumigatus* MR2012, produced luteoride D, a new luteoride derivative and pseurotin G, a new pseurotin derivative, in addition to the production of terezine D and 11-*O*-methylpseurotin[27]. Besides those strategies, the focus of natural products discovery shifted towards biodiversity mining especially in marine and other extreme environments[28,29]. Those biodiversity mining efforts have led to the isolation of several novel extremophilic and extremotolerant Actinobacteria from desert soils[30,31], marine sediments[32], and sponges[33]. The term "extreme" can be defined for both chemical (pH, salinity, water content) and physical parameters (temperature, radiation, pressure)[34]. Some of Actinobacteria that were isolated from the underexplored ecological niches, have been shown to produce several bioactive new compounds, such as cervimycins C[35], hypogeamicins[36]**,** undecylprodigiosin[37]. Iran is a land of diverse ecological habitats, which has a high potential to discover novel species of Actinobacteria. However, the natural habitats of Iran's deserts are underexplored, and the reports of the discovery of rare Actinobacteria are not as many as are expected. Therefore, the potential for discovery of novel species of rare Actinobacteria that might yield new bioactive compounds remains extremely high[30].

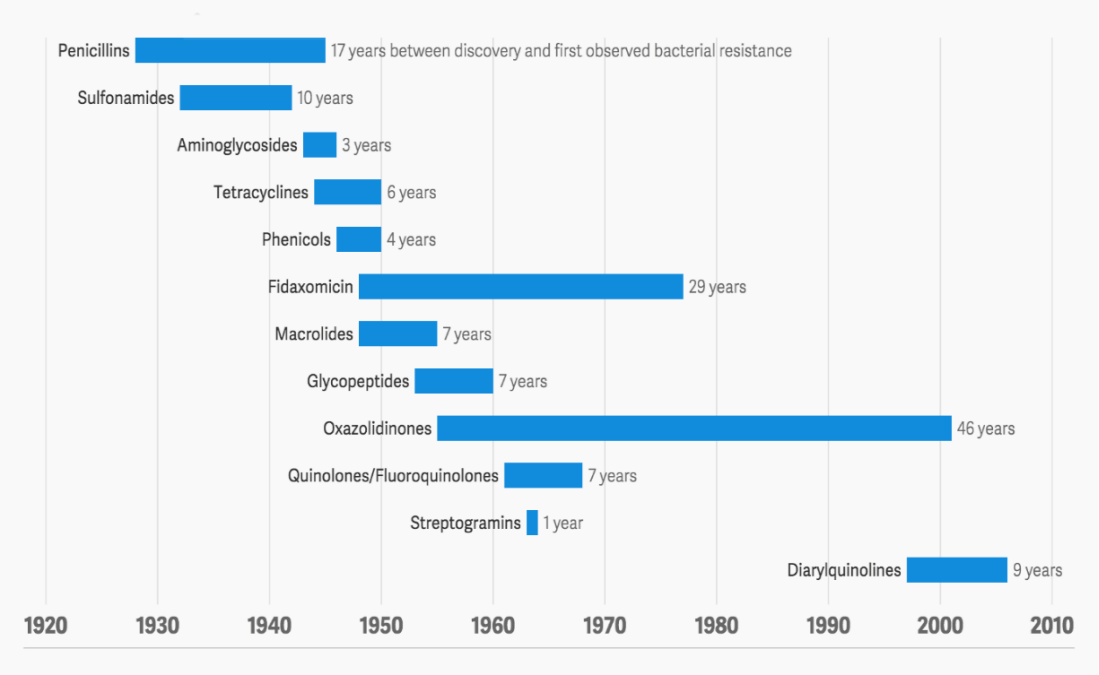

Figure 1. Timeline of antibiotic discovery and first observed antibiotic resistance during 1930–2005. Adapted from Antibiotic history and the winning bacteria 2016.

1.2 The Class of Actinobacteria

The phylum Actinobacteria is one of the major groups within the domain of bacteria and is divided into six classes including Rubrobacteria, Thermoleophilia, Coriobacteriia, Acidimicrobiia, Nitriliruptoria, and Actinobacteria[38]. The class of Actinobacteria includes 29 orders and 62 families (https://www.ncbi.nlm.nih.gov/taxonomy). In the class of Actinobacteria, the order Actinomycetales is now restricted to the members of the family Actinomycetaceae. They are mostly facultative aerobic and, in many cases, form mycelia[39–42]. Among Actinobacteria, morphological differentiation is best studied for the genus *Streptomyces*. In the previous study, it was found that, in the absence of nutrients especially (carbon sources, nitrogen, and phosphor), Actinobacteria form spores[43]. In the process of sporulation, aerial hyphae grow and divide into pre-spore chains. Complete spores with rigid coats capable to survive in dormant state for long periods of time and endure dehydration and other challenging conditions[44]. In many cases, when the spores find appropriate nutritional conditions, they start to germinate and tend to produce hypha, which is multiplied by tip extension and finally develop substrate mycelium. In short, the pattern of growth in Actinobacteria is a combination of tip expansion and hypha branching[44] (Figure 2).

These have a large genome size of between 1 and 12 megabases, with an average of over 5-mega bases (Mb). Their genomes contain a high amount of guanine and cytosine, and the percentage of G+C in some genera, such as *Streptomyces* and *Pseudonocardia*, reaches more than 70%. However, G+C contents of less than 50% have been described for *Tropheryma whipplei* and *Gardnerella vaginalis*[45,46]. Generally, microbial chromosomes are circular, but some genera, such as *Streptomyce*s, *Kineococcu*s, *Gordonibacter*, and *Rhodococcu*s, have linear chromosomes. Actinobacteria are isolated as free-living organisms in the soil and marine environments (*Streptomyces* and *Salinospora* species), some in symbiosis with plants (*Frankia* species), some as animal or plant pathogens (*Mycobacterium*, *Nocardia*, and *Corynebacterium* spp.), and some as normal flora of gastrointestinal (*Bifidiobacterium* species). In addition, several remarkable pathogenic Actinobacteria have been identified, such as *Nocardia* spp. (cause of Nocardiosis), *Actinomyces israelii* (cause of Actinomycosis), and *Mycobacterium tuberculosis* (cause of Tuberculosis)[46]. Large numbers of Actinobacteria live in soils, especially in alkaline soils and soils rich in biological substance, where they form an important proportion of the microbial population. The density of Actinobacteria in the soil can be controlled by several environmental factors, such as temperature, pH, and soil moisture[47]. Actinobacteria have an essential role in the soil for the degradation of complex biopolymers, such as lignocellulose, pectin, hemicellulose, keratin, and chitin[48]. Besides their role in the ecosystem, Actinobacteria are used in pharmacy to produce highly bioactive compounds. Biosynthesis products from Actinobacteria can have diverse bioactivities, including antibacterial, antifungal, antitumor, anticancer, and immunosuppressive[38].

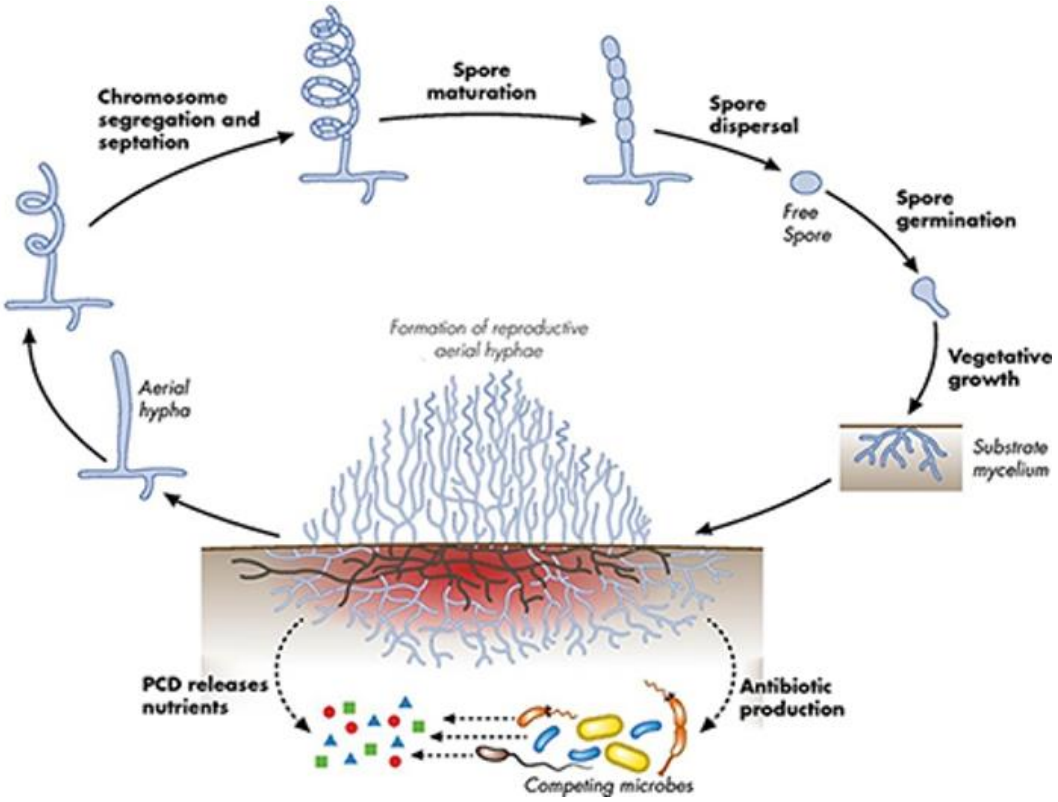

Figure 2.The life cycle of Actinobacteria is a combination of hill-top expansion and branching of the hyphae. The picture was adapted from Van der Meij et al., Chemical ecology of antibiotic production by actinomycetes. *FEMS Microbiology Reviews.* 2017,41:392-416[164].

1.2.1 Rare Actinobacteria

In the classes Actinobacteria, *Streptomyces* is the dominant genus in natural environments. Rare Actinobacteria are referred to as non-*Streptomyces* species that are difficult to isolate, culture, and sustain by standard methods of isolation in the laboratory[49]. They require complicated selective approaches for isolation, preservation, and cultivation because fast growers (such as other bacteria, fungi, and common *Streptomycetes*) frequently overgrow the rare actinomycetes strains of interest[50]. Besides soils and water as the main habitats, Actinobacteria have been isolated from diverse natural ecosystems. Also, many unexplored or underexplored environments, including deserts, caves, plants, volcanic rocks, and stones, can be worthwhile sources for the isolation of rare Actinobacteria[30,51,52]. It has been

reported that the finding of rare Actinobacteria can increase the chances of discovering novel bioactive chemical compounds. Already by September 2010, around 220 genera of rare actinomycetes had been described[28]. Some genera of this group include *Actinomadura*, *Actinoplanes*, *Amycolatopsis*, *Actinokineospora*, *Acrocarpospora*, *Actinosynnema*, *Cryptosporangium*, *Catenuloplanes*, *Dactylosporangium*, *Kibdelosporangium*, *Kineosporia*, *Microbiospora*, *Microtetraspora*, *Nocardia*, *Nonomuraea*, *Planomonospora*, *Planobispora*, *Pseudonocardia*, *Saccharopolyspora*, *Saccharomonospora*, *Saccharothrix*, *Streptosporangium*, *Spirilliplanes*, *Thermomonospora*, *Thermobifida*, and *Virgosporangium*[53].

1.2.2 Bioactive compounds from rare actinomycetes

In the last two decades, antibiotics have been increasingly isolated from rare Actinobacteria, resulting in a 25–30% increase in newly discovered antibiotics[54,55]. More than 50 rare actinobacterial taxa have been reported to produce 2500 bioactive compounds in total[56]. Between 2013 and 2017, a total number of 167 new bioactive compounds were isolated from rare Actinobacteria. Among those isolated strains, some genera, such as *Nocardiopsis* (40 new compounds), *Micromonospora* (37 new compounds), *Salinispora* (21 new compounds), and *Pseudonocardia* (14 new compounds), were predominant with respect to the number of new secondary metabolites[52]. By the end of October 2019, four of those new compounds [Salinosporamide A (Marizomib), Arenamides A and B, and Anthracimycin] were selected for pre-clinical trials[57]. *Micromonospora* genus is considerable with production of several bioactive compounds such as rifamycin, butemycin, micromonophalimane A, quinoline, 1,4 dioxane and paulomycin G[28,52]. Between 2013 and 2017, some unusual bioactive compounds were discovered from rare Actinobacteria, such as, nesterenkoniane isolated from *Nesterenkonia* spp. (anti-allergic)[58], salinipostin A isolated from *Salinospora* spp. (anti-malarial)[59], micromonohalimane A isolated from *Micromonospora* spp. (antibacterial activity)[60], and forazoline A, isolated from *Actinomadura* spp. (antifungal)[61] (Figure 3). The biologically active compounds from rare actinomycetes have actions for inhibiting the growth of bacteria. For instance, inhibition of DNA and RNA synthesis, cell wall synthesis inhibition, cell

membrane destruction, inhibition of protein synthesis, and inhibition of essential enzymes required for folate metabolism[50].

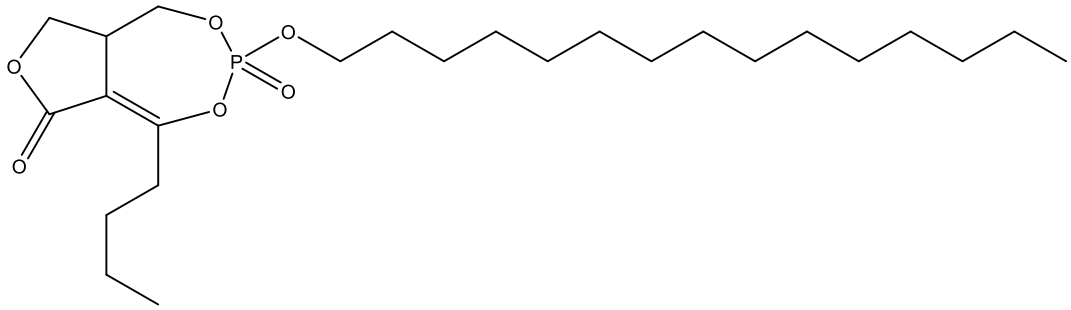

Salinipostin A (Antimalarial activity)

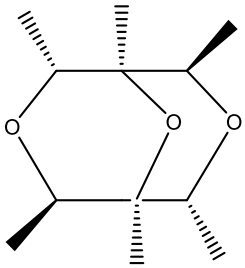

Nesterenkoniane (Anti- allergic activity)

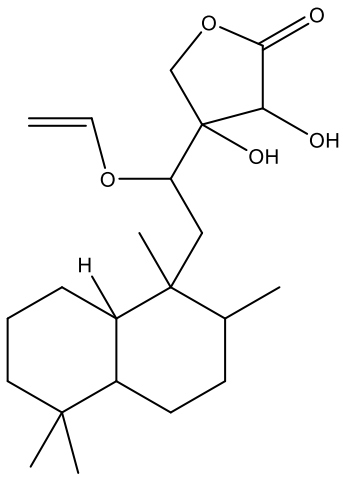

Micromonohalimane A (antibacterial activity)

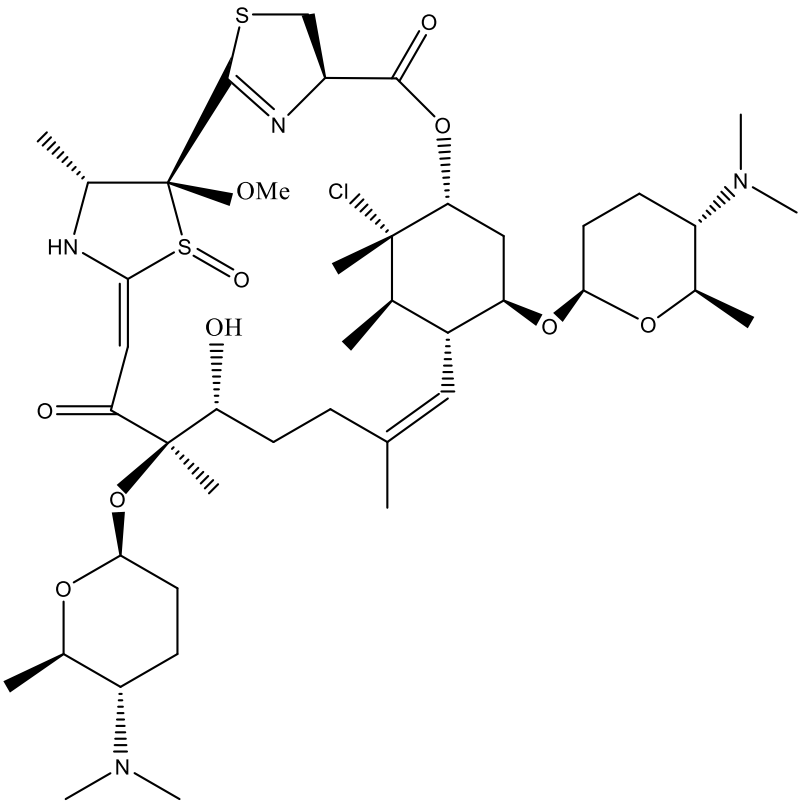

Forazoline A (Anticandida activity)

Figure 3. Some of unusual bioactive compounds from rare Actinobacteria between 2013 and 2017.

1.3 Prokaryotic taxonomy

In general, systematic and taxonomy are used synonymously. However, taxonomy is a part of systematics. Systematic is the general study of all kinds of diversity of all organisms and all relationship among them, whereas taxonomy is the theoretical study of the classification, including its criteria[62]. Taxonomy is divided into three parts: (i) classification that means the arrangements of units into taxonomic groups such as (species, genera, and families), (ii) identification of unknown organisms to confirm that they belong to one of the defined units; and (iii) nomenclature or naming the units defined[63]. The taxonomy techniques established decades ago are not sufficient to provide a comprehensive draft on which bacterial taxonomy could be created. Most of the classifications at that time were based on several

characters, such as shape, colour, size, staining properties, motility, host-range, pathogenicity, and assimilation of a few carbon sources. In 1957, the genus of *Streptomycetes* was subdivided into several distinct clades according to similarities in spore chain morphology, spore surface adornment, colour (spores, substrate mycelium, and soluble pigments), and the production of melanin pigment. In 1970, classification based on the type of cell wall and its chemical composition opened a new scope for classification of aerobic actinomycetes[64]. There was, however, a need for a more comprehensive approach to supply convincing information to derive bacterial lineages. In the 1980s, a new criterion for identifying bacteria was established. It was revealed that phylogenetic relationships among bacteria and all microorganisms could be determined by comparing a conserved part of the genome. In the case of bacteria, the 16S rRNA gene sequence is a more common conserved gene that has been used in taxonomy and in creating a phylogenetic tree[65]. Currently, the classification of prokaryotes is mostly based on the combination of several criteria, such as phenotypic, genotypic, and phylogenic tree data, referred to as polyphasic taxonomy. Phenotypic systems applied for taxonomy include the morphology of single colony and spore, growth variety, metabolic production, pathogenesis, and chemotaxonomical markers. Genotypic analyses include 16S rRNA gene sequence analysis, DNA-DNA hybridization (DDH), multilocus sequence analysis (MLSA), and guanine and cytosine content of DNA (G+C). Recently, RiboPrinter typing analysis and average nucleotide identity (ANI) approaches in whole genome sequencing have been developed as new methods for genotypic classification[66].

1.4 The polyphasic classification in Actinobacteria

1.4.1 Phenotypic classification

1.4.1.1 Microscopic and macroscopic characteristics

Morphological properties remain basic criteria in the description of different taxa, while they are not considered as sufficient factors to individualize different genera. In the International *Streptomyces* Project (ISP), a number of standard media were defined for cultivation and characterization of *Streptomyces* species, and were later used for the characterization of actinomycetes. At present, these media are used to describe strain characteristics, such as the colour of the colony, spore, diffusible

pigment, and aerial mycelium, as well as substrate mycelium features[67].

Actinobacteria represent diverse morphologies, including coccoid or rod-coccoid shapes of cell in *Micrococcus* and *Arthrobacter*, well-differentiated branched mycelium in *Streptomyces*, and fragmented hyphae in *Nocardia*. They produce a range of spore types, either free or encapsulated in sporangia, that are important in the taxonomy of Actinobacteria[67].

The surface of the spores can also distinguish between different species using scanning electron microscopy. The surface of the spores in Actinobacteria varies widely, such as warty, smooth, spiny, or hairy. Long chains of spores are formed on the aerial mycelium of genera *Streptomyces*, *Nocardiopsis*, and *Kitasatospora*. Several genera of Actinobacteria develop sporangia with motile spores (*Oerskovia*, *Actinoplanes*, *Promicromonospora*), spores with flagella (*Ampullariella*), spherical spores on the surface of the colony (*Actinoplanes*), and short chains of conidia without sporangia structure (*Cattellatospora* and *Glycomyces*)[41]. Actinobacteria produce several pigments that make a distinction in the colour of colonies, medium, and aerial mycelium. These pigments are represented in several colours, including red, violet, green, yellow, grey, brown, and black. Production of pigments depends on medium constituents, culture condition, and the age of the strain. One of these pigments is melanin, which is a polymer with different structures and is produced by a broad range of organisms. This pigment is usually brown to black and is used in cosmetics and pharmaceutical products[68].

1.4.1.2 Physiological characteristics

Actinobacteria have different physiological and metabolic characteristics that are unique for each species, and these can be utilized for classification. The physiological characteristic can be accomplished in a microplate and automated monitoring of biology systems or rapid and ready strips of API®, such as API Coryne and API ZYM or API 20 E. Some important physiological properties used in the taxonomical description of Actinobacteria include the utilization of carbohydrates and growth conditions, such as temperature, pH, NaCl tolerance, and enzymatic activities[67].

Actinobacteria are able to use monosaccharides and disaccharides (e.g., glucose,

fructose, galactose, glycerol, maltose, mannitol, raffinose, rhamnose, sucrose, and xylose) and polysaccharides (e.g., starch and cellulose) as a carbon source[41]. Normally, most genera of Actinobacteria grow at an optimum temperature between 25–35°C. However, several thermophilic and psychrophilic species have also been identified. Psychrophilic strains grow between < 0°C and 20°C, with optimum growth at < 10°C, and facultative thermophile types grow between 50°C and 65°C. Actinobacteria grow at a pH ranging from 5 to 9 with an optimum pH of 6.5–8. Nevertheless, alkaliphilic and acidophilic genera have been observed[67].

Another aspect of physiological classification is the detection of enzymes that are produced by Actinobacteria. API ZYM and API Coryne are simple, rapid tests for the detection of bacterial enzymes, which have been successfully applied for Actinomycetaceae and related bacteria in the past[67].

1.4.2 Chemical classification (chemotaxonomy)

Among bacteria, the main compounds of the bacterial cell, such as DNA, cytoplasm, plasma membrane, and cell wall, are almost similar. However, particular structures of the cytoplasm, plasma membrane, and cell wall composition show remarkable differences. The modifications of these components are not distributed in the same way among bacteria, and this facilitates discrimination between groups of Actinobacteria above the genus level[38]. Chemotaxonomy studies referring to the specific composition of the cell wall peptidoglycan and cell membrane, including the identification of amino acid in position 3 of tetrapeptide side chains, the presence or absence of teichoic and/or mycolic acids, sugars, several specific fatty acids, polar lipids, respiratory quinones, and polyamines. Various sugars have been found in the whole-cell hydrolysis of bacteria. Most of these sugars are generally the components of cell wall polysaccharides. The sugar patterns in Actinobacteria are various and noticeable in chemotaxonomy. Phospholipid analyses of lyophilized cells of Actinobacteria can reveal several important pieces of information about the cell wall of these microorganisms. It is notable that members of one genus in Actinobacteria present identical phospholipids. Another noteworthy parameter is the presence of the specific nonproteinogenic amino acid 2,6-diaminopimelic acid (DAP) in the cell wall of Gram-positive bacteria. Two isomers, LL- or DL (meso)-

DAP, depending on the genus, can be detected in the peptidoglycan of Actinobacteria. In chemotaxonomic classification, cellular fatty acids are also important indicators. The chain length of fatty acids in bacteria is in a wide range: between 2 (C2) up to 90 (C90) carbon atoms. However, only those arrays of C10 to C24 are of specific chemotaxonomic value. Quinones are distinguished according to the types of quinones, the length of the isoprenoid side chain, and the number of saturated isoprenoid units. Several types of isoprenoid quinones have been identified in bacteria, and among them, menaquinones were the most common quinones in the cell membrane of Actinobacteria[69].

1.4.3 Genomic classification

In general, the term genomics refers to the whole information about the genome. Since the 1980s, it was revealed that phylogenetic evaluation based on conserved parts of the genome was much more reliable than classification based only on phenotypic characteristics. In the genome, all three types of RNA genes, including 5S rRNA, 16S rRNA, and 23S rRNA, with the spacers between them, are highly conserved and can be used in the phylogenic assay. However, due to the small and large size of, 5S rRNA (120 bp) and 23S rRNA (3300 bp) respectively, their sequencing has not been as popular as 16S rRNA. Therefore, the 16S rRNA (1650 bp) is the best and most commonly used marker and has a huge impact on the systematic classification of microbes[70,71]. The criterion based on 16S rRNA gene sequence similarity is defined with the threshold of 95% for a new genus and 98.7% for new species[72]. Although, it was clearly expressed by Tindal, that "the 16S rRNA gene sequences alone do not describe a species but may provide the first indication that a novel species has been isolated"[73]. Analysis of guanine and cytosine (G+C) nucleosides ratio is one of the classical evaluations in genome analysis. The range of variation of G+C for defining a new species is not more than 3%, and for defining a new genus, more than 10%[74].

DNA-DNA hybridization (DDH) is a technique for comparison of the whole-genome of two bacterial species. According to the committee on systematics, the threshold of 70% DDH is a criterion for describing a new species. Therefore, the members of the same species exhibited a DDH similarity of ≥ 70% with 5°C or less ΔTm values. However, the result of this technique must be reported as a

relative similarity of genomes, not as an absolute value[75,76].

The RiboPrinter microbial system is an automated instrument for genetic fingerprinting. Ribotyping is a method in which genomic DNA is digested in the specific regions, using a restriction endonuclease, such as *Eco*RI, *Pst*I, *Pvu*II, *BamH*I, *Cla*I, and *Hind*III. The resulting DNA fragments are size separated by gel electrophoresis. Following electrophoresis, the DNA is transferred to a membrane by Southern blotting and is probed with Y-^{32}P ATP-labeled rRNA and imagined by autoradiography. The RiboPrinter uses an rDNA probe obtained from the entire ribosomal operon from *Escherichia coli.* The array of DNA fragments hybridizing with this probe serves as a genetic fingerprint, which can be applied to distinguish between individual strains in a population of isolated bacteria[77].

The classical method of whole-genome sequence with the Sanger sequencing was associated with several unique laboratory methods, time consuming, and high cost. *Streptomyces coelicolor* A3 was the first *Streptomyces* genome, which was sequenced in the late 1990s with the use of an automated dideoxynucleotide method developed by Sanger[78,79]. Since the introduction of the next-generation sequencing (NGS) technologies Whole-genome sequences have become a powerful key element of taxonomic studies. Genome to Genome distance comparison (GGDC) based on complete genome data is a state-of-the-art *in silico* method that is reliably mimicking conventional DDH but does not have some important drawbacks[80]. The average nucleotide identity (ANI) is another similarity index between a given pair of genomes that can be applicable to two prokaryotic genome sequences. The cut-off ≈ 95% ANI has been applied for taxonomically defining prokaryotic species[75]. Recently, molecular analysis including 16S rRNA gene sequencing, DNA-DNA hybridization, and whole genome sequencing, is a crucial part of taxonomy[81].

1.5 Dereplication of compounds from Actinobacteria

The process of discovering natural products requires considerable investments in technical equipment, time, and human resources. Therefore, an innovative technique is required to reduce the workflow of isolation and purification of the novel bioactive agent at an appropriate time. In the late of 20 century, John A. Beutler defined the term of “dereplication “as a fast process for identification of known chemotypes[82].

At present, the dereplication method is depending on the different natural resources in the investigation. Dereplication does not relate to a single distinct method. In this term, different methods of dereplication are separated into five systems (DEREP1- DEREP5). All five methods are involved in the identification of new bioactive agents of natural origin but with various workflows: DEREP1 (identification of major compound in a single extract), DEREP2 (increasing of activity-guided fractionation), DEREP3 (chemical profiling of crude extract collection), DEREP4 (chemical profiling of target compounds), and DEREP5 (taxonomic identification of microbial strains)[83]. Therefore, dereplication of natural products from Actinobacteria sources might be achieved by using 16S rDNA analysis with the combination of the LC-MS-bioassay method. This process could be accomplished following the bioassay-guided isolation strategies that connect information on the chemical profiles of extracts and the active fractions. Extraction of compounds might be completed using organic solvents of various polarity, water, and their mixtures[84,85]. Some bioactivity analyses can be performed, such as antibacterial, antifungal, antitumor, or antiviral activity. The further isolation process requires column chromatographic and thin-layer chromatography (TLC) methods. Lastly, for the structure elucidation of the separated compound, high-resolution mass spectrometry (HR-MS) and NMR spectroscopy are applied to the identification and structure elucidation of novel natural products[86] .

1.6 Previous work in search of novel Actinobacteria and their secondary metabolites

In the past two decades, much effort has been directed to identifying novel actinobacterial species with the high potential of producing antibiotics. The Middle East, with its biological diversity, represent a variety of ecosystems and related habitats, including high-to low-density jungles, deserts, grasslands, and mountains[87]. Iran is called the land of extremes, and 34 biodiversity hotspot areas are within its borders[87]. In a review article, it has been reported that the diverse climate in this land, such as the cold temperature of the Zagros regions and the hot desert climates in the center and east, might affect the diversity of microorganisms in Iran[88]. One study has reported the isolation of *Glycomyces sediminimaris* as a

novel species from marine samples collected from the south of Iran[89]. In another study in this area, a novel genus and species of halophilic actinomycetes of the family Pseudonocardiaceae was discovered from the Meighan wetland[90]. Recently, another study described *Saccharothrix xinjiangensis* as a novel isolate from Caspian beach in Iran, which produced several new compounds[91]. The findings of the above-cited studies show that Iran, with its diverse ecosystems, has a remarkable potential for the investigation of new Actinobacteria. Therefore, in this study, we search for novel rare Actinobacteria in the neglected area of Iran and in other underexplored areas, such as Cuxhaven beach, in Germany.

1.7 Study aims

1) The isolation of Actinobacteria from Iran and Germany;
2) The cultivation and optimization of media;
3) The extraction and screening of bioactivity, including antimicrobial and antiviral activity;
4) The fermentation, purification, and structure elucidation of metabolites produced by isolated Actinobacteria;
5) Taxonomic study of the identified novel Actinobacteria strains.

2. Materials and Methods

2.1 Materials

2.1.1 Media

Table 1. List of media utilized in this study

Media	Ingredients	g/l
5336 - medium	Soluble starch	10.0 g/l
Isolation medium - Actinobacteria	Casein	1.0 g/l
	K_2HPO_4	0.5 g/l
(pH 7.3)	$MgSO_4 \times 7\ H_20$	5.0 g/l
	Agar	20.0 g/l
	D.W	1000 ml
5336+ Antifungal- medium	Sterilized 5336 medium	1000 ml
Isolation medium- Actinobacteria	Nalidixic acid solution (25 mg/ml in 0.2 M NaOH)	1.0 ml
	Cyclohexamide acid solution (50 mg/ml in	
(pH 7.3)	methanol)	2.0 ml
GYM-medium	Glucose	4.0 g/l
Maintenance and revitalization	Yeast extract	4.0 g/l
	Malt extract	10 g/l
	$CaCO_3$	2.0 g/l
(pH 7.2)	D.W	1000 ml
GYM+ ASW (Artificial Sea Water)	GYM medium	1000 ml
Maintenance medium	Coral reef salt(Coral Ocean), ATI	39 g/l
(pH 7.2)		
Sodium chloride tolerance-medium	Casein peptone	10 g/l
	Yeast extract	5.0 g/l

(pH 7.0)	Agar	20 g/l
	D.W	1000 ml
Basal medium	$(NH_4)_2 SO_4$	2.64 g/l
Carbohydrate utilization medium	KH_2PO_4	2.38 g/l
	K_2HPO_4	4.31 g/l
	$MgSO_4 \times 7 H_2O$	1.0 g/l
(pH 7.3)	Agar	15.0 g/l
	Trace element solution 3 (5342)	1.0 ml/l
	D.W	1000 ml
5341 solution	$CuSO_4 \times 5 H_2O$	10 g/l
(Trace element solution 2)	$CaCl_2 \times 2 H_2O$	10 g/l
	$FeSO_4 \times 7 H_2O$	10 g/l
	$ZnSO_4 \times 7 H_2O$	10 g/l
	$MnSO_4 \times 7 H_2O$	40 g/l
	D.W	1000 ml
5342 solution	$CuSO_4 \times 5$ H2O	0.64 g/l
(Trace element solution 3)	$FeSO_4 \times 7$ H2O	0.11 g/l
	$ZnSO_4 \times 7$ H2O	0.15 g/l
	$MnCl_2 \times 4$ H2O	40 g/l
	D.W	1000 ml
5343 solution	$FeSO_4 \times H_2O$	1.0 g/l
(Trace element solution 4)	$ZnSO_4 \times H_2O$	1.0 g/l
	$MnCl_2 \times H_2O$	1.0 g/l
	Agar	20 g/l
(pH 7.0)	D.W	1000 ml
5006- medium	Sucrose	3.0 g/l
Sterility control medium	Dextrin	15 g/l
	Meat extract	1.0 g/l
(pH 7.2)	Yeast extract	2.0 g/l

	Tryptone soy broth	5.0 g/l
	NaCl	0.5 g/l
	K_2HPO_4	0.5 g/l
	$MgSO_4 \times 7\ H_2O$	0.5 g/l
	$FeSO_4 \times 7\ H_2O$	0.01 g/l
	Agar	20 g/l
	D.W	1000 ml
ISP2 (Yeast malt agar)-medium	Malt extract	10.0 g/l
Maintenance and taxonomy	Yeast Extract	4.0 g/l
	Glucose	4.0 g/l
(pH 7.0)	Agar	15 g/l
	D. W	1000 ml
ISP 3 (Oat meal agar)-medium	Oatmeal (Quaker white oats)	20.0 g/l
Maintenance and taxonomy		
medium	Agar	18.0 g/l
	Trace salt solution ISP3	1.0 ml
(pH 7.2)	D. W	1000 ml
Trace solution ISP3	$FeSO_4 \times 7\ H_2O$	0.1 g
	$MnCl_2 \times 4\ H_2O$	0.1 g
	$ZnSO_4 \times 7\ H_2O$	0.1 g
	D. W	1000 ml
ISP4- medium	Soluble starch	10.0 g/l
Maintenance and taxonomy		
medium	$(NH_4)_2\ SO_4$	2.0 g/l
	K_2HPO_4	1.0 g/l
	$MgSO_4 \times 7\ H_2O$	1.0 g/l
(pH 7.3)	NaCl	1.0 g/l
	$CaCO_3$	2.0 g/l
	Agar	20 g/l

	D.W	1000 ml
ISP5- medium	L-Arginine	1.0 g/l
Maintenance and taxonomy		
medium	Glycerol	10.0 g/l
	K_2HPO_4	1.0 g/l
	Trace salt solution ISP 5	1.0 ml/l
(pH 7.2)	Agar	20 g/l
	D. W	1000 ml
Trace salt solution ISP 5	1,0 g $FeSO_4 \times 7\ H_2O$	1.0 g
	1,0 g $MnCl_2 \times 4\ H_2O$	1.0 g
	1,0 g $ZnSO_4 \times 7\ H_2O$	1.0 g
	D.W	1000 ml
ISP 6 (Peptone Iron Agar)-		
medium	Peptone	15.0 g/l
Production of melanoid pigment	Proteose Peptone	5.0 g/l
	Ferric ammonium citrate	0.5 g/l
	Sodium glycerophosphate	1.0 g/l
(pH 7.2)	Sodium thiosulfate-5-hydrate	0.12 g/l
	Yeast extract	1.0 g/l
	Agar	20 g/l
	D. W	1000 ml
ISP7-medium	Glycerol	15.0 g/l
Production of melanoid pigment	L-Tyrosine	0.5 g/l
	L-Asparagine	1.0g/l
	K_2HPO_4	0.5 g/l
(pH 7.3)	NaCl	0.5 g/l
	$FeSO_4 \times 7\ H_2O$	0.01 g/l
	Trace salt solution (5343)	1.0 ml/l
	Agar	20.0 g/l
	D. W	1000 ml

Synthetically Sutter medium	Glycerol	15 g/l
Production of melanoid pigment	Tyrosine	1.0 g/l
	L-arginine	5.0 g/l
(pH 7.2)	L-glutamic acid	5.0 g/l
	L-methionine	0.3 g/l
	L-isoleucine	0.3 g/l
	K_2HPO_4	0.5 g/l
	$MgSO_4 \times 7\ H_2O$	0.2 g/l
	Trace element solution (5341)	1.0 ml/l
	Agar	20.0 g/l
	D. W	1000 ml
Middlebrooks Broth medium	Becton, Dickinson and Company France	
Müller-Hinton Bouillon (MHB)	Carl Roth GmbH+Co.KG, Germany	
Myc medium	Phytone peptone	0.1 g/l
	Glucose	0.1 g/l
pH (7.0)	HEPES	11.9 g/l
	D. W	1000 ml
Trypticase soy broth	Becton, Dickinson and Company France	
Tryptone soy broth		
5294 -medium	Yeast extract	2.0 g/l
Metabolite production medium	Starch (soluble)	10 g/l
	Glucose	10 g/l
	Glycerol	10 g/l
(pH 7.2)	Corn steep liquor	2.5 g/l
	Peptone	2.0 g/l
	NaCl	1.0 g/l
	$CaCO_3$	3.0 g/l
	D.W	1000 ml
	Glucose	15.0 g/l

5254- medium		
Metabolite production medium	Soy flour	15.0 g/l
	Corn steep liquor	5.0 g/l
(pH 7.0)	$CaCO_3$	2.0 g/l
	NaCl	5.0 g/l
	D.W	1000 ml
5080-medium	Soy flour	20 g/l
Metabolite production medium	Mannit	21 g/l
(pH 7.2)	D.W	1000 ml
5304-medium	Glucose	1.0 g/l
	Starch	24.0 g/l
	Tryptone	5.0 g/l
	Meat extract	3.0 g/l
(pH 7.0)	$CaCO_3$	4.0 g/l
	D. W	1000 ml
5305-medium	Potato starch	30.0 g/l
Metabolite production medium	Soy flour	15.0 g/l
	Corn steep liquor	5.0 g/l
	Yeast extract	2.0 g/l
(pH 7.0)	Trace element solution 5314	1.0 ml/l
	D. W	1000 ml
Trace element solution 5314	$CaCl_2 \times H_2O$	3.0 g/l
	Iron (III) citrate	1.0 g/l
	$MnSO_4$	0.2 g/l
	$ZnCl_2$	0.1 g/l
	$CuSO_4 \times 5\ H_2O$	0.025 g/l
	$Na_2B_4O_7$	0.2 g/l
	$CoCl_2 \times 6\ H_2O$	0.004 g/l
	Na_2MoO_4	0.01 g/l
	D.W	1000 ml

5319-medium	Glycerol	30.0 g/l
Metabolite production medium	Casein peptone	2.0 g/l
	K_2HPO_4	1.0 g/l
	NaCl	1.0 g/l
(pH 7.0)	$MgSO_4 \times 7\ H_2O$	0.5 g/l
	Trace element solution 5314	5.0 ml/l
	D.W	1000 ml
5330-medium	Glucose	10 g/l
Metabolite production medium	Dextrin	10 g/l
	Yeast extract	5.0 g/l
	Casein peptone	5.0 g/l
(pH 6.5)	$CaCO_3$	1.0 g/l
	Celite	5.0 g/l
	D.W	1000 ml
5333-medium	Yeast extract	4.0 g/l
Metabolite production medium	Starch (soluble)	15.0 g/l
	K_2HPO_4	1.0 g/l
(pH 7.0)	$MgSO_4 \times 7\ H_2O$	0.5 g/l
	D. W	1000 ml
5334-medium	Glucose	20.0 g/l
Metabolite production medium	Soy flour	10 g/l
	$CaCO_3$	0.2 g/l
	$CoCl_2 \times 6\ H_2O$	0.001 g/l
(pH 7.0)	D.W	1000 ml
5288-medium	Glucose	15 g/l
Metabolite production medium	Soy flour	15 g/l
	Corn steep	10 g/l
	NaCl	5.0 g/l
(pH 7.0)	$CaCO_3$	2.0 g/l
	D. W	1000 ml

5010-medium	Sucrose	30 g/l
Metabolite production medium	$NaNO_3$	2.0 g/l
	KH_2PO_4	1.0 g/l
(pH 6.8)	$MgSO_4 \times 7\ H_2O$	0.5 g/l
	KCl	0.5 g/l
	$FeSO_4$	0.01 g/l
	D.W	1000 ml

All of the media were autoclaved for 20 min at 121°C.

2.1.2 Chemicals

Table 2. List of chemicals applied for this study

Chemical material	**Manufacturer**
1 kb DNA ladder	BioLabs
Acetic acid	Carl Roth
Acetone	J.T. Baker
Acetonitrile	J.T. Baker
Agarose	Gibco BRL
Ammonium acetate	Carl Roth
Ammonium iron (III) citrate $((NH_4)_5Fe(C_6H4O_7)_2$	Carl Roth
Ammonium Sulfate $(NH_4)_2SO_4$	Merck
Aniline phthalate spry solution for Polar lipid	Roth CP35.1
Anisaldehyde spry solution for Polar lipid	Sigma SRA1
Arabinan	Merck
Artificial sea water “Coral Ocean	ATI aquarium
Arabinose	Merck

Arabinoxaylan	Merck
Bacto Agar®	Becton Dickinson
Calcium carbonate (CaCO3)	Panreac Appli Chem
Casein (peptone Type M)	Marcor
Calcium chloride ($CaCl_2$ x $2H_2O$)	Merck
Cellulose	Serva, Heidelberg
Chloroform dnp for NMR	Carl Roth
Chloroform	Merck
Corn steep liquor	Schering
Copper (III) sulfate $CUSO_4 \times 5\ H_2O$)	Merck
Cyclohexamide	Serva
Dextran	Sigma-Aldrich
DL –valine	Sigma-Aldrich
DL-alanine	Sigma-Aldrich
Dulbecco´s modified Eagle´s medium (DMEM)	Bio Whittaker, Walkersville, MD
Dichloromethane	J.T. Baker
Dimethyl sulfoxide (DMSO) for NMR	Carl Roth
Ethylenediaminetetraacetic acid (EDTA)	Honeywell
Ethanol	J.T. Baker
Ethyl acetate	J.T. Baker
Fetal bovine serum	FBS, JRH Bioscience, Lenexa, KS
Formic acid	Carl Roth
Fructose	Carl Roth

Galactan	Carl Roth
Galactose	Carl Roth
Galactomannan	Carl Roth
Gelatin	Merck
Glucose	Carl Roth
Glycerol	Carl Roth
n-Heptane	Carl Roth
Hexane	Merck
Hydrochloric acid (HCl)	Carl Roth
HEPES 4-(2-Hydroxyethyl)-1-piperazine ethanesulfonic acid	Carl Roth
Inositol	Merck
Iron(III) citrate ($FeC_6H_6O_7 \times H_2O$)	Merck
Iron (III) chloride ($Fecl_3 \times 6H_2O$)	Merck
Iron (II) sulfate ($FeSO_4 \times 6H_2O$)	Honeywell
Isoamyl alcohol	Sigma-Aldrich
Jump Star Taq Ready Mix	Sigma-Aldrich
L-Alanine	Panreac Appli Chem
L-Asparagine	Panreac Appli Chem
L-Isoleucine	Fluka
L-Glutamic acid	Merck
L- valin	Sigma- Aldrich
L-Tyrosine	Merck
Magnesium sulfate ($MgSO_4 \times 7H_2O$)	Carl Roth

Mannitol	Merck
Malt extract	Carl Roth
Marfey regent FDAA	Thermo Scientific
Methanol	J.T. Baker
Middlebrook Broth medium	Becton Dickinson
Molybdenum blue	Molybdenum blue (Sigma No.3389)
Muller hinton Bouillon	Carl Roth GmbH + Co.KG, Germany
α-Naphtol α-Naphtol spray reagent composition: 15% α-naphtol in ethanol (10.5 ml) Concentrated H2SO4 (6.2 ml) Ethanol (40.5 ml) Deionized water (4 ml)	Merck
Ninhydrin	Merck spray reagent Na.6758
Pachyman	Megazyme
Pectin	Sigma
Petrol ether	Sigma-Aldrich
Pepton	Becton Dickinson
Pepton S	Marcor
Potassium chloride (KCl)	Sigma- Aldrich
Potassium dihydrogen phosphate (KH_2PO_4)	Carl Roth
Potassium hydrogen phosphate (K_2HPO_4)	Merck
Potassium nitrate	Merck
Pullulan	Megazyme
Sodium chloride (NaCl)	Merck
Sodium-hydrogen-carbonate ($Nahco_3$)	Merck
Sodium glycerophosphate	Serva

Sodium thiosulfate-5-hydrate	Merck
Sulfuric acid (H_2SO_4)	Merck
Soy flour	Cargill
Soy peptone	Merck
Sucrose	Merck
Starch	Carl Roth
Soluble Starch	Carl Roth
XAD AmberLite™ XAD™16N Polymeric Adsorbent	Rohm and Hass
Xylose (Xyl)	Merck
Water (nuclease free)	Carl Roth
Yeast extract	Carl Roth
Zinc sulfate (ZnSO4 x 7H2O)	Merck

2.1.3 Equipment

Table 3. List of equipment used in this study

Equipment	**Manufacturer**
Evaporator	Zymark
Bath water	Julabo
Centrifuge	Eppendorf Centrifuge 5804 R
Centrifuge	Eppendorf Centrifuge 5427 R
Centrifuge Multifuge 1S-R	Thermo Scientific
Clean Bench	Thermo Scientific Type MS 2020 1.2
CO2 incubator	Thermo Scientific Heracell 150i CO2

	Incubator
Optical rotation detector	PerkinElmer 241 polarimeter
HR-ESIMS	MaXis ESI-TOF-MS spectrometer (Bruker) equipped with an Agilent 1260 series RP-HPLC system
HPLC	Aligent 1100 series; Aligent technology, USA
HPLC	Agilent 1260 Series; Aligent technology, USA
HPLC preparative	Reverse-phase liquid chromatography HPLC 2020, Gilson, Middleton, WI, USA
HPLC column	VP Nucleodur 100−5C 18 ec column (250 mm × 40 mm, 7 μm) Macherey-Nagel
HPLC column	Column 2.1 × 50 mm, 1.7 μm, C18 Acquity UPLC BEH (waters)
HPLC column	XBridge® C-18 3.5 μm, 2.1 mm x 100 mm, Waters
Incubator	Biometra ov5
Incubator	Hereus Instruments Function Line
Light microscope	Zeiss Axio Sc pie. A1 microscope
Milli-Q, Millipore, deionized water	Schwalbach, Germany
Multichannel pipette	RAININ 8-Kanal-Pipette ED P3 Plus 100-1200 μL
N2 dryer (plates)	MiniVap (Porvair science)
NanoPhotometer	NanoPhotometer UV/Vis Spectrophotometer From Implen GmBH
Pipettes	Eppendorf Research plus

Eppendorf thermocycler	GBF
Gel Doc imagine system	Herolab
Electrophrese	Bio Rad
\Rotator (overhead shaker)	Heidolph
Rotary evaporator	Heidolph Laborata 4003
Shaker (plates)	Heidolph Titramax 1000
Shaker	Pilot-Shake System Kühner RC-6-U
Magnetic stirrer	MR 3002 s / Hiedolph
Thin layer chromatography (TLC) plates cellulose	Merck
Thin layer chromatography (TLC) plates silica gel 6	Merck
UV detector	Herolab RH-5.1 darkroom hood + B1393-3K7N
DNA sequencer	96-capillary-system from Applied Biosystems (ABI), 3730xl DNA Analyzer

2.1.4 Primers

Table 4. List of primers used in this study for PCR and sequencing

Primer	Sequence (5'–3')	Orientation	Function	Position (bp)*
F27	AGA GTT TGA TCM TGG CTC AG	Forward	PCR	9-27
R1492	TACGGYTACCTTGTTACGA CT	Reverse	PCR	1492-1531
F1100	YAA CGA GCG CAA CCC	Forward	sequencing	1100-1114
R1100	GGG TTG CGC TCG TTG	Reverse	sequencing	1100-1114
R518	GTA TTA CCG CGG CTG CTG G	Reverse	sequencing	518-537
R1541	GAAGGAGGTGWTCCARCCG CA	Reverse	PCR	1526-1541

*Number relative to *Escherichia coli*[92]

2.1.5 Kits and Enzymes

Table 5. List of kits and enzymes applied for polyphasic approach.

Kits or enzymes	Utilization	Manufacturer
API® ZYM	Semiquantitation of enzymatic activities	BioMérieux
API® Coryne	24-hour identification of Corynebacteria and coryne like organisms	BioMérieux
Bacterial alkaline phosphatase	Removing 3 and 5 phosphates from DNA and RNA	Thermo Fisher Scientific
Invisorb® Spin Plant Mini Kit	DNA extraction	Stratec/Invitek
JumpStart™ Taq Ready-mix™	PCR	Sigma-Aldrich
Lysozyme from chicken egg white	DNA digestion	Sigma-Aldrich
Nuclease P1 from Penicillium citrinum	DNA digestion	Sigma-Aldrich
NucleoSpin® Gel and PCR Clean-up	PCR cleaning	Macherey-Nagel
Proteinase K	Extraction Protein digestion in DNA	Carl Roth

2.1.6 Microorganisms

Table 6. List of standard test microorganisms for antibiotic assay.

Microorganisms	media	temperature	Time of incubation
Micrococcus luteus (DSM 1790)	Müller Hinton	30°C	24 h
Mycobacterium semegmatis (ATCC700084)	Middle brook	30°C	24-48 h
Staphylococcus aureus Newman	Müller Hinton	30°C	24 h
Bacillus subtilis (DSM 10)	Müller Hinton	30°C	24 h
Escherichia coli TolC	Müller Hinton	30°C	24 h
Escherichia coli (DSM 1116)	Müller Hinton	30°C	24 h
Chromobacterium violaceum (DSM 30191)	Müller Hinton	30°C	24 h
Pseudomonas aeruginosa PA14 (DSM 19882)	Müller Hinton	37°C	24 h
Candida albicans (DSM 1665)	Myc	30°C	24 h
Pichia anomala (DSM 6766)	Myc	30°C	24 h
Mucor himalis (DSM 2656)	Myc	37°C	24 h
Clostridium difficile 630	Columbia blood agar (BD)	37°C	72 h
Legionella pneumophila (NCTC 11192)	BCYE	37°C	72 h

2.2 Method

2.2.1 Sampling

The samples of Iran were taken from the upper 5-10 cm of surface soil, in different locations from the west, north, and center of Iran, collected in boxes. The sample of Germany was collected by Dr. Kathrin Mohr from the Cuxhaven beach/waden sea. Region of collecting samples are shown in Figure 4.

Figure 4. Regions of collecting samples a) Map of Iran with the sampling sites. The sampling locations are marked with a red circles. Credit picture from https://www.mapsofworld.com/answers/geography/what-are-the-key-facts-of-iran/

b) Map of Germany with sampling sites. The sampling location is marked with a red circle. https://www.mapsofworld.com/answers/geography/what-are-the-key-facts-of-germany/

2.2.2 Isolation

For the isolation of Actinobacteria an amount of 1 gram, wet or dry samples were used for serial dilutions up to 1/1000. The volume of 100 µl of each dilution was inoculated on agar plate 5336 supplemented with cyclohexamide (100 µg/ml) as antifungal agent, also supplemented with artificial sea water for the sand samples[93]. The plates were incubated for 7-21 days at 30°C. Based on the typical morphology of Actinobacteria, supposed colonies were picked with the sterile inoculating loop and streaked on the GYM agar medium.

2.2.3 Cultivation

2.2.3.1 Cultivation of Actinobacteria strains

A portion of pure culture in agar medium was cultivated in 100 ml of liquid GYM or GYM+ASW medium in a 250 ml flask and incubated at 30°C, for five days on a rotary shaker (160 rpm). The well grown culture was sub-cultured 1:10 to 100 ml of GYM medium, incubated for 5-7 days (30°C, 160 rpm).

2.2.3.2 Cultivation in production media and extraction of secondary metabolites

For the extraction of secondary metabolites, 10% of a 5-day-old culture were transferred to different production media (5254, 5295, 5254+ASW, 5294+ASW). All strains were cultured in 250 ml flasks filled with a volume of 100 ml medium, incubated at 30°C for 5-7 days on a rotary shaker (160 rpm). An amount of 25 ml of the growth culture was transferred to a 50 ml falcon tube and well mixed with 25 ml of ethyl acetate for 30 min on a rotator shaker. The tube was centrifuged at 9000 rpm for 15 min to separate the phases between the two immiscible solvents. The upper phase was transferred to a small 50 ml round flask and evaporated with reduced pressure at 40°C. The dried extract was re-dissolved in 500-µl methanol for the final concentration of 1/50[107,95].

2.2.4 Taxonomic classification

To characterize a new isolated strain the polyphasic approach including molecular, morphological, physiological, and chemotaxonomical analysis was conducted. In this study morphological and physiological analysis were completed in our lab. The chemotaxonomy analysis was accomplished in cooperation with Dr. Richard Hahnke and Dr. Peter Schumann, Leibniz Institute DSMZ-Braunschweig. For evaluation of DNA-DNA hybridization, the isolated DNA was sent to the group of Prof. Dr. Peter Kämpfer, University of Gießen, Germany. The whole genomes sequencing of isolated strains were completed by Christian Rückert, University of Bielefeld. All steps of the polyphasic approach, which is necessary for description of novel species, have been summarized in the flow chart (Figure 5).

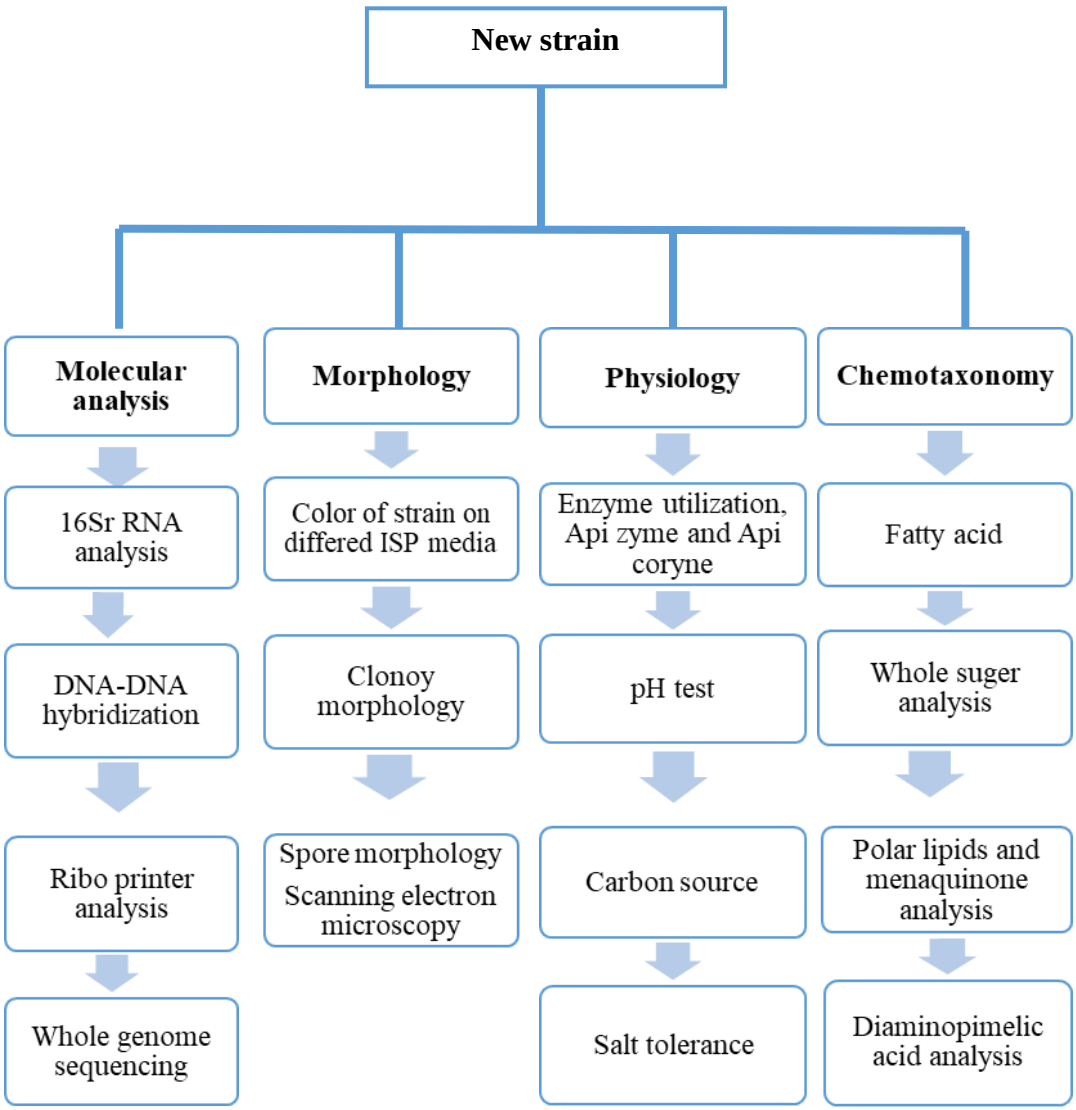

Figure 5. Flow-charts of polyphasic classification

2.2.4.1 Extraction, amplification, sequencing of 16S rRNA

Extraction of genomic DNA was achieved by using Invisorb Spin Plant Mini Kit (250) (Stratec Molecular, Germany). In this study, from the well-grown liquid culture, about 500 µl was transferred to a 2 ml microtube and centrifuged at 11000 rpm for 2 min. The supernatant was discarded, and the cell pellet was mixed with 100 µl of lysis buffer. About 300 µl lysis buffer was added again, incubated at 95°C for 5 min. Then amount of 20 µl protein kinase K was added and incubated

for 30 min at 65°C. The remaining steps were handled following the manufacturer's instruction. Amplification of 16S rRNA gene was conducted with MOHR52 PCR program with the following protocol: initial denaturation at 95°C (5 min); 34 cycles of denaturing at 94°C (30 s); annealing at 52°C (30 s); elongation at 72°C (120 s); final elongation at 72°C (10 min). The two specific primers 27 (forward) and 1492 (reverse) or 1541 (reverse) were applied for 16S rRNA PCR. For preparation the PCR ingredient, the sufficient amount of mastermix containing "Jump Start Ready Mix" (JSRM) (25 µl), water (22 µl), forward primer (1 µl), reverse primer (1 µl) was prepared. The amount of 49 µl of mastermix was transferred to the 200 µl PCR reaction tube and 1 µl of the DNA template was added. The JSRM contains JumpStart Taq DNA polymerase, 99% pure deoxynucleotides, and buffer in an optimized reaction concentration. The PCR reaction was accomplished in a Master cycler Gradient (Eppendorf, Hamburg, Germany)[96]. The PCR product was purified using the NucleoSpin® Gel and PCR Clean-up Kit (Macherey-Nagel, Germany). Almost full-length16S rRNA gene fragment (1501bp) was sequenced by using the 96-capillary system from applied bio- systems (ABI), 3730 xl DNA analyzer. The primers for sequencing were F27, R518, F1100, R1100, and R1541.

The 16S rRNA gene sequences were compared with sequences from the NCBI database by BLAST analysis (http://www.ncbi.nlm.nih.gov/BLAST), as well as with sequences available at EzBioCloud (www.ezbiocloud.net)[97]. The 16S rRNA gene sequences were assayed by using MEGA X[98] software package and the sequences of all type strains were aligned using the CLUSTAL W algorithm[99]. Phylogenetic analysis was accomplished using the neighbor-joining[100] and maximum likelihood[101] methods. The topologies of the assumed trees were evaluated by bootstrap analyses based on 1000 replicates[102].

2.2.4.2 MALDI-TOF analysis

MALDI-TOF (matrix-assisted laser desorption/ionization-time of flight) analysis was done according to the ethanol/formic acid extraction protocol from Schumann & Maier[103] described in detail by Wink *et al.*[104]. About 10 mg of biomass from a liquid culture (cultivated in GYM medium for 6-8 days at 30°C) was suspended in H_2O (300 µl) and homogenized carefully. Then, 900 µl ethanol was added to the

suspension. Further preparation steps as well as the MALDI-TOF measurements and following analyses were done by Dr. Peter Schumann. MALDI-TOF mass spectra were recorded using a Microflex L20 mass spectrometer (Bruker Daltonics) with a N2 laser unit. The spectra were measured in linear positive mode and the acceleration voltage was 20 kV. The spectra were collected from 250 shots across a spot. To analyze the data, a mass range of m/z 2000-20,000 Da was observed. Using the Flex analysis software (version 3.3, Bruker Daltonics), the MALDI-TOF MS spectra were smoothed, baseline corrected and re-calibrated. A score-orientated dendrogram was calculated by using the BioTyper software (version 3.1, Bruker Daltonics).

2.2.4.3 RiboPrinter® analysis

Automated ribotyping of the isolates was accomplished according to Schumann & Pukall[105], by using the RiboPrinter system (Hygiena) and *Pvu*II as restriction enzyme. A dendrogram based on pattern similarity was created using the software package BioNumerics, Applied Maths (Sint-Martens-Latem, Belgium). The analysis was divided to five parts: sample preparation, DNA preparation, separation and transfer, membrane processing and pattern detection. For the sample preparation, 1ml of well grown liquid GYM medium was centrifuged, supernatant discarded, the biomass was sent out for further analysis. RiboPrinter® analysis was conducted by the working group of Dr. Peter Schumann, Leibniz Institute DSMZ-Braunschweig.

2.2.4.5 DNA-DNA hybridization

Preparation and isolation of DNA for DNA-DNA hybridization was done based on the method described in practical *Streptomyces* genetic by T. Kieser *et al.*[106]. The procedure was started with centrifugation of 30 ml well grown culture, supernatant was discarded. The pellet was suspended in 5ml TE25S buffer, the volume of 100 µl lysozyme solution was added, incubated at 37°C for 30-60 min on tube rotator. The amounts of 50 µl of proteinase K and 300 µl of 10% SDS solution were added, incubated at 55°C for 1 hour on a tube rotator, followed by adding 1ml of 5M NaCl and mixed by inversion. Then, amount of 0.65 ml CTAB/NaCl was added, incubated at 55°C for 10 min on tube rotator. The tube was cooled to 37°C, the amount of 5 ml chloroform/isoamyl alcohol was added and mixed for 30 min by

inversion. The tube was centrifuged for 15 min at 13,500 *g at 20°C. At the end, the supernatant was transferred to a fresh tube, 0.6 vol isopropanol was added and mixed by inversion. After 3 min the DNA was spooled to a 2ml Pasteur pipette, the DNA was rinsed 3 times with ethanol 70%, air-dried and dissolved in 0.5 ml of distal water.

The DNA-DNA hybridisation (DDH) experiments were performed between the new strain and its closest type strains with 16S rRNA gene sequences higher than 98.7% similarity according to the method of Ziemke *et al*. (except that for nick translation 2 µg of DNA were labelled during 3 hrs of incubation at 15°C)[107]. The genomic DNA G+C content of isolated strains was determined as described previously by Glaeser *et al*.[108]. The DNA-DNA hybridization and G+C content analysis were analyzed by Prof. Dr. Peter Kämpfer, University of Gießen.

2.2.4.6 Whole genome sequencing

Genomic DNA was used to construct two sequencing libraries, one using the Rapid Barcoding Kit run on an R9.4.1 flow cell (Oxford Nanopore Technologies, Oxford, UK), and using the TruSeq PCR-free Library Prep Kit run on a MiSeq sequencing platform (lllumina, Eindhoven, NL). The first resulted in the acquisition of 26,561 reads containing, base called with guppy v.2.3.1, a total of 337.1 Mb. The second delivered 3,864,942 reads containing 1,077.9 Mb. The ONT data were assembled using Canu v.1.7.1, resulting in a single contig of 5,878,427 bp. After trimming of the overlapping ends and rotating the genome based on *dnaA*, the resulting contig was first polished using minimap2 v.2.10 and nanopolish v.0.11.0 using the ONT raw fast5 data. The polished contig was then subjected to 10 rounds of additional polishing using pilon v.1.22 and the Illumina data mapped with either bwa mem v.0.7.12 (round 1-5) or bowtie2 v.2.3.3 (round 6-10). In all cases, samtools v.1.9 was used for handling mapping data. In parallel, the Illumina data were assembled using the newbler v.2.8 assembler (454 Life Sciences, Branford, CT, USA), resulting in an assembly consisting of 89 contigs in 26 scaffolds. Both assemblies were combined using consed v27.0 with the Illumina contigs were used for manual correction of the remaining errors in repetitive regions in the polished Canu assembly. The whole genome sequencing was conducted by the Dr. Christian Rückert, University of Bielefeld.

2.2.5 Morphology analysis and diffusible pigment production

For culture characterization the isolates were grown on various International *Streptomyces* Project (ISP) media such as yeast extract-malt extract agar (ISP2), oatmeal agar (ISP3), inorganic salts starch agar (ISP4), glycerol-asparagine agar (ISP5), peptone-yeast extract-iron agar (ISP6), tyrosine agar (ISP7), SSM+T (synthetically Suter medium with tyrosine), and SSM-T (synthetically Suter medium without tyrosine)[92,109]. For those strains, which have been isolated from the sand of beach all the media were supplemented with 7% NaCl. Colors of substrate mycelium, aerial mycelium, and diffusible pigments were identified after 10-14 days incubation at 30°C using the RAL color card (https://www.ralfarben.de)[110].

2.2.5.1 Spore chain morphology

To analyze the structure of the aerial mycelium and spores, the strains were grown on the complex solid growth medium ISP3 and incubated for 10-14 days at 30°C[109]. A section of the agar containing a bacterial lawn was fixed in 5% glutaraldehyde solution[111]. Samples were critical-point-dried and gold-palladium-sputtered, and the morphology of the spores was determined using a Zeiss Merlin field emission scanning electron microscopy (FESEM) with an Everhart-Thornley SE-detector and an Inlens-SEM detector in a 25: 75% ratio applying the SEM Smart software version 5.05[112].The electron microscopic analysis was done by Prof. Dr. Manfred Rhode, HZI Braunschweig.

2.2.6 Physiological and biochemical features

2.2.6.1 Growth at different temperature and pH

The growth of strains was observed at different temperatures 15, 20, 25, 30, 37, 44 and 55°C on GYM medium agar. The pH tolerance was detected in the pH range of 2, 3, 4, 5, 6, 7, 8, 9 and 10 on ISP2 liquid medium after incubation for 14 days**.**

2.2.6.2 Utilization of carbohydrates

The utilization of carbohydrates was followed employing microtiter plates filled with ISP9 medium as a basic medium. Additional carbohydrates were added with (1%, w/v) to each micro well as a source of carbon, including glucose (Glu), arabinose (Ara), sucrose (Suc), xylose (Xyl), inositol (Ino), mannitol (Man), fructose (Fra), rhamnose (Rha), raffinose (Raf) and cellulose (Cel)[109]. Then, the

amount of 100 µL of the well-grown liquid culture was transferred to each well. The plates were incubated 10-14 days at the optimum temperature for individual strain.

2.2.6.3 Sodium chloride tolerance

The sodium chloride tolerance analysis was accomplished with different concentration of NaCl: 0%, 2.5%, 5.0%, 7.5%, and 10% in a 6 well plate, incubated at 30°C for 14 days[113].

2.2.6.4 Enzymatic activity via API® stripes

To detect an enzymatic reaction a homogenized suspension of a well-grown liquid culture was transferred to the test stripes, which contain different substrates. The enzyme utilization was investigated by using API ZYM[114] and API Coryne strips[115]. The enzymes that can be detected with API ZYM strip, include alkaline phosphatase, butyrate esterase (C4), caprylate esterase lipase (C8), myristate lipase (C14), leucine arylamidase, valine arylamidase, cystine arylamidase, trypsin, α-chymotrypsin, acid phosphatase, naphtol-AS-BI-phosphohydrolase, α-galactosidase, β-galactosidase, β-glucuronidase, α-glucosidase, β-glucosidase, n-acetyl-β-glucosaminidase. The enzymes that can be detected with API Coryne strip are including nitrate reduction, pyrazinamidase, pyrrolidonyl arylamidase, alkaline phosphatase, β-glucuronidase, β-galactosidase, α-glucosidase, α-fucosidase, n-acetyl-β-glucosaminidase, esculin (β-glucosidase), urease, gelatin (hydrolysis), glucose fermentation, ribose fermentation, xylose fermentation, mannitol fermentation, maltose fermentation, lactose fermentation, sucrose fermentation, glycogen fermentation.

2.2.6.5 Polysaccharides microarray

The decomposition of polysaccharides and peptides was investigated in 96-well plates, following the protocol of Panschin *et al.*[116]. In short: each well was filled with 100 µl of either GYM medium with 10% NaCl (w/v) or minimal GYM medium (without carbon source) with 10% NaCl (w/v). One of the azurin-cross-linked –polysaccharide was added to each well and 100 µl of a culture (stationary phase) was added. Each strain was tested in triplicates with negative control. This procedure was conducted in cooperation with Dr. Richard Hahnke, Leibniz Institute DSMZ-Braunschweig.

2.2.7 Chemotaxonomic analysis

2.2.7.1 Freeze-dried cells preparation

For chemotaxonomical characterization, freeze-dried cells were applied in this study. The method of preparation was done by cultivating the strain for 5-7 days in the GYM liquid medium. The biomass was collected by centrifugation at 9000 rpm for 10 min. The pellet was washed three times with demineralized water and centrifuged three times at 9000 rpm for 10 min. The wet biomass was kept overnight at - 80°C and subsequently was dried in the freeze-dried machine for 24-48 hours.

2.2.7.2 Diaminopimelic acid of cell wall

Freeze-dried cells (10 mg) were mixed with 200 µl of HCL (6N) in a 5 ml teflon-lined screw capped tube and incubated overnight in the water bath (95°C). The mixture was filtrated by a 5 cm filter paper (Schleicher @ Scheull 589). The filtrate was dried with nitrogen flow for 45 min. The residue was dissolved in H_2O (0.3ml) and the solvent transferred to the Eppendorf tube. The amount of 5 µl of sample was applied on a cellulose thin layer plate (20*20 cm), thickness of the layer (0.3 mm). The standard mixture (1 mg/ml DL/LL-DAP) was employed as a reference. The plate was placed in a TLC tank, containing solvent mixture (Methanol- water-10N HCl-pyridine) with (8:17, 5:2, and 5:10 v/v), developed for almost 3 hours. The TLC plate was dried under fume hood and spots of amino acids were determined by spraying with ninhydrin solution and heating at 100°C for 3 min[117].

2.2.7.3 Cell wall sugars

About 50 mg freeze-dried cell material was mixed in a hydrolysis tube with 1 ml 1N H_2SO_4 and incubated at 95°C for 2 hours. After cooling down the tube, the sample was transferred to a 50 ml beaker. The pH was adjusted with ($Ba(OH)_2$. H_2O = 3 gr/10 ml) solution to 5.2-5.5, controlled by pH indicator. The precipitate was removed by centrifugation (3000 rpm, 5 min). The liquid phase was dried under reduced pressure on a rotatory evaporator. The residue was dissolved in 400 µl of H_2O. The particle was removed by centrifugation (3000 rpm, 1 min). The amount of 5 µl of the clear cell hydrolysate was spread on to a cellulose TLC plate (20×20). The standard mixture was applied as reference. The plate was developed

in ethyl acetate/pyridine/water (100:35:25 v/v) for 2 hours. The plate was dried under the fume hood, sprayed with anilinphathlate reagent. Spots of sugars were determined after heating the plate at 100°C for 5 min[117].

2.2.7.4 Extraction of quinones

About 100 mg freeze-dried cells was transferred into a 30 ml teflon- lined screw cap from Schott (GL18) and were mixed with 25 ml chloroform-methanol (2:1). The sample was filtered through 0.90 mm ashless filter paper circle (Schleicher and Schuell, Nr. 589). The supernatant was evaporated (40°C). About 25 ml of chloroform-methanol (2:1) was added to the cell material again, mixed for 1 hour, filtrated and added to the first elute and dried together in the evaporator (water bath 40°C). Finally, the residue was dissolved in 400-600 µl isopropanol. The solvent was filtered over *dyna Gard* and transferred to a micro vial, applied for the HPLC analysis[118]. The best separations of menaquninone mixtures were performed by HPLC using RP-18 columns with following condition: 250 mm, i.d 4 mm, mobile phase: acetonitrile/iso-propanol (56:45 v/v) at 40°C and 20 bar pressure. The flow rate was 1ml/min, UV detector, 254 nm, and sensitivity 0.005 abs.

2.2.7.5 Phospholipid identification

The polar lipids were extracted by the method of Blight and Dyer (1595), modified by Card (1973)[119]. About 100 mg of freeze-dried cells were mixed with 2 ml aqueous methanol and 2 ml light petrol in a 10 ml teflon- lined screw cap tube for 15 min in the tube rotator, centrifuged for 5 min at low speed, the supernatant was transferred to the small flask. About 1 ml petrol ether (60°C) was added to the aqueous phase, mixed for 15 min, centrifuged for 5 min and the supernatant was transferred to the small flask. The combined upper layers were reduced to dryness on the rotary evaporator (water bath 40°C). The lower phase was heated for 5 min in a boiling water bath, cooled down to room temperature with a water bath at 30°C for 5 min. The amount of 2.3 ml of $CHCl_3$-CH_3OH-0.3% NaCl (90:100:30) was added, mixed for 1 hour on a rotatory shaker, centrifuged and the supernatant was transferred to a 10 ml screw cap tube. About 0.75 ml $CHCl_3$-CH_3OH-0.3% NaCl (50:100:40 v/v) was added to the sediment (cells), extracted for 30 min, centrifuged and the supernatant was combined. This step of extraction was repeated, the solvents combined, and the cells were discarded. The amounts of 1.3

ml of $CHCl_3$ and 1.3 ml of 0.3% NaCl were added to the combined extracts, centrifuged for 5 min. The upper phase was discarded with a Pasteur pipette and the lower phased was concentrated to dryness on a rotary evaporator (water bath 40°C). The dried residue was dissolved in the CHCl-CH3OH (2:1) (0.4 ml). The sample was maintained for the thin layer chromatographic analysis of the phospholipids.

About 15 µl of each extract was applied as a small spot on the three different thin layer plates (silica gel 60 pre-pared plates of Merck Art. NO. 5553, 10*10 cm). Each plate was developed in two dimensions, first in solvent 1: chloroform-methanol-water (65:25:4), second in solvent 2: chloroform-acetic acid-methanol-water (80:15:12:4). The plate was developed in the first direction for 30 min, dried and the second direction was progressed. For detecting all polar lipids, the amount of 10% molybdophosphoric acid in ethanol was sprayed and spots were determined after the plate was heated for 15 min at 140°C. Observation of specific lipid was performed by spraying different reagents. Anisaldehyde was applied for detecting mannose-containing substance the plate was heated (10 min, 100°C)**.** Ninhydrin was used for free amino groups (PE) and the plate was heated (5 min, 100°C). Dragendrof reagent was sprayed for detecting phosphatidyl colin (PC) without heating.

2.2.7.6 Fatty acids

For extraction of the whole-cell fatty acids, cells were harvested at the logarithmic phase of growth according to the standard protocol of microbial identification system (Sherlock Version 6.1; MIDI database: TSSA6)[120]. About 10 mg freeze-dried cells were mixed with 1 ml saponification regent (45 g sodium hydroxide, 150 ml methanol and 150 ml distal water) for 5-10 seconds; the rack of tube was putted in boiling water bath for 30 min. After cooling down, amount of 2 ml methylation reagent (325 ml HCl 6N, 275 ml methanol) was added. The capped tube, briefly was vortexed for 5-16 seconds, and heated at 80°C for 10 min. The mixture was cooled down and 1.25 ml extraction reagent (200 ml hexane, 200 ml methyl- tert-butyl ether) was added. The tube was mixed end-over in a tube rotator for 10 min. The aqueous (lower) phase was discarded with a Pasteur pipette. About 3 ml of washing reagent (10.8 g NaOH dissolved in 900 ml distilled water) was

added to the organic phase, the tube was capped and rotated end-over-end for 5 min. Then tube was centrifuged at 2000 rpm for 3 min. The upper solvent phase was transferred to the suitable vial for gas liquid chromatography analysis.

2.2.8 Antimicrobial test with serial dilution method

With the purpose to identify compounds with anti-infective activity, the crude extracts were screened against a set of different test microorganisms including bacteria, fungi, and yeast as a standard panel. The antibacterial assay was performed in the 96- well plates according to the method described by Bauman *et al.*[121]. All the 96 wells were filled with 150 µl of the microbial suspension (OD600 0.01 for bacteria and 0.05 for fungi and yeast). The first row was filled with another 130 µl of the suspension of the test strains. Then 20 µl of the crude extracts was added to the first well (A1) and the last well of first row (A12) was mixed with 20 µl of the particular antibiotic as a positive control. The amount of 150 µl of the mixture was transferred to the next rows (B) and serially diluted with two-fold dilution until the last rows. The lasting 150 µl of the row (H) was discarded. The plates were incubated at 30°C or 37°C for 1-2 days based on the growth conditions of individual test strains. Antibacterial activity against two strains *Legionella pneumophila* NCTC11192 and *Clostridium difficile* 630 was performed in the lab of Prof. Dr. Michael Steinert, TU Braunschweig.

2.2.9 Cytotoxicity assay

The cytotoxicity assay against different mammalian cells was carried out based on the method of Landwehr *et al.*[122]. The cells were cultivated at 37°C with 10% CO_2 in DME medium (high glucose) supplemented with 10% fetal calf serum (CFS). The cell culture reagents came from Life Technologies Inc. (GIBCO BRL). Then, 60 µl of the test compound was given to 120 µl of suspended cells (50,000/ml) in wells of 96-well plates. After 5 days of incubation the growth inhibition (IC_{50}) was determined using an MTT assay[123]. Different cell lines were selected for the assay including L-929 (murine fibroblast), KB-3-1 (human cervix carcinoma), A-549 (human lung carcinoma), PC-3 (human prostate carcinoma), MCF7 (human breast adenocarcinoma), A-431 (human epidermoid carcinoma), SK-OV-3 (human Caucasian ovary adenocarcinoma), and HUVEC (human umbilical vein endothelial cell). The cytotoxic assay was accomplished by Wera Collisi, HZI-Braunschweig**.**

2.2.10 Antiviral assay

The antiviral assay was performed based on the method of Mulwa *et al*.[124]. Huh-7.5 cells (human hepatocellular carcinoma cells) stably expressing firefly luciferase (Huh-7.5 Fluc) were inoculated with RLuc Jc1 reporter viruses and the extracts were given also to the cells. The cells were incubated at 37°C with 5% CO_2 stream. After 4 hours of incubation, the inoculum was discarded, and the cells were washed with PBS (phosphate buffer saline) and new medium without extracts was added. The medium for the cells was Dulbecco's modified minimum essential medium (DMEM, Life Technologies Manchester UK) containing 2 mM glutamine, 1 × minimum essential medium nonessential amino acids (MEM NEAA, Life Technologies), 100 µg/mL streptomycin, 100 IU/ml penicillin (Life Technologies), 5 µg/ml blasticidin and 10% FBS (fetal bovine serum). After 3 days of incubation, the infected cells were lysed. The reporter virus infection and the cell viability were determined by renilla luciferase and firefly luciferase activities, respectively. The measurement of luciferase activity was performed by using Berthold Technologies Centro XS3 Microplate Luminometer. The antiviral assays were conducted by Dimas F. Praditya and Prof. Dr. Eike Steinmann, TWINCORE-Hannover.

2.2.11 Compound analysis: HPLC fractionation and mass spectrometry (MS)

HPLC fractionation was carried out in 96-well plates. An Agilent 1260 Series HPLC–UV system equipped with a Waters, XBridge BEHC18, 2.1 mm 100 mm column (poresize135 Å, particle size 3.5 µm; solvent A: H_2O-acetonitrile (95/5),5 mmol NH_4Ac, 0.04 mL/L CH_3COOH, solvent B: H_2O-acetonitrile (5/95), 5 mmol NH_4Ac, 0.04 mL/L CH_3COOH; gradient system: 10% B increasing to 100% B in 30 min; flow rate 0.3 mL/min; 40°C; UV-detection at 210–450 nm) was used for the chromatographic fractionation of crude extract. The same HPLC gradient was used for the high-resolution electrospray ionization mass spectrometry (HRESIMS) instrument. The fractionated crude extract in the 96-well plate was dried at 40°C with heated nitrogen in a MiniVap (Porvair science) for 30 min. Then, 150 µl of the certain test organisms were added to each well and the plate was incubated at 30°C or 37°C for 24 h.

2.2.12 Optimization of media

Analyzing and optimization of best production media was carried out in different production media. About 10% of well- grown culture was transferred to the several standard production media (5010, 5038, 5080, 5288, 5304, 5305, 5319, 5321, 5330, 5333, and 5334). The flasks were incubated at 30°C and 160 rpm for 7 days. All extracts were measured by HPLC; the area of the selective molecular mass was evaluated for each extract. Based on the statistical analysis the best medium, which the compound was produced in the highest amount, was selected.

2.2.13 Fermentation, extraction, and isolation of compound from strain M2^T

The 5-day-old culture was transferred to the production medium 1:10 in eight 1000-ml flasks, filled with 800 ml of medium 5294 (1% soluble starch, 0.2% yeast extract, 1% glucose, 1% glycerol, 0.25% corn steep liquor, 0.2% peptone, 0.1% NaCl, 0.3% $CaCO_3$; pH 7.2) and incubated at 30°C for 8 days on rotary shaker (160 rpm). The 8-day-old culture medium was centrifuged using a Sorvall RC-5 refrigerated super speed centrifuge, at 8500 rpm for 30 min. The supernatant was discarded, and 311 g cell mass was extracted with two liters of acetone three time in an ultrasonic bath (3×30 min). The obtained solution was evaporated to yield an aqueous phase, which was further extracted with ethyl acetate (3×500 ml) and the ethyl acetate portion was dried out with evaporator, yielded 575.2 mg of crude cell mass extract. An initial pre-separation of 575.2 mg crude extract was applied on the Strata TM-X 33 UM polymeric reversed phase (1g/12 ml giga tube Phenomenex). It was washed three times with methanol. After separation the fatty acids, the amount of 265.2 mg crude extract was used for injection to preparative HPLC (Gilson) (1 run using a linear gradient of solvent B from 20% to 50% solvent B in 30 min, 50% to 100% B in 20 min followed by isocratic conditions for 10 min at a flow rate of 50 ml/min). Fractions were collected and combined according to UV absorption at 220, 280 and 350 nm and yielded 5.6 mg of compound 1 at a retention time of 37.5–38.5 min and 0.5 mg of 2 at 36.5–37 min, respectively.

Data acquisition, processing, and spectral analyses of NMR data was performed by Dr. Frank Surup at microbial drug group- HZI Braunschweig.

2.2.14 Ozonolysis, hydrolysis, and Marfey's Derivatization with l-FDAA

For determination the final structure of compound 1, several assessments including ozonolysis reaction, hydrolysis, and Marfey's derivatization evaluations were conducted. For the ozonolysis reaction a stream of O3 was bubbled through a solution of pure compound 1 (2.3 mg) dissolved in methanol (6 ml) at -78°C until the solution obtained a characteristic blue color and stirred for 30 min. Subsequently, the solvent was removed in vacuum and the resulting oxidized material was subjected to hydrolysis in 3 ml of 6 N HCl at 110°C for 24 h according to Yun *et al.*[125]. Then, the solvent was removed under a stream of nitrogen for 3 h and the remainder dissolved in H_2O (200 µl), of which 100 µl were proceeded further. A total of 1 N $NaHCO_3$ (20 µl) and 1% 1-fluoro-2,4dinitrophenyl-5-Lalaninamide (100 µl in acetone) were added, and the mixture was heated at 40°C for 40 min[126]. After being cooled to room temperature, the solutions were neutralized with 2 N HCl (20 µl) and evaporated to dryness. The residues were dissolved in MeOH and analyzed by HPLC−MS. Retention times in minutes of FDAA-derivatized amino acids were 6.5 for Val and 5.0 for Ala. Retention times of the authentic amino acid standards were L-Val 6.5, DL-Val 6.5/7.5, L-Ala 5.0, DL-Ala 5.0/6.0.

3 Result

3.1 Identification of isolated Actinobacteria based on 16S rRNA gene sequence similarity from soil and sand samples

48 Actinobacteria strains were isolated from Iran's samples and 2 additional from the sand of Cuxhaven beach in Germany. Among the 48 isolates, 34 strains were characterized as *Streptomyces* and the rest were identified as a rare Actinobacteria (Table S 11). From the sand samples, two isolates were belonged to the rare Actinobacteria.

3.2 Polyphasic taxonomy of strains M2^T and M3 isolated from Cuxhaven beach, Germany

Two strains M2^T and M3 were isolated from the sand of Cuxhaven beach. The color of substrate mycelium varied depending on the medium; in ISP2 (honey yellow), ISP3 (white), ISP4 (white), ISP5 (light ivory), ISP6 (golden yellow), ISP7 (ivory). Aerial mycelium was detected in all media except of ISP4. The color of aerial mycelia was pure white. Diffusible pigments were produced on ISP2, ISP3, ISP5, ISP7, and SSM+T and SSM-T. Melanin was not produced on ISP6, ISP7 and SSM+T and SSM-T (Figure 6). At maturity on ISP3 medium, aerial mycelium forms spore chains (wrinkled surface) and single non-motile spores (smooth surface) (Figure 7). In this study, to compare morphological characteristics of selected isolates with other type strains of the genus, the growth of all members of genus *Streptomonospora* was analyzed in our laboratory conditions (Table S 1).

3.2.1 Utilization of carbohydrates, sodium chloride tolerance, and pH tolerance

Strains M2^T and M3 utilized glucose, xylose, arabinose, fructose, rhamnose as carbone sources (Figure 8). Utilization of carbohydrates for all species of genus *Streptomonospora* in our laboratory conditions were shown in Table S 2. They grew in media with NaCl concentration 0-15 (optimum7-10% NaCl) (Figure 9), at pH 4-9 (optimum7-8) and at temperature betwee n 20- 37°C (optimum 30°C).

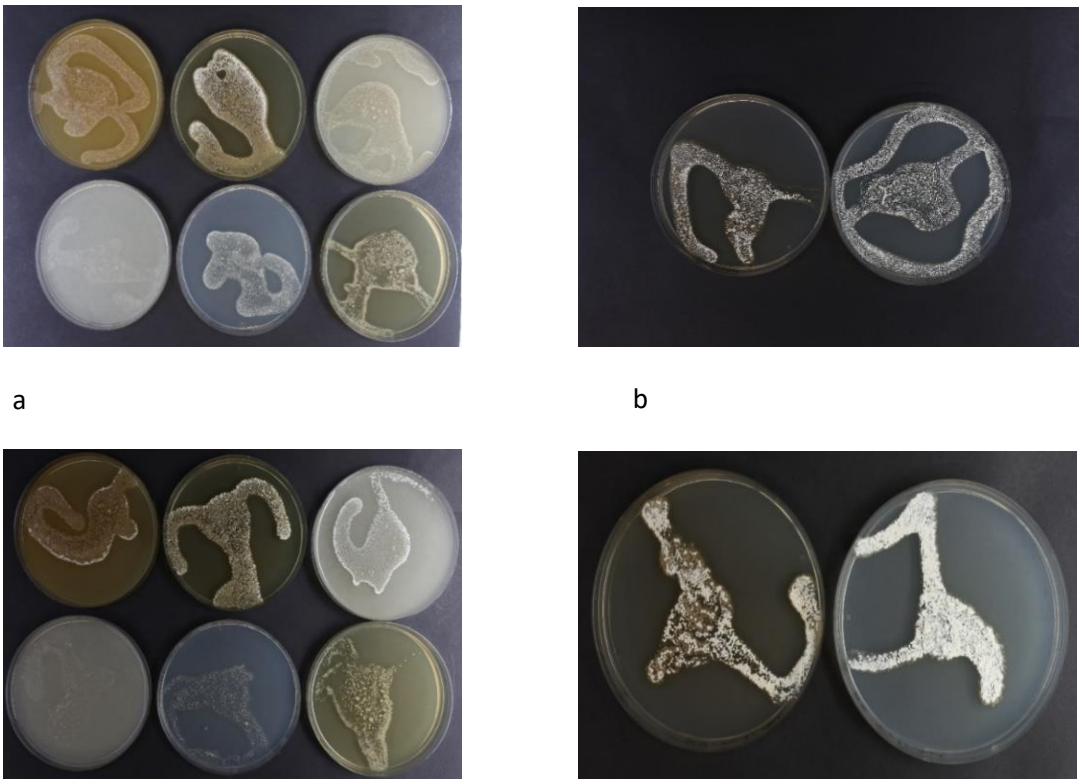

a b

c d

Figure 6. Morphological characteristics of two strains $M2^T$ and M3 on ISP media. a) The growth of strain $M2^T$ on GYM, ISP2, ISP3, ISP4, ISP5, and ISP7; b) The growth of strain $M2^T$ on SSM+T and SSM-T; c) The growth of strain M3 on: GYM, ISP2, ISP3, ISP4, ISP5, ISP7; d) The growth of strain M3 on: SSM+T left and SSM-T. right.

a

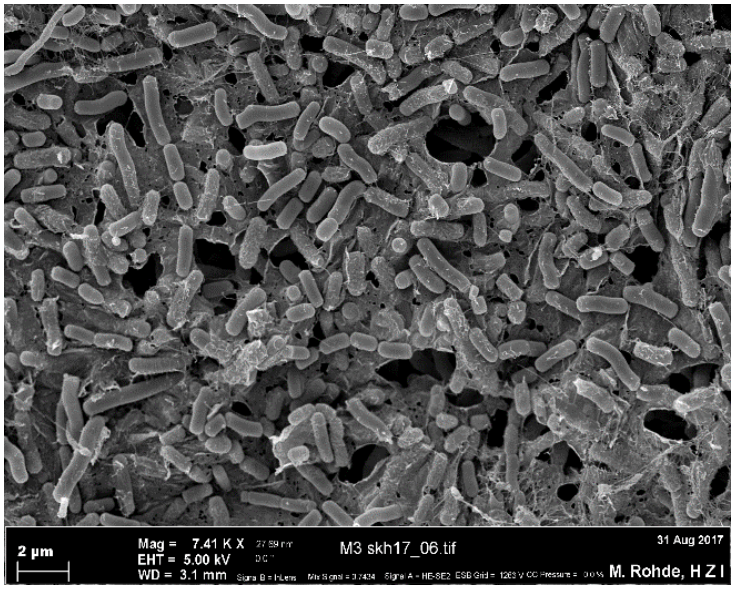

b

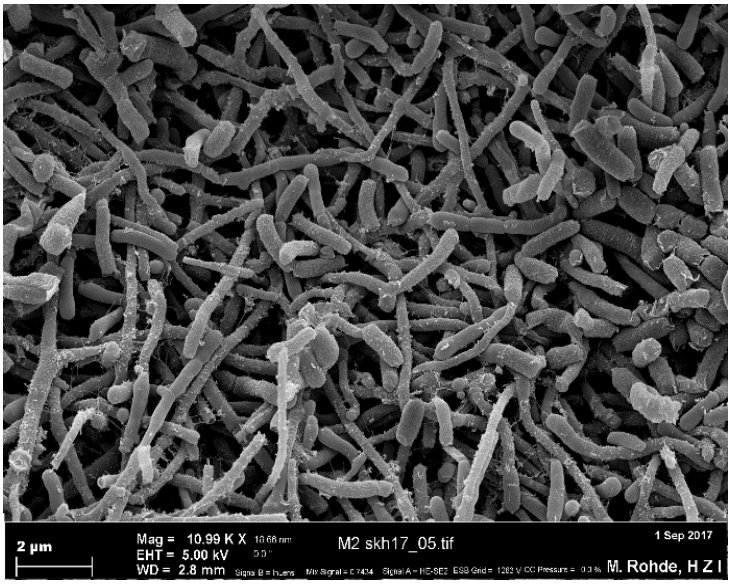

Figure 7. Scanning electron microscopy, a) strain M2^{T} b) strain M3.

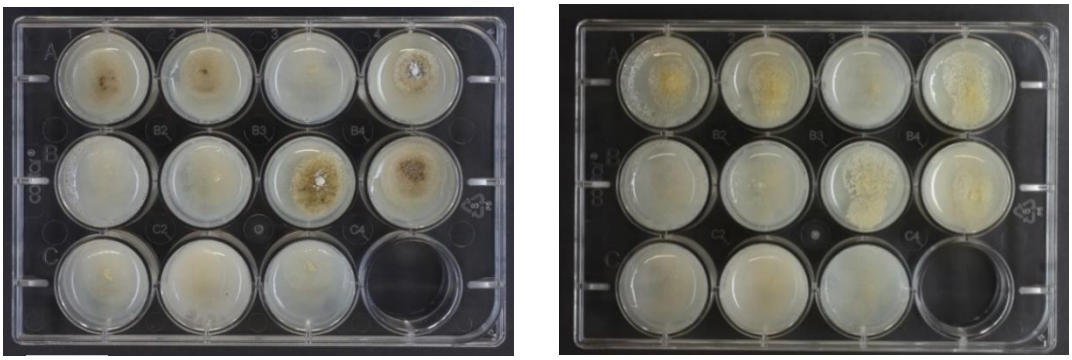

a b

Figure 8. Carbon utilization test results of strains M2^T and M3 in different single carbon sources. From top left to bottom right: glucose, arabinose, sucrose, xylose, inositol, mannose, fructose, rhamnose, raffinose, cellulose. a) Strain M2^T b) Strain M3.

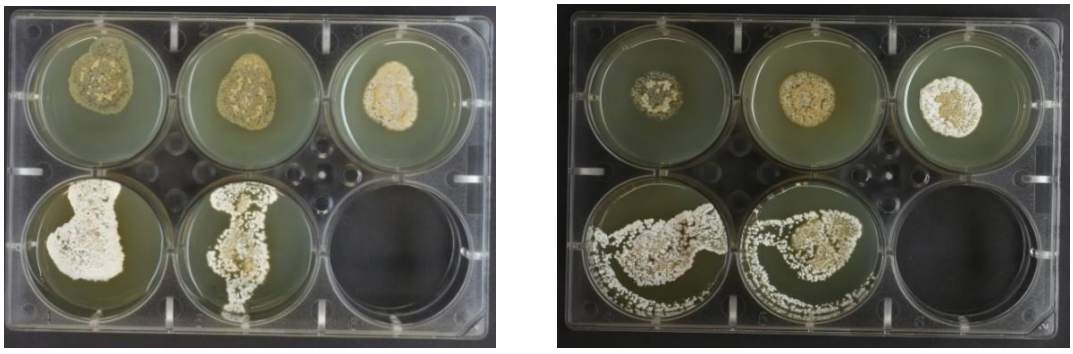

Figure 9. Sodium chloride tolerance test results of strains M2^T and M3. From top left to bottom right (0, 2.5, 5, 7.5, 10) % NaCl. The picture of the left side shows the growth of strain M2^T on all wells and right side the growth of strain M3.

3.2.2 Enzymatic activity via API® stripes

The strips of API ZYM and API coryne were evaluated after 24 h incubation at 30°C of both strains M2^T and M3 (Figure 10). With this test in triplicate, it was determined that both strains M2^T and M3 were positive for alkaline phosphatase, esterase (C4), esterase lipase (C8), leucine aryl amidase, valine aryl amidase, acidic phosphatase, naphthol-AS-BI- phosphohydrolase, α-galactosidase, α-glucosidase, glucosidase. Nevertheless, the color of the well was negative in both strains for lipase (C14), alpha mannosidase, α-fucosidase, pyrrolidonyl arylamidase, n-acetyl-beta glucoseamidase, pyrazinamidase, xylose fermentation, β-glucuronides, β-galactoronidase, mannitol, maltose, ribose fermentation, lactose fermentation, glucose fermentation, and sucrose fermentation (Figure 10) (Table 7)The physiological characteristic of enzyme activity basis on to API ZYM and API coryne for all species of genus *Streptomonospora* were analyzed (Table S 3).

A

B

Figure 10. API coryne and API ZYM test analysis of strain M2^T (a) and M3 (b).

Table 7. API ZYM and API Coryne test results of strains $M2^T$ and M3; + positive, - negative, w weak, v variable.

API ZYM	**$M2^T$**	**M3**	**API Coryne**	**$M2^T$**	**M3**
Phosphatase alkaline	+	+	nitrate reduction	-	-
Esterase (C4)	+	+	Pyraziamidase	-	-
Esterase Lipase (C8)	+	+	Pyrrolidonyl arylamidase	-	-
Lipase (C14)	-	-	Alkaline phosphatase	-	+
Leucin arylamidase	+	+	beta glucuronidase	-	-
Valine arylamidase	+	+	beta galactosidase	-	-
Cystine arylamidase	-	+	alpha glucosidase	+	+
Trypsin	-	+	N-acetyl-beta glucoseamidase	-	-
Chymotrypsin	-	+	Esculin (beta glucosidase)	+	+
Phosphatase acid	+	+	Urease	-	+
Naphthol-AS-BI-phosphohydrolase	+	+	Gelatin (hydrolysis)	+	+
alpha galactosidase	+	+	Glucose fermentation	-	-
beta galactosidase	-	-	Ribose fermentation	-	-
beta glucuronidase	-	-	Xylose fermentation	-	-
alpha glucosidase	+	+	Mannitol fermentation	-	-
beta glucosidase	+	+	Maltose fermentation	-	-
N- acetyl-beta-glucoseamidase	+	-	Lactose fermentation	-	-
alpha mannosidase	-	-	Sucrose fermentation	-	-
alpha fucosidase	-	-	Glycogen fermentation	-	-

3.2.3 Polysaccharides microarray

Both strains $M2^T$ and M3 showed the same pattern of degradation of polysaccharides. The results after week 1 to week 4 confirmed they were positive for hydrolyzing of pachyman laminarin, rhamnogalacturunan, pectin, xylose, arabinose xylose, hydroxyethyl-cellulose, barley-b-glucan, and gelatin. Both strains were negative for hydrolyzing amylose, pullulan, dextran, galectin, rhamnose, galactorunan, alpha-cellulose, beta-cellulose, chitosan, casein. The whole type species of the genus *Streptomonospora* were tested, and the results obviously showed that whole genus has potential for degradation of the polysaccharides xyloglucan and arabinan (Figure 11).

3.2.4 Chemotaxonomy

The result of diaminopimelic acid clearly showed in both isolates $M2^T$ and M3, DL-DAP was the main diaminopimelic acid in the cell wall (Figure 12 a). The cell wall sugars were ribose, mannose, and glucose (Figure 12 b). The polar lipids of both strains $M2^T$ and M3 were diphosphatidyl glycerol, phosphatidyl ethanolamine, phosphatidyl inositol, phosphatidylcholine, phosphatidylinositol mannosides, phosphatidyl glycerol, and glycolipids (Figure 13). The predominant fatty acids (>10%) of strain $M2^T$ were, iso-$C_{16:0}$ (33.1%), anteiso- $C_{17:0}$ (24.4%) and 10 methyl $C_{18:0}$ (13.6%) (Figure 14). The pattern of major fatty acids for strain M3 was similar, but the percentages of iso-$C_{16:0}$ with (45.74%), anteiso- $C_{17:0}$ with (12.78%) and 10 methyl $C_{18:0}$ with (11.94%). Quinone analysis revealed MK10 (H4), MK10 (H6), MK11 (H6), and MK11 (H8) as predominant quinones. Comparative profiles of physiological and cellular properties of both strains $M2^T$ and M3 in comparison with all members of genus *Streptomonospora* are shown in Table S 4.

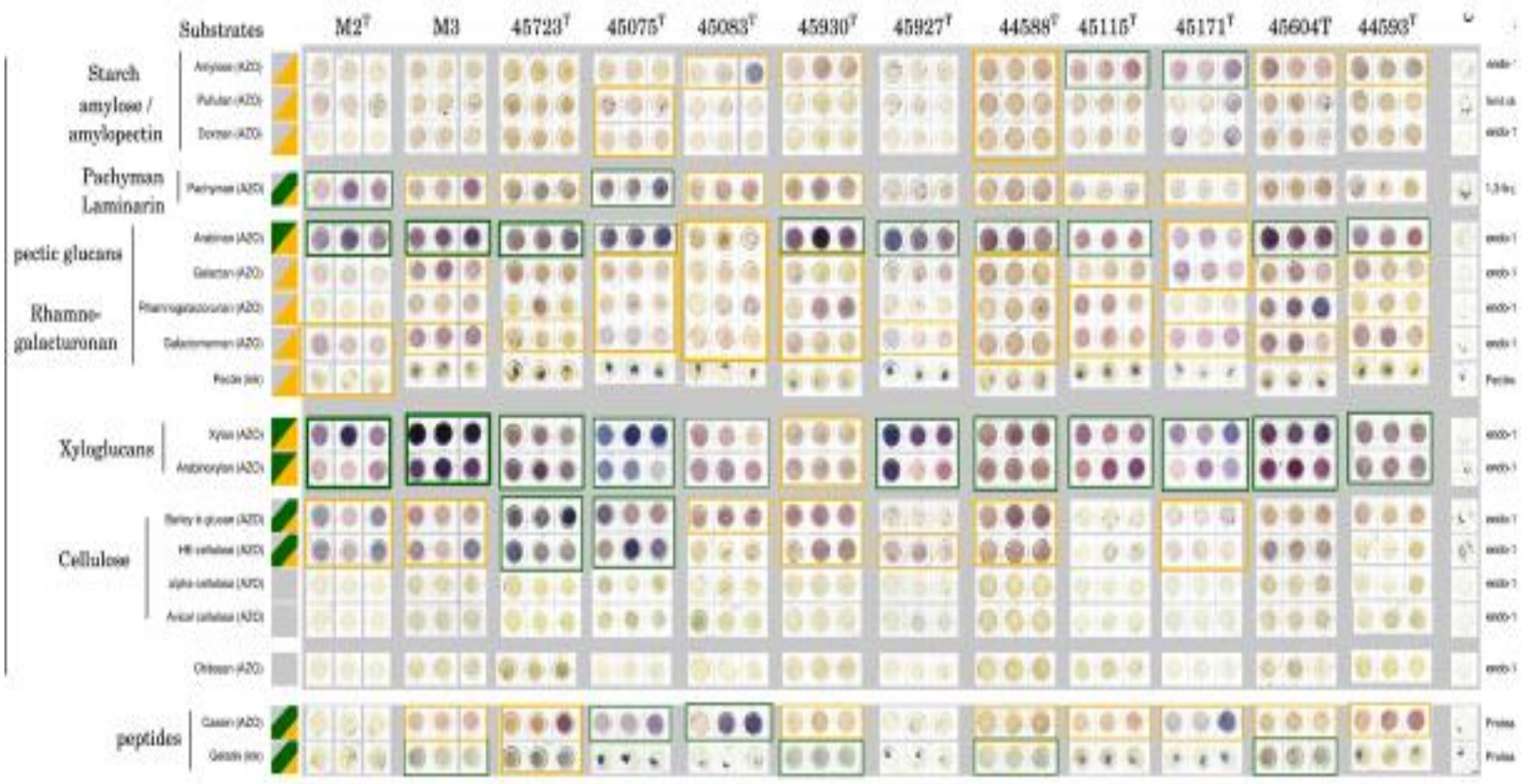

Figure 11 Hydrolysis of polysaccharides of all members of genus *Streptomonospora*. The green colure represents the strong activity, the yellow color for moderate activity and light grey for no activity.

a

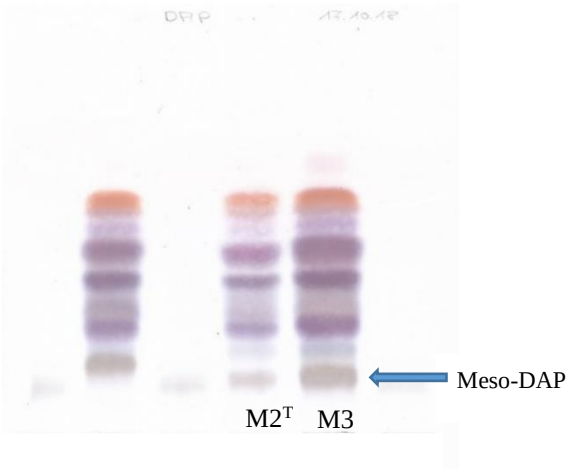

b

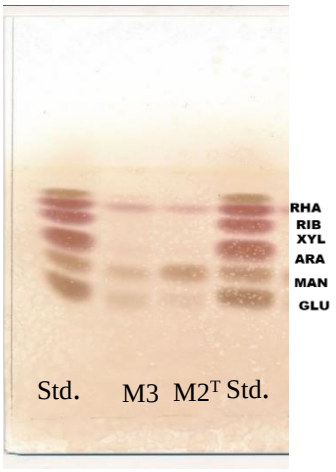

Figure 12. TLC chromatogram of whole cell sugars and analysis amino acids of the cell wall for both strains $M2^T$ and M3 a) DL- aminopimelic acid (meso- DAP) detected as the amino acid of cell wall b) The whole cell sugars in both strains were determined as glucose (GLU), mannose (MAN), arabinose (ARA), xylose (XYL), ribose (RIB), and rhamnose (RHA).

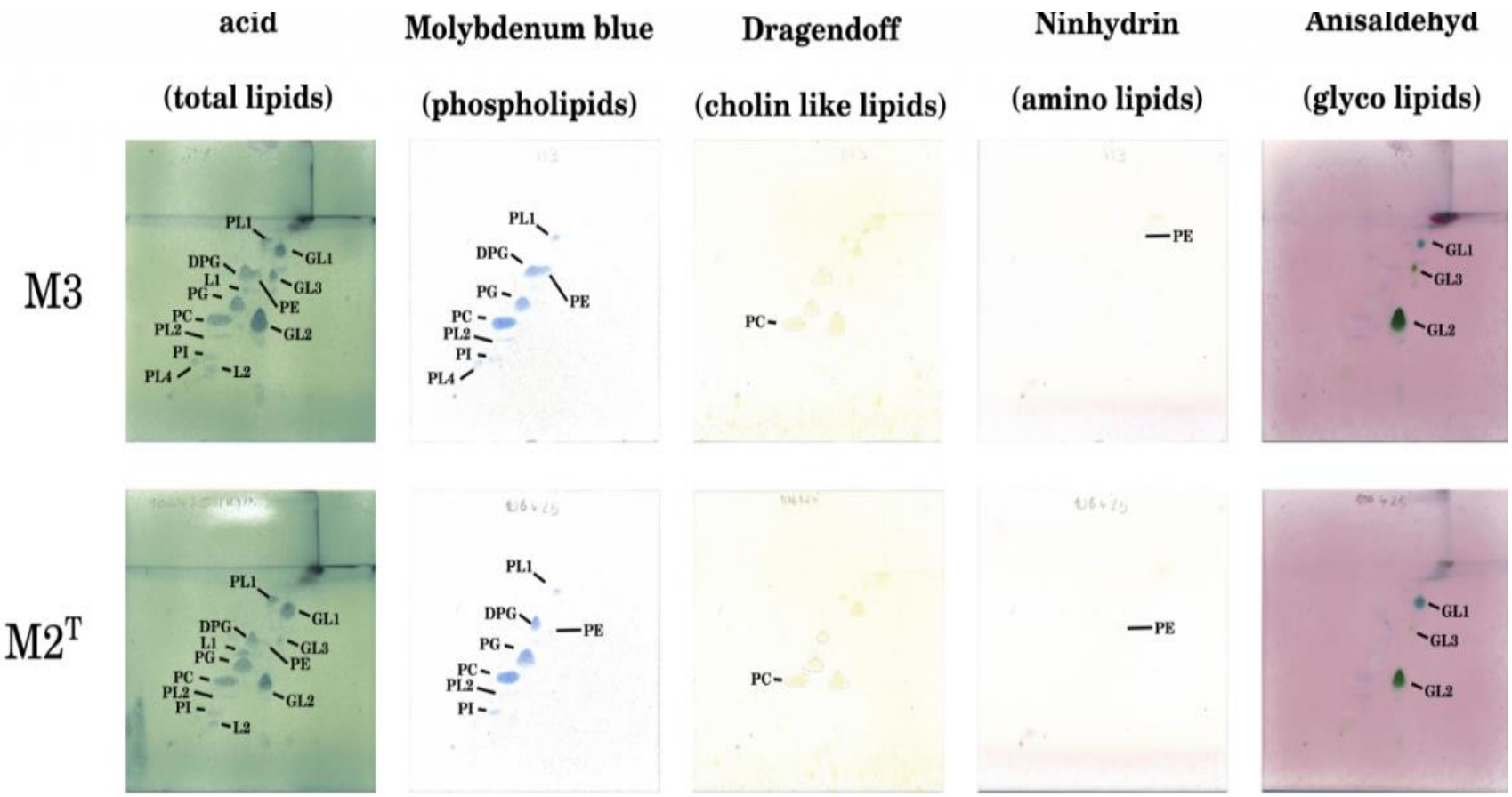

Figure 13. Polar lipid observed in strain $M2^T$ and strain M3 in five different TLC plates.

RT	Response	Ar/Ht	RFact	ECL	Peak Name	Percent	Comment1	Comment2	
1.624	3.649E+8	0.026	----	7.019	SOLVENT PEAK	----	< min rt		
2.925	324	0.024	1.245	9.604	10:0 ISO	0.29	ECL	Reference	
6.721	956	0.035	0.994	13.618	14:0 ISO	0.69	ECL deviates	Reference -0.004	
6.795	388	0.026	----	13.672		----			
8.203	957	0.043	0.960	14.624	15:0 ISO	0.66	ECL	Reference	
8.340	2758	0.041	0.957	14.713	15:0	1.91	ECL	Reference	
9.825	54242	0.041	0.935	15.627	16:0 ISO	36.59	ECL deviates	Reference -0.002	
10.145	439	0.030	0.931	15.819	16:1 CIS 9	0.29	ECL		
10.441	1069	0.039	0.927	15.997	16:0	0.72	ECL	Reference	
11.192	2906	0.039	0.920	16.430	16:0	1.93	ECL		
11.535	4237	0.051	0.918	16.628	17:0 ISO	2.81	ECL	Reference	
11.694	23628	0.044	0.917	16.721	17:0 ANTEISO	15.63	ECL deviates -	Reference -0.004	
11.819	741	0.042	0.916	16.792	17:1 CIS 9	0.49	ECL		
12.171	800	0.042	0.914	16.995	17:0	0.53	ECL deviates -	Reference -0.006	
12.350	443	0.039	----	17.097		----			
12.896	11100	0.045	0.910	17.406	17:0	7.29	ECL		
13.287	5067	0.043	0.908	17.627	18:0 ISO	3.32	ECL	Reference	
13.531	2683	0.043	0.908	17.766	18:1 CIS 9	1.76	ECL		
13.961	13525	0.085	0.907	18.009	18:0	8.85	ECL	Reference	
14.622	23654	0.046	0.906	18.385	TBSA 18:0 10METHYL	15.46	ECL deviates -		
14.855	573	0.035	----	18.517		----			
15.	1212	0.057	0.905	18.719	19:0 ANTEISO	0.79	ECL deviates -		

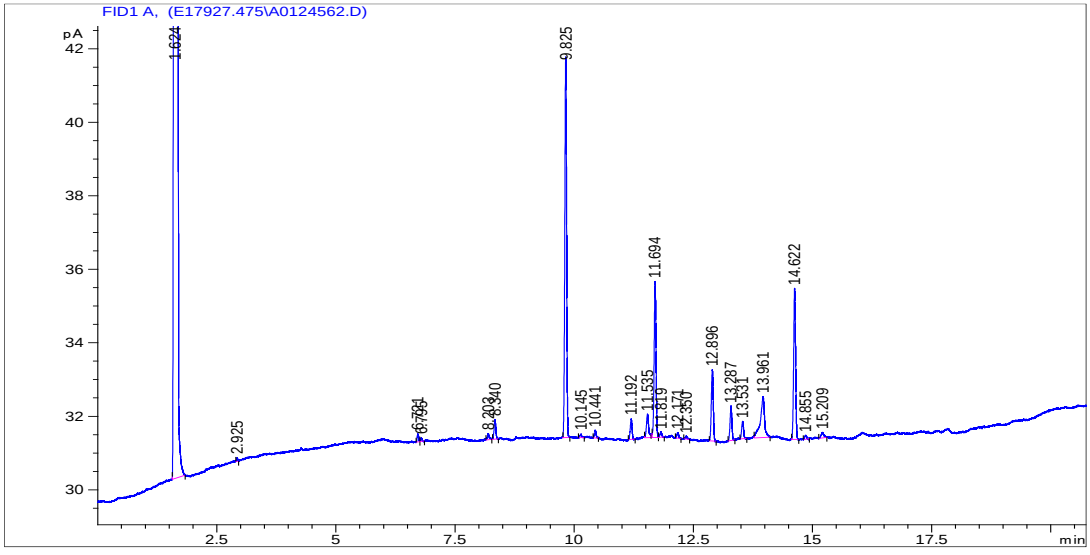

Figure 14. GC chromatogram of fatty acid analysis in strain M2^{T}.

3.2.5 Molecular analysis result

The comparison of the 16S rRNA sequences with EZbiocloud and NCBI database indicated that both strains M2^T and M3 belong to the genus *Streptomonospora.* They form a stable clade with the three validly named *Streptomonospora*, *Streptomonospora sediminis* DSM 45723^T, *Streptomonospora arabica* DSM 45083^T, and *Streptomonospora halophila* DSM 45075^T. The 16S rRNA similarity of M2^T and M3 with *Streptomonospora halophila* DSM 45075^T, *Streptomonospora arabica* DSM 45083^T and *Streptomonospora sediminis* DSM 45723^T were 97.85, 97.74, and 97.66% respectively. The 16S rRNA gene sequences for both strains M2^T and M3 were identical. This relation is shown in phylogenic tree generated with the Neighbour-joining method (Figure 15).

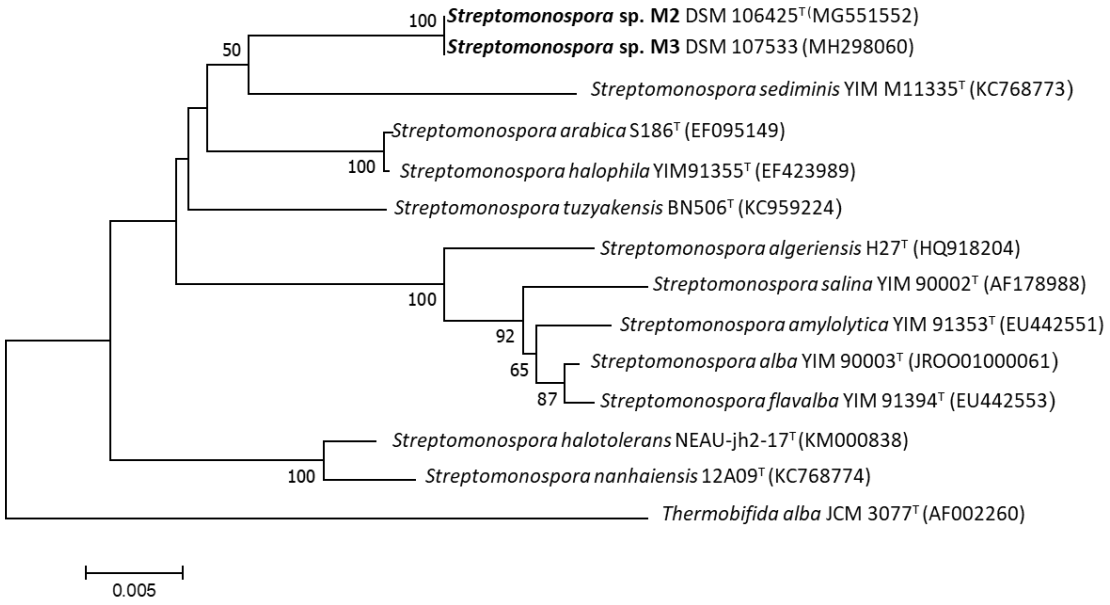

Figure 15. Neighbour-joining tree of both strains M2^T and M3 based on complete 16S rRNA gene sequences. It shows both strains M2^T and M3 belong to the *Streptomonospora* genus. The evolutionary distances were determined using the Tamura-Nei method[127]model. Numbers at the nodes are percentage bootstrap values based on a neighbor-joining analysis of 1,000 replicates, only values above 50 % are shown.

The level of DDH similarity between strain M2^T and *Streptomonospora halophila* DSM 45075^T, *Streptomonospora arabica* DSM 45083^T and *Streptomonospora sediminis* DSM 45723^T were 52.8/ 45.8, 44.4/39.2 and 21.3/38.9 respectively. The level of DDH similarity between M2^T and M3 was 65/69%.

The dendrogram based on MALDI-TOF mass spectra (Figure 16) shows that the spectra of strains M2^T and M3 differ from those of *Streptomonospora halophila* DSM 45075^T and other phylogenetically related actinomycetes.

The RiboPrinter dendrogram (Figure 17) shows that the patterns of both strains M2^T and M3 differ from one another and from the pattern of the closest related type strain *Streptomonospora halophila* DSM 45075^T.

The Chromosome is circuler with a size of 5,914,311 bp, G+C number of 4251521 (71.89%) and one plasmid is determined with 89,998 bp. The total gene number is 52391bp, from the entire genes, protein-coding genes with functional protein is 3904 bp, tRNA gene 57, RNA genes 68 and coding genes without function prediction is 1267 bp. The statistic attribute of gene with more details is summarized in the table (Table S 5). Based on the COGs function categories the distribution of genes is determined, see the details in (Table S 6).

The genome sequence of strain M2^T was analyzed for secondary metabolite biosynthesis gene clusters (BGCs) using the bioinformatic tool antiSMASH 5.0[128] which predicted 12 BGCs. Four of the BGCs matched with known clusters for isorenieratene[129], geosmin[130], ectoine[131], and SapB[132] with 100% similarity. Another two BGCs showed > 80% similarity to clusters encoding fusachelin[133] and radamycin/globimycin[133]. The remaining BGCs were predicted to encode three polyketides, one nonribosomal peptide, one lanthipeptide, and one ectoine (Figure S 1). Gene cluster region 4 detected by antiSMASH analysis harbors a predicted thiopeptide BGC (BGC4), which is expected to code for the thiopeptide biosynthesis (Figure S 1). BGC4 shows similarity to other known thiopeptide BGCs encoding radamycin/globimycin in *S. globisporus* subsp. *globisporus*, berninamycin A from in *S. bernensis*[134], and TP-1161 from a marine *Nocardiopsis* strains[135] (Figure S 2). BLASTP analysis additionally revealed high similarity of BGC4 to the recently published sulfomycin I BGC of *S. viridochromogenes*[136] (Figure S 3). Both BGCs only differ in the thiopeptide precursor encoding gene, whereby one gene (*sulA*) is present in the sulfomycin cluster of *S.*

viridochromogenes but two small open reading frames (ORFs) (*lit11, lit12*) are found within BGC4 of M2^T (Table S 7). *lit11* and *lit12* encoding the predicted precursor peptides Lit11 (51-aa) and Lit12 (50-aa), whereby Lit11 harbours a N-terminal 17-aa core peptide (CP) sequence consisting of the amino acid sequence pattern SCTTTGCTTSSSSSSSS and Lit12 a 16-aa CP sequence of SCVGCACTCSSTSSSS. The Lit11 CP sequence is 100% identical to the SulA CP sequence described for sulfomycin biosynthesis in *S. viridochromogenes*, suggesting that Lit11 encodes the sulfomycin I thiopeptide precursor in M2^T (Figure S 3). The Lit12 CP is highly similar to the CP sequence of WP_078651956.1 involved in radamycin biosynthesis in *S. globisporus* subsp. *globisporus* with a difference of only two amino acids (Figure S 3).

Due to the structural similarity of the litoralimycins with radamycin[137] it can be expected that Lit12 encodes the peptide precursor for litoralimycin biosynthesis in M2^T. The analysis of genome mining is accomplished by Prof. Dr. Yvonne Mast, Leibniz Institute DSMZ-Braunschweig.

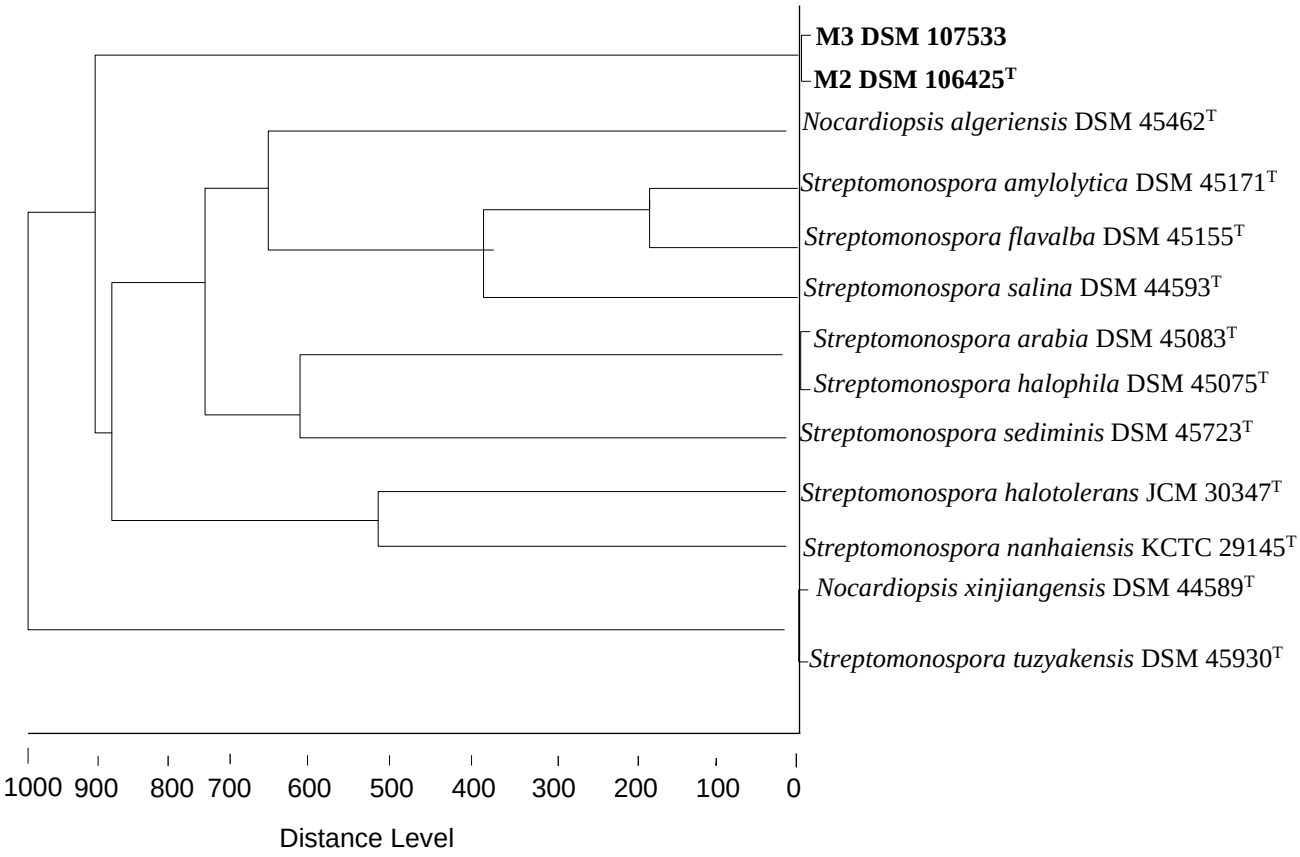

Figure 16. MALDI-TOF dendrogram of cell extracts of strains M2^T and M3.The tree shows the similarity of mass spectra of cell extracts of strains M2^T, M3 and of closely related type strains of the genera *Streptomonospora* and *Nocardiopsis*.

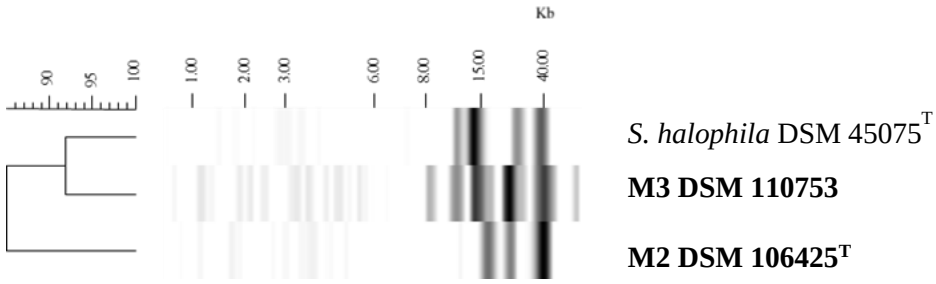

Figure 17. RiboPrinte patterns of strains M2^T, M3 and the closely related type strain *Streptomonospora halophila* DSM 45075^T.

3.3 Compound isolated from *Streptomonospora* sp. M2^T

The crude extracts of *Streptomonospora* sp. M2^T showed inhibitory activity against Gram-positive indicator organisms including *Micrococcus luteus*, *Staphylococcus aureus* and *Bacillus subtilis*. By a fractionation of the crude extracts in 96-well plates, it was possible to link the antibacterial activity to a region containing two major peaks (Figure 18). The chromtogram of crude extract is showen in (Figure 19). At the end, we isolated compounds **1** and **2** by preparative HPLC (Figure 20). This compounds were named Litoralimycins and were described in the recent publication[137].

Litoralimycin A (**1**) was isolated as a light-yellow oil. The molecular formula of $C_{48}H_{45}N_{15}O_{10}S_4$ was derived from its high-resolution electrospray ionization mass spectrometry (HRESIMS) peak observed at *m/z* 1120.2429 (Figure S 5). Litoralimycin **2** gave a molecular formula of $C_{45}H_{42}N_{14}O_9S_4$, implying the formal loss of a C_3H_3NO fragment compared to Litoralimycin **1**, with the molecular mass of: *m/z* 1051.2219 $[M+H]^+$ (Figure S 6). After ozonolysis, hydrolyzation and derivatization with FDAA, we detected l-Val and l-Ala according to Marfey's method (Figure S 7). Compound 1 showed the toxicity against all different test cell lines while compound 2 showed a weak activity just versus cell line 929 (Table 8). Both compounds 1 and 2 showed the activity versus Gram-positive bacteria such as *Bacillus subtilis* and *Staphylococcus aureus* with 66.8 ug/ml (Table 9). Furthermore, compound 1 showed the significant activity versus *Legionella pneumophila* (Figure 21). The crude extract of strain M2^T showed no antiviral activity against Hepatitis C virus (Figure 22).

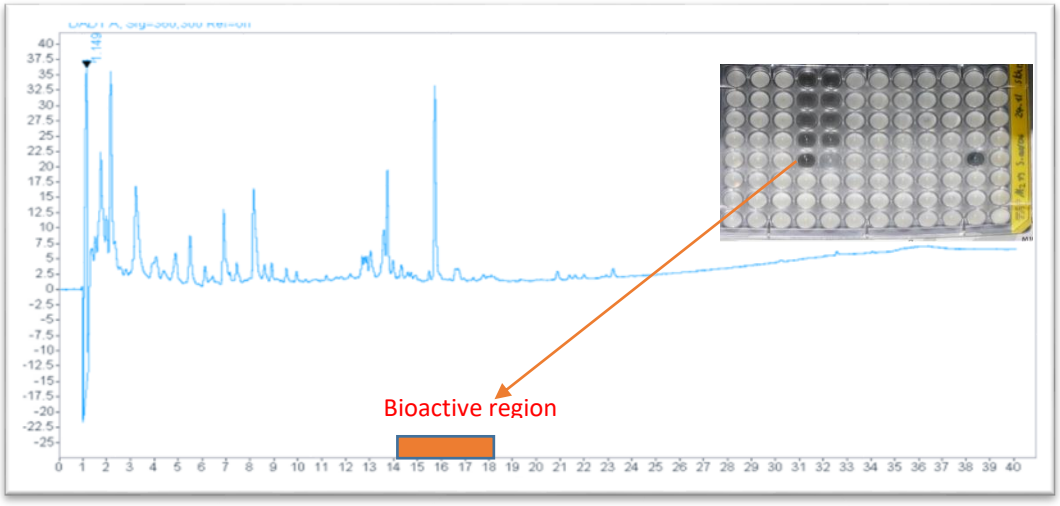

Figure 18. Fractionation analysis of *Streptomonospora* M2^T crude extract. By fractionation of 5µl *Streptomonospora* sp. M2^T raw extract (100x concentrated in methanol compared to culture volume) the reproducible growth inhibition of test organism *Staphylococcus aureus* was caused in wells D5 until E4, which had been collected from 13.5 to 17 minutes by HPLC fractionation.

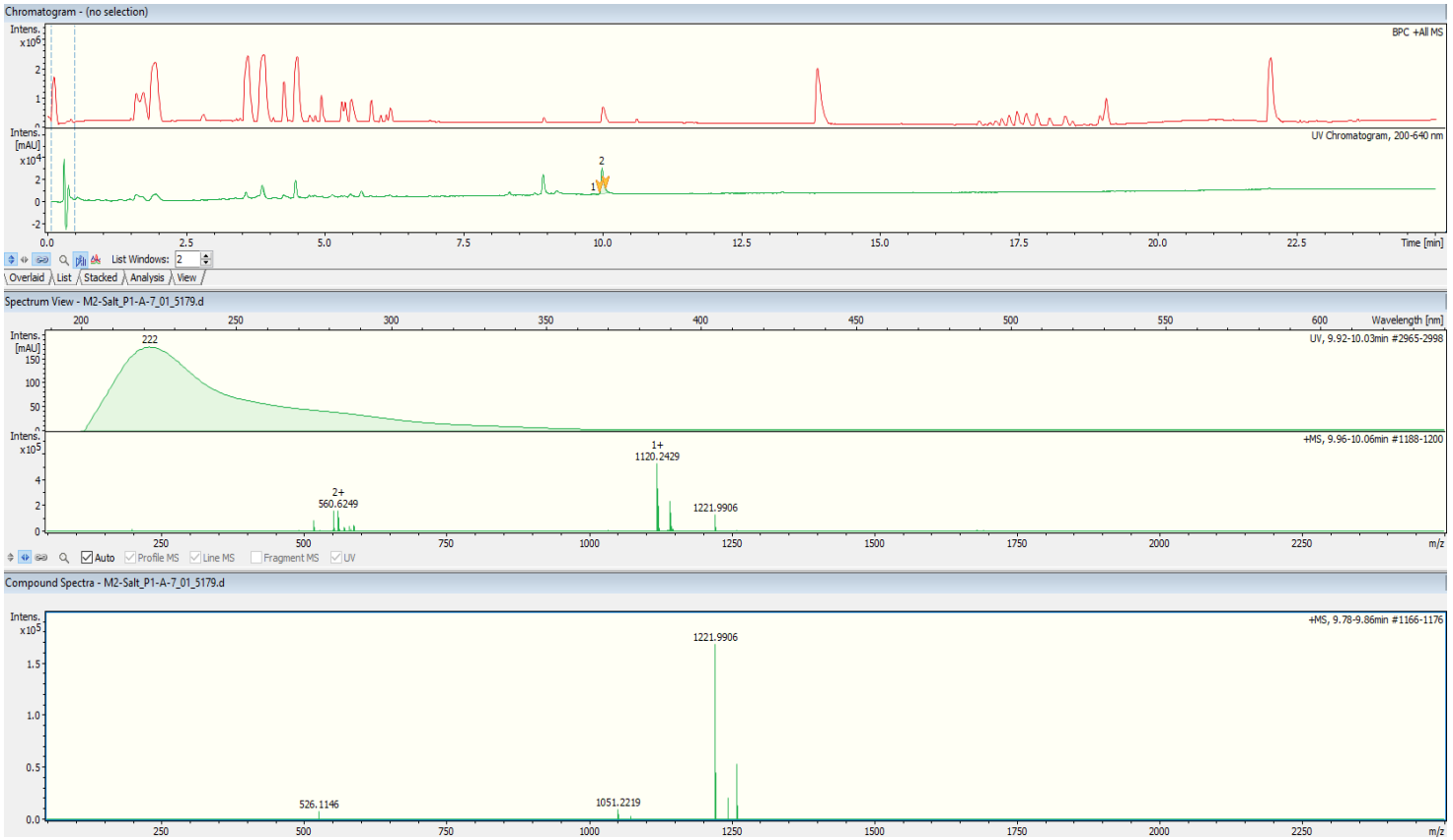

Figure 19. HPLC-MS (base peak) and UV/Vis (200-640nm) chromatograms of a crude extract of *Streptomonospora* sp. M2^{T}.

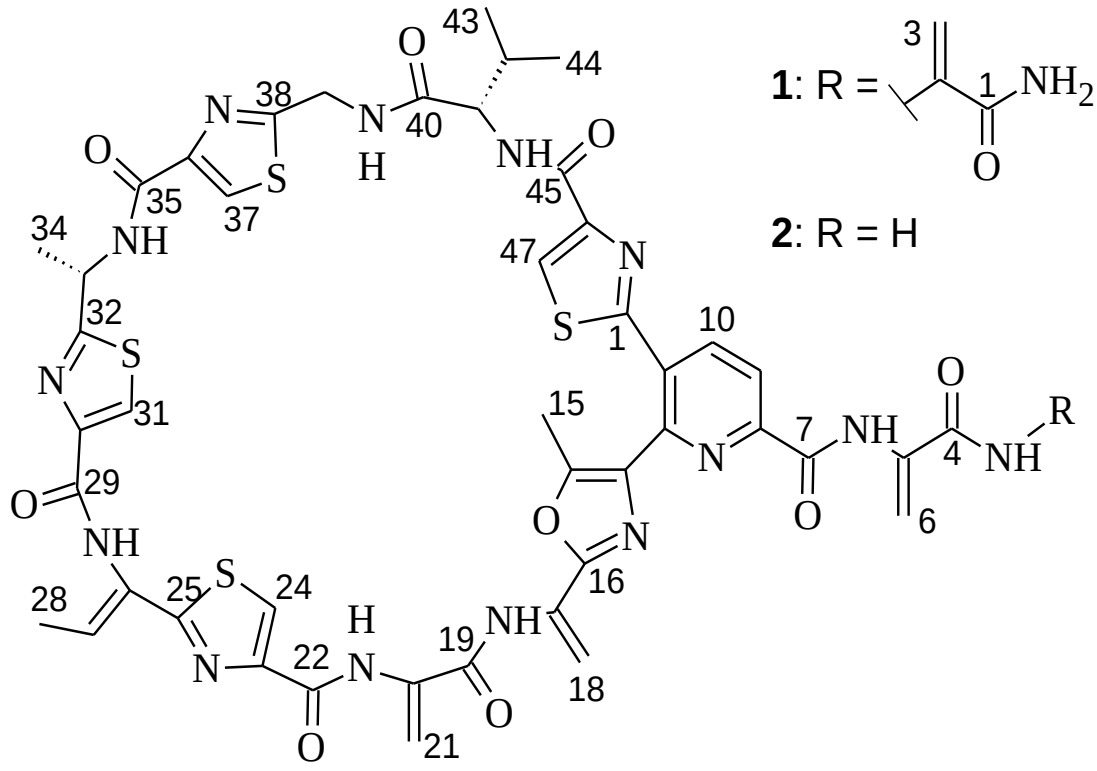

Figure 20. Chemical structure of compounds 1 and 2.

Table 8. Toxicity test results of pure compounds 1 and 2 isolated from strain M2^T against different cell lines. n.t. means not tested.

Compound	**L929**	**KB3.1**	**MCF-7**	**SKOV-3**	**A431**	**PC-3**
1	2.9	2.6	1.0	28	0.8	31
2	24.0	/	n.t.[1]	n.t.	n.t	n.t
epothilon B	0.00082	0.000065	0.000048	0.000095	0.000045	0.0001

Table 9. Antimicrobial activity of compounds 1 and 2 isolated from strain M2^T.

n.i: no inhibition, T: Tetracycline, G: Gentamycin, N: Nystatin, K: Kanamycin.

Test organisms	**compound 1**	**comound 2**	**Ref G-K-N-T**
Bacillus subtilis DSM10^T	66.7	66.7	16.6 T
Staphylococcus aureus Newman	66.7	66.7	1.02 G
Escherichia coli WT BW25113	n.i	n.i	1.02 G
Escherichia coli acrB JW0451-2	n.i	n.i	1.02 G
Pseudomonas aeruginosa PA14	n.i	n.i	1.2 G
Acinetobacter baumannii DSM 24110^T	n.i	n.i	1.2 G
Citrobacter freundii DSM 30039^T	n.i	n.i	1.02 G
Mycobact semegmatic ATCC700084	n.i	n.i	4.1 K
Mucor himalis DSM 2656^T	n.i	n.i	16.6 N
Candida albicans DSM1665^T	n.i	n.i	33.35 N
Pichia anomala DSM6766^T	n.i	n.i	33.35 N

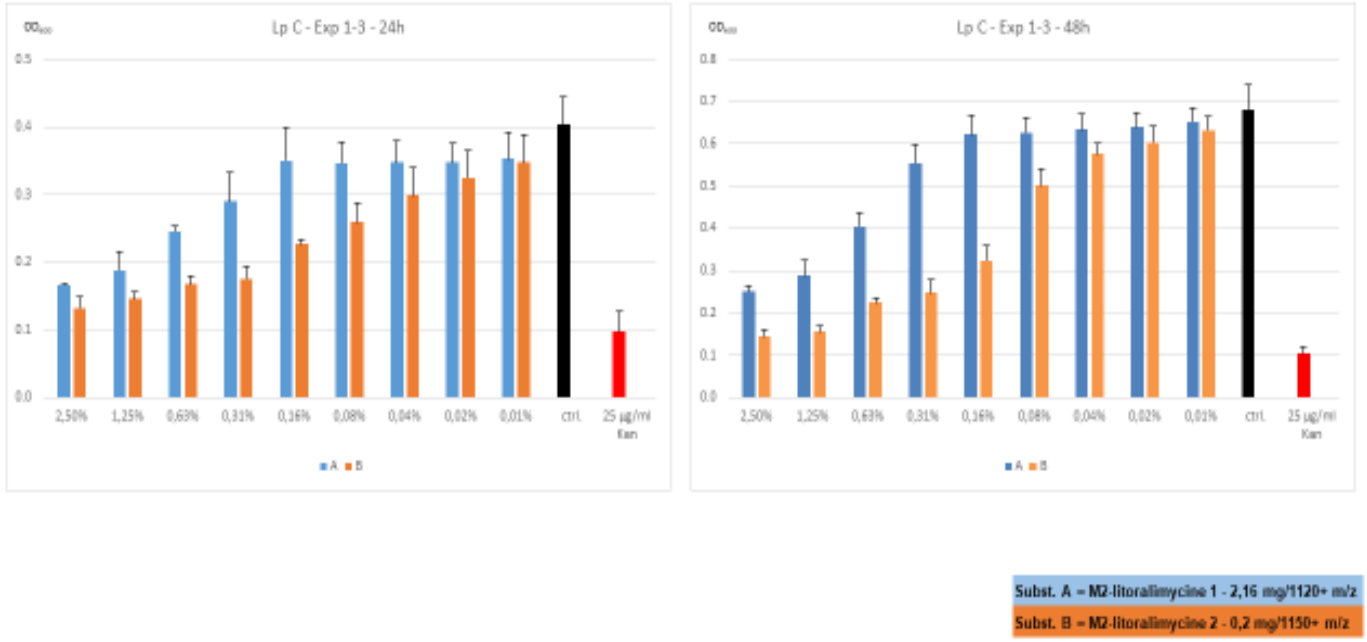

Figure 21. Graph of antibacterial activity of compound 1 and compound 2 against *Legionella pneumophila.*

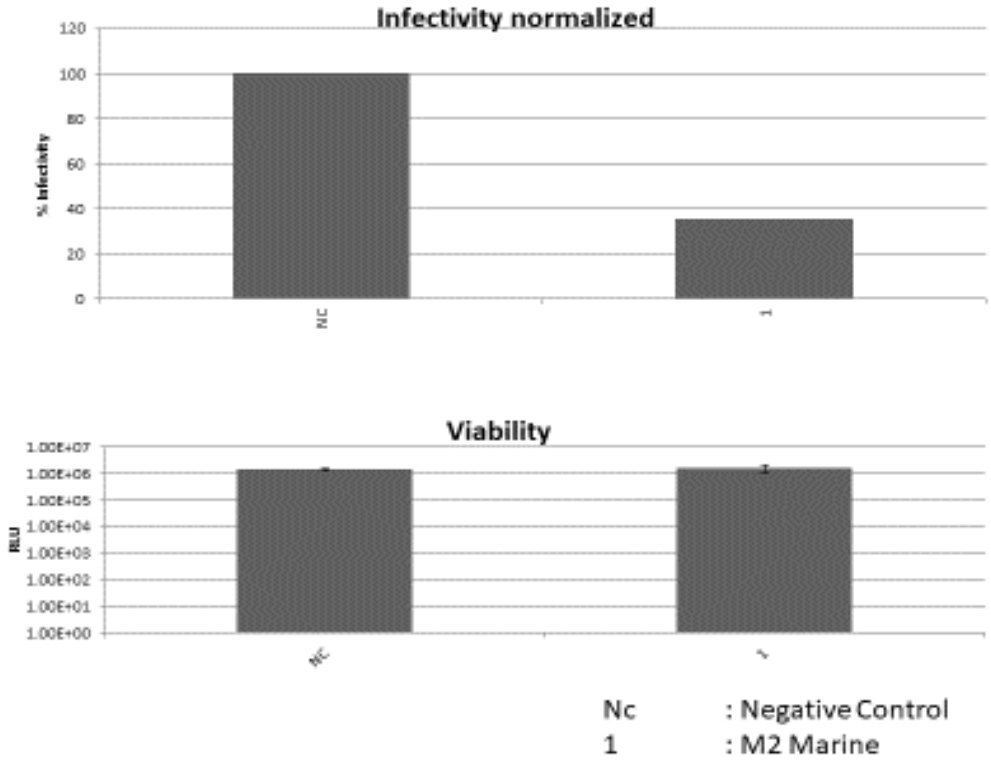

Figure 22. Chart of antiviral activity of crude extract of strain $M2^T$ against Hepatitis C virus.

3.4 Polyphasic taxonomy for *Streptomyces* sp. 86D

3.4.1 Morphological characterization

Strain 86D was isolated from Lavasan/ Tehran/ Iran. Strain 86D could grow well on GYM and all ISP media (ISP2-ISP7) after 2 weeks. Aerial mycelium was observed in cream white color on ISP3 and grey color on ISP5, but no aerial mycelium was found on other ISP media. The colony colors varied from maize yellow to light ivory (Table 10). The morphology of the strain in GYM and ISP 3 media was shown in Figure 23. Scanning electron microscopy, after 14 days of growth on ISP3, showed long spore chain with smooth surface (Figure 24).

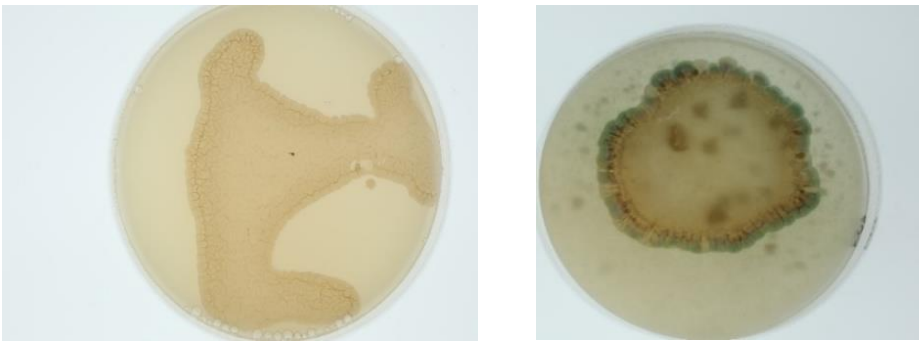

Figure 23. Morphology of *Streptomyces* sp. 86D on GYM (left) and ISP3 (right).

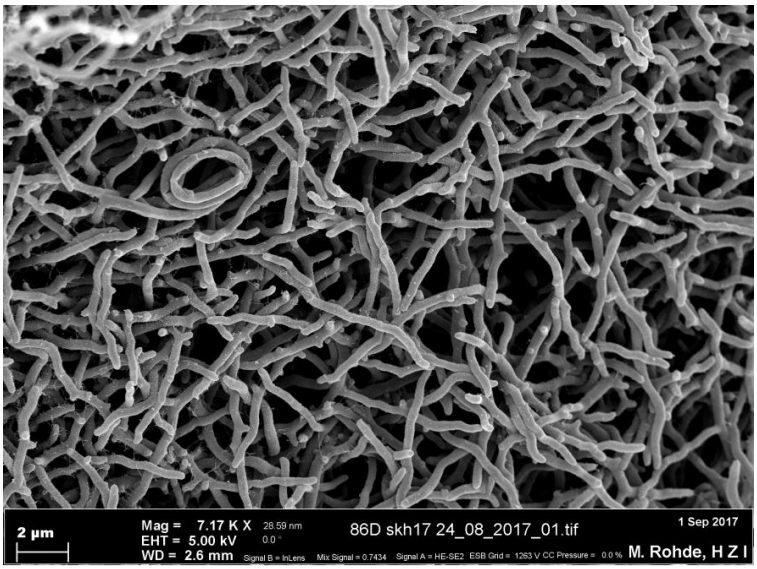

Figure 24. Scanning electron micrographs of aerial mycelium and spores of strain 86D after incubation on ISP3 agar at 30°C for 14 days.

3.4.2 Physiological and biochemical characteristic

Streptomyces sp. 86D could grow at 25-37°C (optimum 30°C) and at pH of 6-9 (optimum pH 7). The strain was also able to grow in the range of 0- 2.5% NaCl. Strain 86D utilized different carbohydrates such as glucose, arabinose, sucrose, xylose, inositol, mannose, fructose, rhamnose, raffinose as the source of carbon. The results from API ZYM determined the high enzyme activities for hydrolyzing phosphatase alkaline, esterase (C4), esterase lipase (C8), leucine arylamidase, valine arylamidase, alpha-glucosidase, n-acetyl-beta-glucoseamidase, lipase (C14), cysteine arylamidase, phosphatase acid, naphthol-AS-BI-phosphohydrolase, beta-galactosidase, and beta-glucosidase; nevertheless, it had weak activity for chymotrypsin and no enzyme activity was detected for beta glucuronidase. API Coryne tests showed the positive activity for pyrrolidonyl arylamidase, alkaline phosphatase, alpha glucosidase, n-acetyl-beta-glucoseamidase, esculin (beta-glucosidase), urease, and gelatinase (Table 11). The enzyme activities of strain 86D in compare with closest species including *Streptomyces violaceus*, *Streptomyces roseoviolaceus,* and *Streptomyces spiralis* were shown in Table S 8.

3.4.3 Results of Chemotaxonomy for *Streptomyces* sp. 86D

The whole cell sugars contained galactose, glucose, ribose mannose (Figure 25a). LL- diaminopimelic acid was detected as a major diamino acid in the cell wall (Figure 25b). The phospholipids observed were diphosphatidylglycerol (DPG), phosphatidylethanolamine (PE), phosphatidylinositol (PI), phosphatidyl-myo-inositol mannosides (PIMs) (Figure 26). The composition of menaquinones of whole cells of strain 86D as MK-9 (H_8), MK-9(H_6), MK-9 (H2), MK-9, MK-9 (H_4) with (50:46:2:1:1) respectively (Figure 27).The predominant methyl ester fatty acids were determined as *iso*-$C_{14:0}$ (9.40%), *iso*-$C_{15:0}$ (14.13%), *anteiso*- $C_{15:0}$ (17.59%), *iso*-$C_{16:0}$ (19.82%), $C_{16:0}$ (19.89%) (Figure 28).

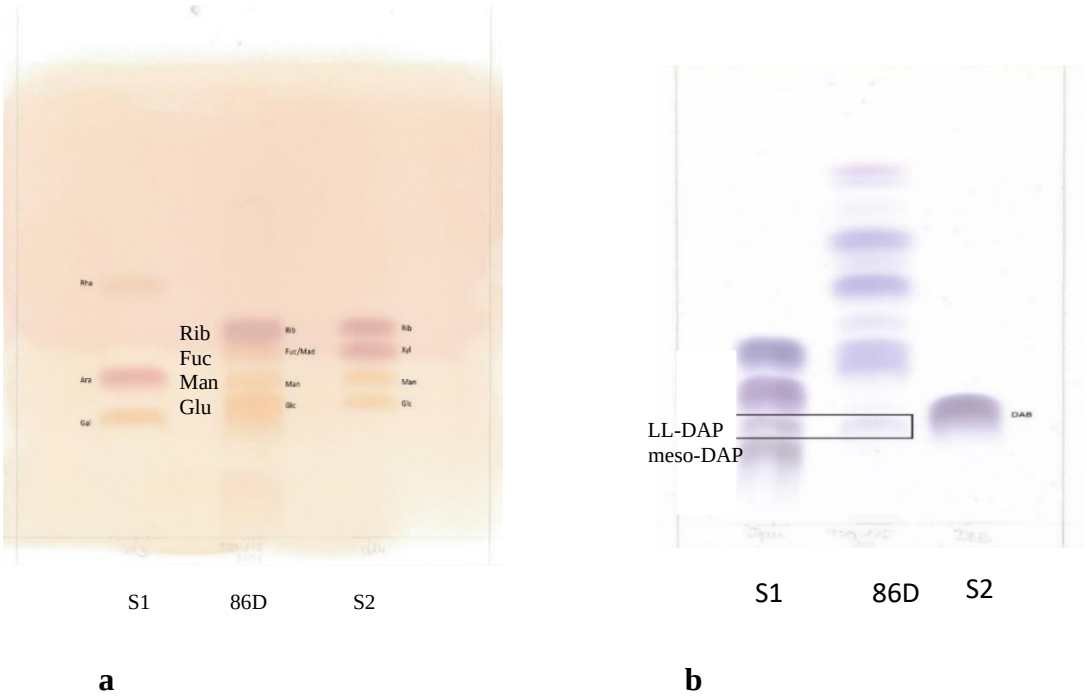

Figure 25. Whole-cell sugars and amino acids observed in strain 86D. a) ribose (Rib), fucose (Fuc), glucose (Glu) and mannose (Man) detected as a whole cell sugar; LL- diaminopimelic acid detected as a cell wall amino acid. S1: Standard 1; S2: Standard 2.

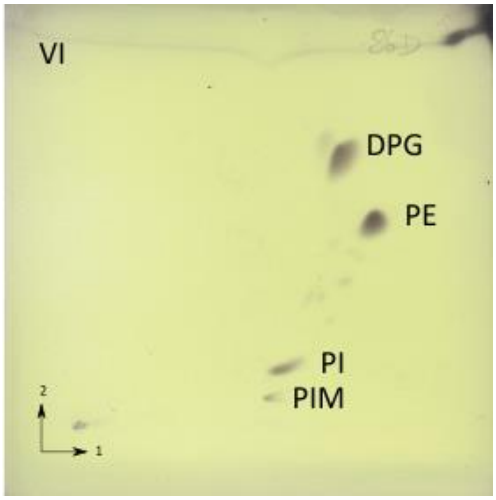

Figure 26. Polar lipids observed in *Streptomyces* sp. 86D. Diphosphatidylglycerol (DPG), phosphatidylethanolamine (PE), phosphatidylinositol (PI), phosphatidylinositol mannosides (PIMs).

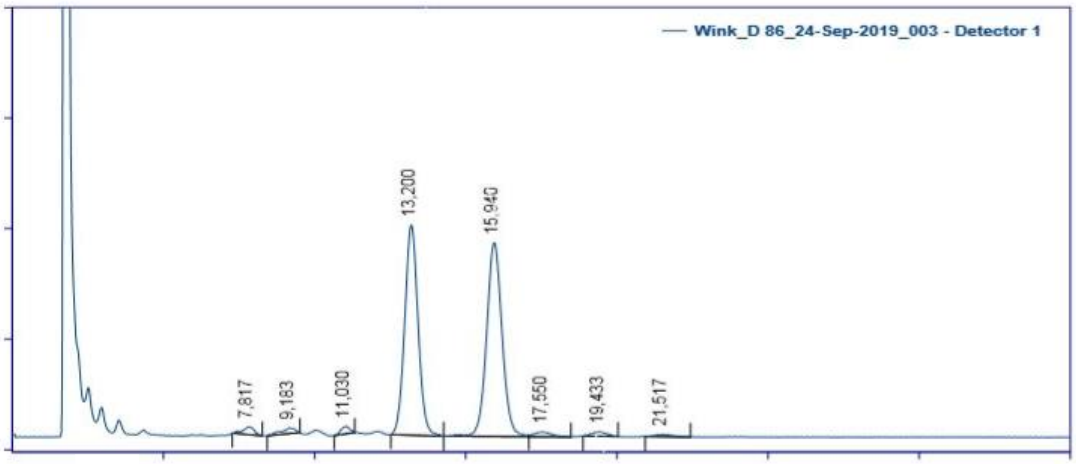

A

Result Table (Uncal - Wink_D 86_24-Sep-2019_003 - Detector 1)

	Reten. Time [min]	Area [mV.s]	Height [mV]	Area [%]	Height [%]	W05 [min]
1	7,817	9,446	0,354	1,5	1,8	0,42
2	9,183	8,122	0,258	1,3	1,3	0,41
3	11,030	6,778	0,342	1,0	1,7	0,35
4	13,200	291,849	9,506	45,0	48,1	0,47
5	15,940	312,119	8,763	48,1	44,3	0,54
6	17,550	8,816	0,224	1,4	1,1	0,65
7	19,433	6,973	0,201	1,1	1,0	0,60
8	21,517	4,463	0,111	0,7	0,6	0,55
	Total	648,567	19,759	100,0	100,0	

B

Figure 27. Menaquinones detected in strain 86D. A) Chromatogram from LC-MS of detected menaquinones; B) Retention time and area of detected menaquinones.

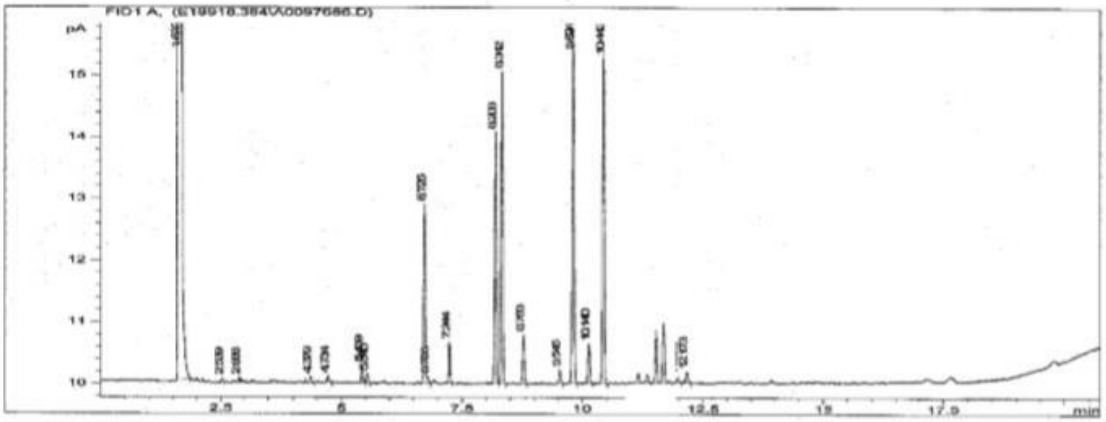

RT	Response	Ar/Ht	RFact	ECL	Peak Name	Pt	Comment1	Comment2
1.633	3.654E+8	0.026	----	7.012	SOLVENT PEAK		< min rt	
2.539	184	0.020	----	8.820			< min rt	
2.888	256	0.025	1.234	9.515	unknown 9.521		ECL deviates -0.006	
4.379	683	0.046	1.086	11.610	12:0 ISO		ECL deviates 0.002	Reference 0.001
4.734	521	0.034	1.064	11.998	12:0		ECL deviates -0.002	Reference -0.003
5.439	1196	0.032	1.034	12.613	13:0 ISO		ECL deviates 0.001	Reference 0.000
5.540	665	0.032	1.030	12.701	13:0 ANTEISO		ECL deviates 0.000	Reference -0.001
6.725	12849	0.035	0.992	13.618	14:0 ISO		ECL deviates 0.000	Reference -0.001
6.798	496	0.033	----	13.671				
7.244	3162	0.037	0.979	13.998	14:0		ECL deviates -0.002	Reference -0.003
8.203	19952	0.039	0.961	14.622	15:0 ISO		ECL deviates 0.001	Reference 0.000
8.342	24895	0.039	0.959	14.713	15:0 ANTEISO		ECL deviates 0.002	Reference 0.001
8.783	3859	0.039	0.951	15.000	15:0		ECL deviates 0.000	Reference -0.001
9.545	1099	0.038	0.941	15.459	16:1 ISO H		ECL deviates -0.002	
9.824	28663	0.042	0.938	15.626	16:0 ISO		ECL deviates 0.000	Reference -0.001
10.140	3334	0.042	0.935	15.817	16:1 CIS 9		ECL deviates 0.000	
10.443	28963	0.042	0.932	15.999	16:0		ECL deviates -0.001	Reference -0.003
11.169	852	0.042	0.926	16.419	16:0 9? METHYL		ECL deviates 0.003	
11.349	797	0.037	0.925	16.523	17:1 ANTEISO C		ECL deviates -0.002	
11.533	4584	0.043	0.923	16.630	17:0 ISO		ECL deviates 0.001	Reference -0.002
11.694	5214	0.041	0.922	16.723	17:0 ANTEISO		ECL deviates 0.001	Reference -0.002
11.978	423	0.037	0.921	16.887	17:0 CYCLO		ECL deviates -0.001	Reference -0.004
12.173	1013	0.047	0.920	17.000	17:0		ECL deviates 0.000	Reference -0.004

Figure 28. GC chromatogram of fatty acid analysis of strain 86D.

Table 10**.** Morphology of *Streptomyces* sp. 86 D on ISP and Sutter synthetic media+/- tyrosine. No: not produced.

Medium	**characterization**	***Streptomyces sp.* 86D**
Isp2	Substrate mycelium	Maize yellow
	Aerial mycelium	No
	Soluble pigments	Ochre yellow
ISP3	Substrate mycelium	Sepia brown and Green
	Aerial mycelium	Signal white
	Soluble pigments	Pare brown
ISP4	Substrate mycelium	Beige
	Aerial mycelium	No
	Soluble pigments	Light ivory
ISP5	Substrate mycelium	Light ivory
	Aerial mycelium	white
	Soluble pigments	Grey
ISP 6	Substrate mycelium	Sand yellow
	Aerial mycelium	No
	Soluble pigments	No
ISP7	Substrate mycelium	Ivory
	Aerial mycelium	No

	Soluble pigments	Ochre yellow
	Substrate mycelium	Ochre yellow
SSM+T	Aerial mycelium	No
	Soluble pigments	Sand yellow
	Substrate mycelium	Sand yellow
SSM-T	Aerial mycelium	No
	Soluble pigments	Ivory

Table 11. API ZYM and API Coryne results of *Streptomyces* sp. 86D. + positive, - negative, (+) weak positive.

***Streptomyces* sp. 86D**			
API ZYM	activity	**API Coryne**	activity
Phosphatase alkaline	+	Nitrate reduction	-
Esterase (C4)	+	Pyrazinamidase	-
Esterase Lipase (C8)	+	Pyrrolidonyl arylamidase	+
Lipase (C14)	-	Alkaline phosphatase	+
Leucin arylamidase	+	beta glucuronidase	-
Valine arylamidase	+	beta galactosidase	+
Cystine arylamidase	(+)	alpha glucosidase	+
Trypsin	(+)	N-acetyl-beta glucoseamidase	-
Chymotrypsin	-	Esculin (beta glucosidase)	+
Phosphatase acid	+	Urease	(+)
Naphthol-AS-BI-phosphohydrolase	+	Gelatin (hydrolysis)	+
alpha galactosidase	(+)	Glucose fermentation	-
beta galactosidase	+	Ribose fermentation	-
beta glucuronidase	-	Xylose fermentation	-
alpha glucosidase	+	Mannitol fermentation	-
beta glucosidase	+	Maltose fermentation	-

N- acetyl-beta-glucoseamidase	+	Lactose fermentation	-
alpha mannosidase	+	Sucrose fermentation	-
alpha fucosidase	(+)	Glycogen fermentation	-

3.4.4 Molecular analysis

Based on 16S rRNA gene sequences blasting in the EZBioCloud, strain 86D belongs to the genus *Streptomyces* and the highly comparable strains were determined as *Streptomyces violaceus* DSM 44391^T (98.44%), *Streptomyces roseoviolaceus* DSM 44631^T (98.44%), and *Streptomyces spiralis* DSM 44106^T (98.36%). The phylogenic tree by neighbor joining supported the stable clade of strain 86D within the genus *Streptomyces*. The bootstrap value of 100% was applied (Figure 29). This affiliation was also confirmed by maximum-likelihood algorithm. The level of relatedness of DNA-DNA hybridization between strains 86D, *Streptomyces roseoviolaceus* DSM 44631^T and *Streptomyces violaceus* DSM44391^T were 52.1 and 63.8/42.4 respectively. The result of the dendrogram based on the MALDI-TOF mass spectra also supported the previous result that strain 86D belongs to the genus *Streptomyces* and the most related species detected were *Streptomyces violaceus* DSM44391^T, *Streptomyces roseoviolaceus* DSM 44631^T,and *Streptomyces spiralis* DSM 44106^T (Figure 30). The complete genome sequencing of the strain was performed at GMAK group at HZI Braunschweig. The whole amount of G+C content was 69.9%. Entire genome include 77 contigs, 10,851,282 bases, 959 CDS, 9700 genes, 24 misc_ RNA, 4 rRNA, 885-sig_peptide, 76 tRNA and 1mRNA.

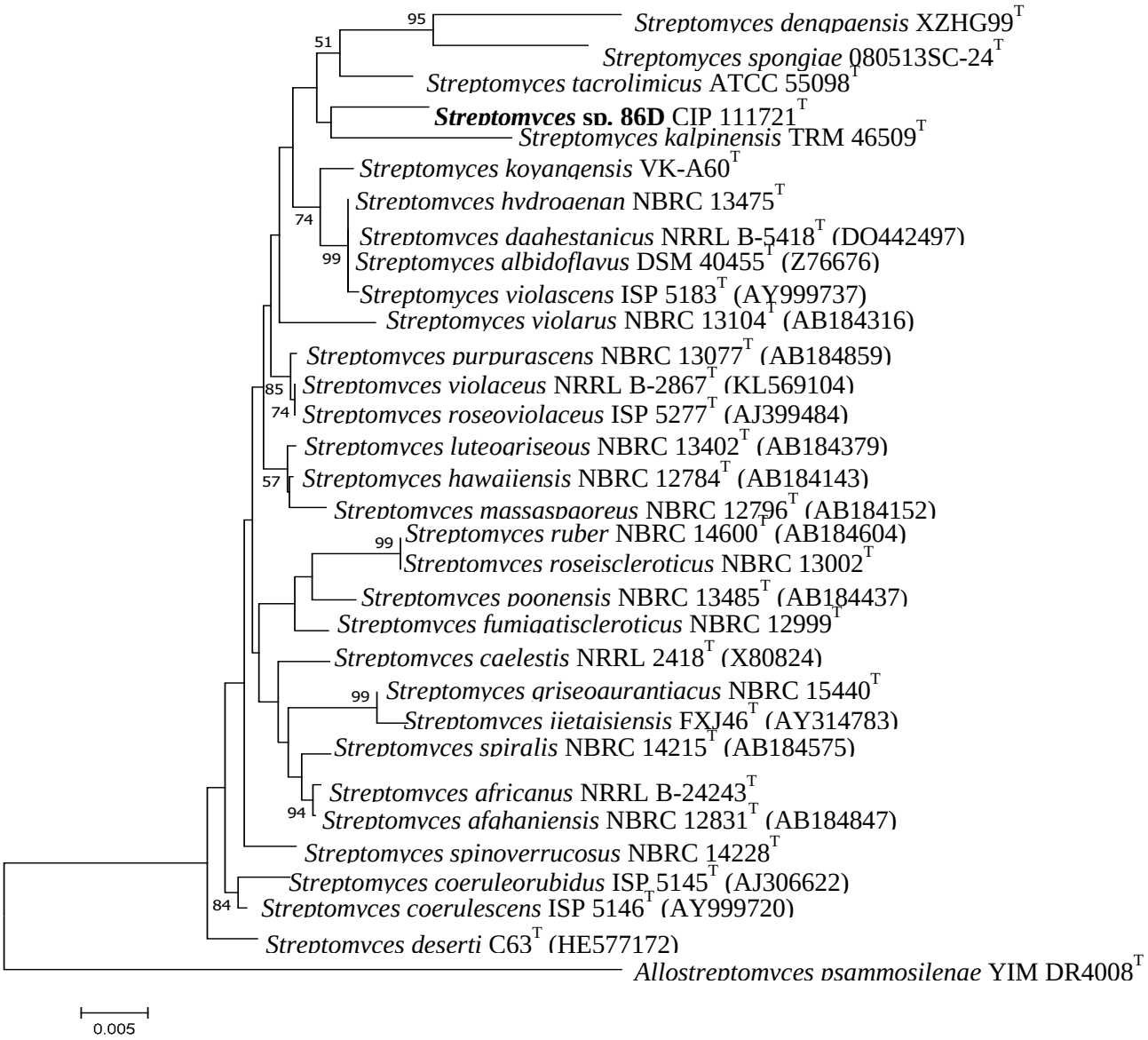

Figure 29. Neighbour-joining tree based on 16S rRNA (1496 bp) gene sequence of *Streptomyces* sp. 86D and related type strains. The corresponding algorithms were achieved using the mega 7.0, with 1000 replicates. Only values above 50% are indicated. Bar, 0.005 substitutions per nucleotide position.

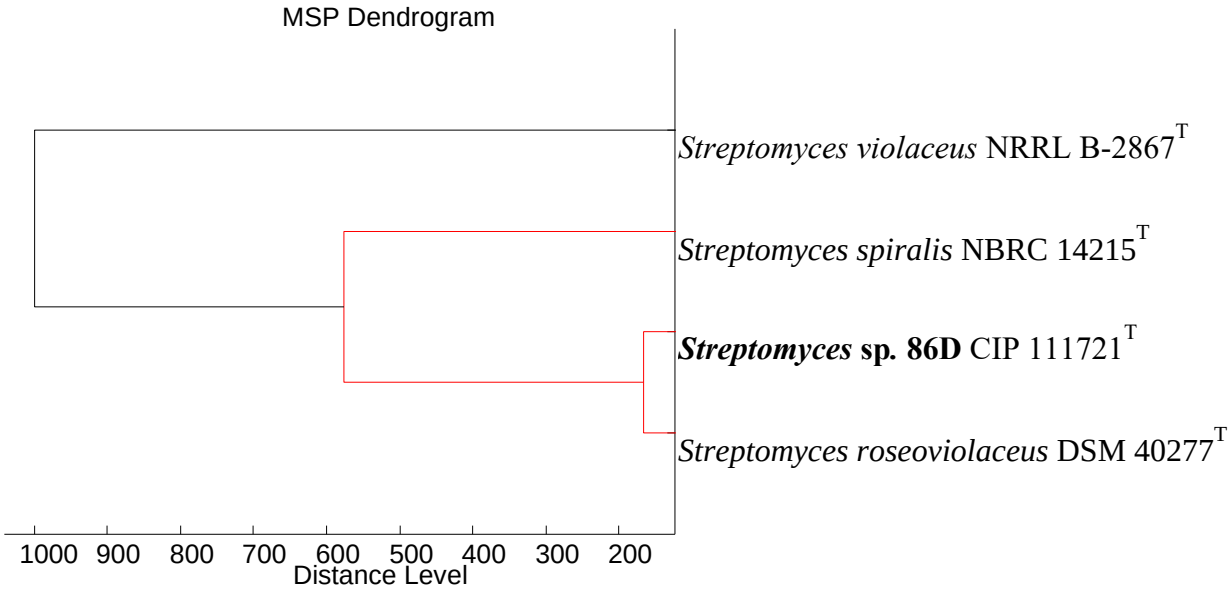

Figure 30. MALDI-TOF dendrogram of cell extract of *Streptomyces* sp. 86D. It is showing the similarity of MALDI-TOF mass spectra of cell extracts of strain *Streptomyces* sp. 86D and of closely related type strains.

3.5 Polyphasic taxonomy for strain 31sw

Strain 31sw isolated from soil sample collected from the Garmsar/Semnan/Iran. Strain 31sw could grow well on GYM agar after 2 weeks and aerial mycelium was observed in cream white. The growth on ISP3 and ISP4 was spare while the strain could grow well on ISP2- ISP5 and ISP7 media. The white aerial mycelium was observed on all ISP media and the colony colors varied from sand yellow to light ivory. Soluble pigments were not detected, and brown melanin pigments were not observed on ISP6 and Suter synthetic media. The morphology features of strain 31sw on GYM, ISP2, ISP3, ISP4, ISP5, ISP6 are shown in Figure 31a. The morphology of spore formations, which was detected by scanning electron microscopy (SEM), was observed as circular, non-motile single spore with smooth surface (Figure 31b). The evaluation of utilizing carbohydrates showed that strain 31sw could use glucose, sucrose, xylose, mannose, and fructose as a carbon sources. Strain 31sw could grow at 15-45°C (optimum 30°C), pH ranges 4.0- 8.0 (optimum pH 7.0) and in the present of 0-5% NaCl (w/v). The results of API ZYM and API Coryne showed that strain 31sw was able to produce some enzymes such as phosphatase alkaline, esterase (C4), esterase lipase (C8), lipase (C14), nitrate reduction, α-glucosidase, urease, and gelatin. More details of results are presented

in Table 12. The whole cell sugars contained arabinose, galactose, and ribose (Figure 32). Meso-DL-diaminopimelic acid was detected as a major diamino acid in the cell wall. The phospholipids analysis determined that the cell wall of 31sw contains phosphatidylglycerol (PG), diphosphatidylglycerol (DPG), phosphatidylethanolamine (PE), phosphatidylmonomethylethanolamine (PME), phosphatidyldimethylethanolamine (PDE), phosphatidylserine (PSer), unidentified phospholipids (PL1-5), and unidentified glycolipid (GL) (Figure 33). The composition of menaquinones of whole cells consisted of MK-9 (H_2), MK-9 (H_4), MK-8 (H_4), MK-9 (H_8), MK-9 (H_6), (46:42:7:4:1) respectively. The profile of methyl ester fatty acids was determined as C_{13}:$_0$ (0.18%) *iso*-C_{14}:$_0$ (1.24%), C_{14}:$_0$ (0.36%), *iso*-C_{15}:$_0$ (4.20%), *anteiso*- C_{15}:$_0$ (1.17%), C_{15}:$_1$ w8c (3.15%), C_{15}:$_0$ (7.66%), iso H-C_{16}:$_0$ (4.38%), *iso*-C_{16}:$_0$ (22.90%), *anteiso*- C_{16}:$_0$ (1.08%), C_{16}:$_0$ (4.14%), C_{16}:$_1$ w7c (6.16%), 10 methyl C_{16}:$_0$ (0.73%) *iso*-C_{17}:$_0$ (2.41%), *anteiso*-C_{17}:$_0$ (5.79%), C17:1 w8c (12.09%), C_{17}:$_1$ w6c (13.58%), C_{17}:$_0$ (7.70%), 10 methyl C_{17}:$_0$ (0.24%), *anteiso*- C_{17}:$_1$ w9c (0.21%), C_{18}:$_1$ w9c (0.26%) (Figure 34).

Based on 16S rRNA gene sequences blasting at the EZBioCloud the strain 31sw belongs to the genus *Saccharomonospora* and the highly comparable strains determined as *Saccharomonospora xinjiangensis* DSM 44391^T (99.65%), *Saccharomonospora azura* DSM 44631^T (98.82%) and *Saccharomonospora cyanea* DSM 44106^T (98.48%). The phylogenic tree with neighbor joining algorithm supported the previous result by detecting the stable clade within the genus of *Saccharomonospora*. The bootstrap value of 100% was applied (Figure 35). This affiliation was confirmed by the maximum-likelihood algorithm as well. The level of relatedness of DNA-DNA hybridization between strain 31sw and *Saccharomonospora xinjiangensis* DSM 44391^T and *Saccharomonospora cyanea* DSM 44106^T and *Saccharomonospora azura* DSM 44631^T were 60.5, 41.3 and 72.1 respectively. The result of MALDI-TOF dendrogram also proved that strain 31sw belongs to the genus of *Saccharomonospora* and the most related strains detected as *Saccharomonospora xinjiangensis* DSM 44391^T, *Saccharomonospora azura* DSM 44631^T and *Saccharomonospora cyanea* DSM 44106^T respectively (Figure 36). The complete genome sequencing of the strain 31sw has been revealed with accession number CP038101.1 in the NCBI gene bank.

a

b

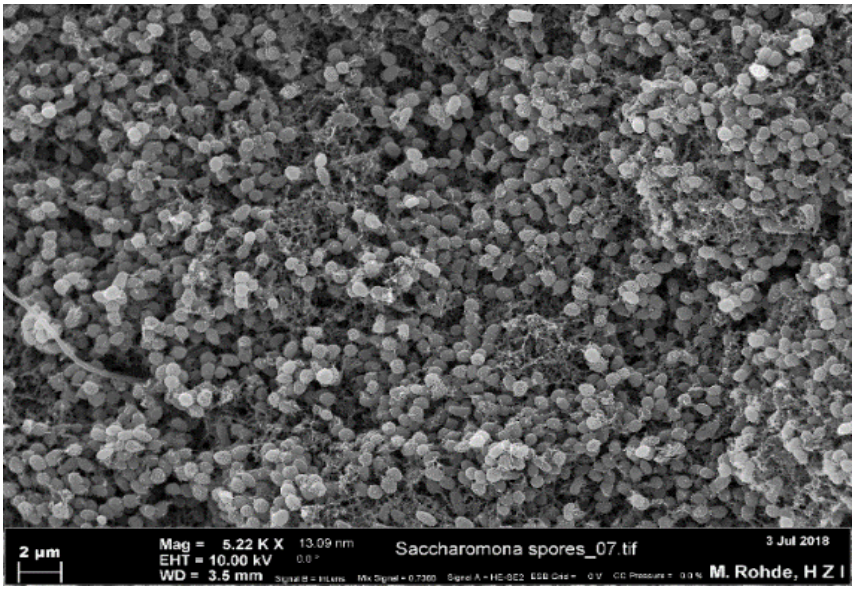

Figure 31. Morphological characteristics of strain 31sw. a) Morphology of strain 31sw on GYM and ISP media; b) Morphology of aerial mycelium and spores under scanning electron microscopy.

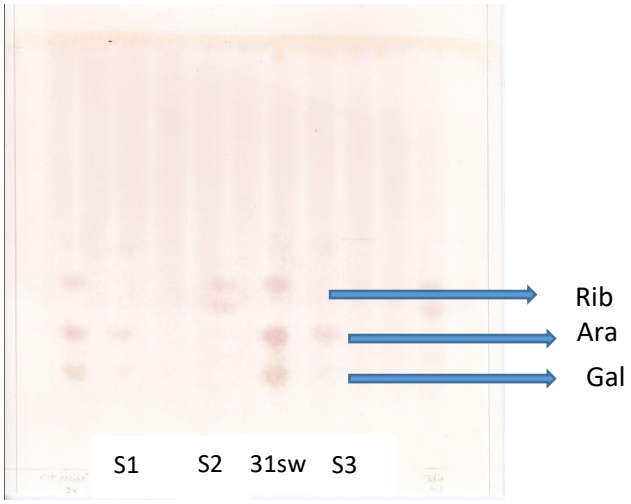

Figure 32. Whole- cell sugars detected in strain 31sw. The whole cell contains Galactose (Gal), Arabinose (Ara), and Ribose (Rib).

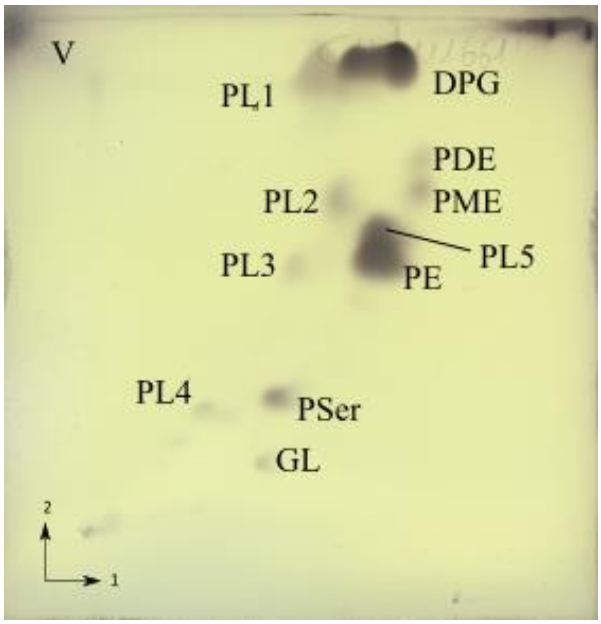

Figure 33. Polar lipids observed in strain 31sw; DPG, diphosphatidylglycerol; PE, phosphatidylethanolamine; PME, phosphatidylmonomethylethanolamine; PDE, phosphatidyldimethylethanolamine; PSer, phosphatidylserine; PL1-5, unidentified phospholipids; GL, unidentified glycolipid.

RT	Response	Ar/Ht	RFact	ECL	Peak Name	Percent	Comment1	Comment2
1.631	3.707E+8	0.026	----	7.012	SOLVENT	----	< min rt	
5.874	358	0.035	1.015	13.000	13:0	0.18	< min rt	Reference -
6.718	2484	0.035	0.997	13.619	14.0 ISO	1.24	ECL	Reference -
6.788	384	0.033	----	13.671		…		
7.236	736	0.038	0.988	14.000	14.0	0.36	ECL	Reference -
8.195	8646	0.038	0.974	14.623	15:0 ISO	4.20	ECL	Reference -
8.332	2409	0.039	0.972	14.713	15:0 ANTEISO	1.17	ECL	Reference -
8.552	6509	0.043	0.970	14.856	15:1 w6c	3.15	ECL	
		0.039				7.66	ECL	Reference -
8.774	15883	0.039	0.967	15.000	15:0	4.38	ECL	
9.537	9158	0.041	0.959	15.460	16:1 ISO H	22.90	ECL	Reference -
9.815	47989	0.040	0.956	15.627	16:0 ISO	1.08	ECL	
9.964	2270	0.042	0.955	15.717	16:0 ANTEISO	6.16	ECL	Reference -
10.335	969	0.052	----	15.941		….	ECL	
10.433	8227	0.040	0.951	16.000	16:0	4.14	ECL	Reference -
10.815	776	0.041	0.948	16.221	15:0 2OH	0.37	ECL	
11.180	1557	0.046	0.946	16.432	16:0 10	0.73	ECL	
11.340	450	0.042	0.945	16.525	ANTEISO 17:1	0.21	ECL	
11.523	5117	0.044	0.943	16.630	17:0 ISO	2.41	ECL	Reference -
11.682	12308	0.044	0.942	16.722	17:0 ANTEISO	5.79	ECL	Reference -
11.807	25737	0.044	0.942	16.794	17:1w8c	12.09	ECL	
11.925	28930	0.046	0.941	16.862	17:1w6c	13.58	ECL	
12.164	16430	0.047	0.940	17.001	17:0	7.70	ECL	Reference -
12.878	514	0.038	0.936	17.407	17:0 10 methyl	0.24	ECL	
13.513	567	0.035	0.933	17.767	18:1w9c	0.26	ECL	

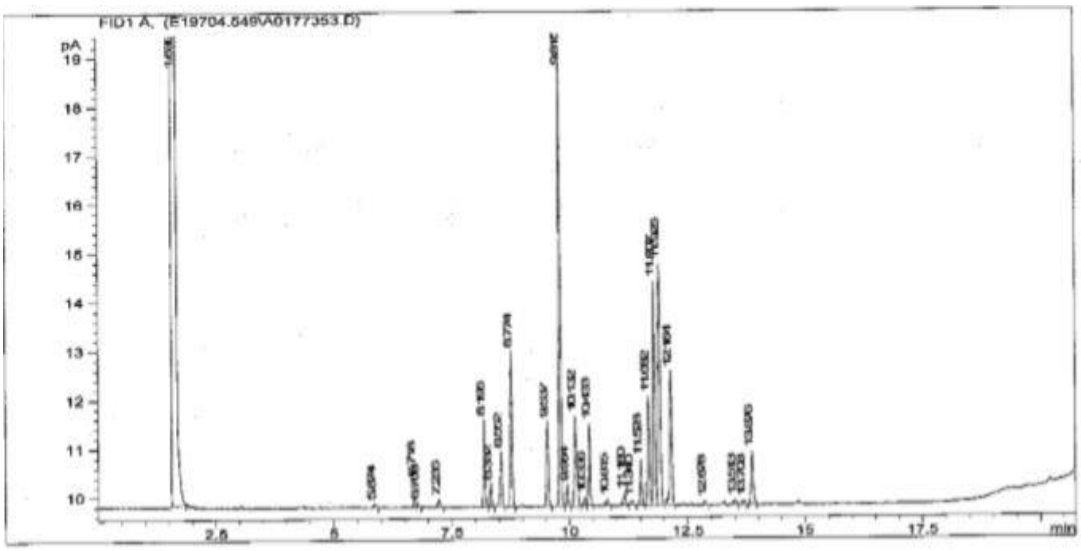

Figure 34. GC chromatogram of fatty acid analysis of strain 31sw.

Table 12. API ZYM and API Coryne test result of strain 31sw. + positive result; - negative result.

Strain 31sw			
Api ZYM	activity	**API Coryne**	activity
Phosphatase alkaline	+	nitrate reduction	+
Esterase (C4)	+	Pyraziamidase	-
Esterase Lipase (C8)	+	Pyrrolidonyl arylamidase	-
Lipase (C14)	+	Alkaline phosphatase	+
Leucin arylamidase	+	beta glucuronidase	-
Valine arylamidase	+	beta galactosidase	-
Cystine arylamidase	+	alpha glucosidase	+
Trypsin	-	N-acetyl-beta glucoseamidase	+
Chymotrypsin	+	Esculin (beta glucosidase)	-
Phosphatase acid	-	Urease	+
Naphthol-AS-BI-phosphohydrolase	+	Gelatin (hydrolysis)	+
alpha galactosidase	-	Glucose fermentation	-
beta galactosidase	-	Ribose fermentation	-
beta glucuronidase	-	Xylose fermentation	-
alpha glucosidase	+	Mannitol fermentation	-
beta glucosidase	+	Maltose fermentation	-
N- acetyl-beta-glucoseamidase	+	Lactose fermentation	-
alpha mannosidase	-	Sucrose fermentation	-
alpha fucosidase	-	Glycogen fermentation	-

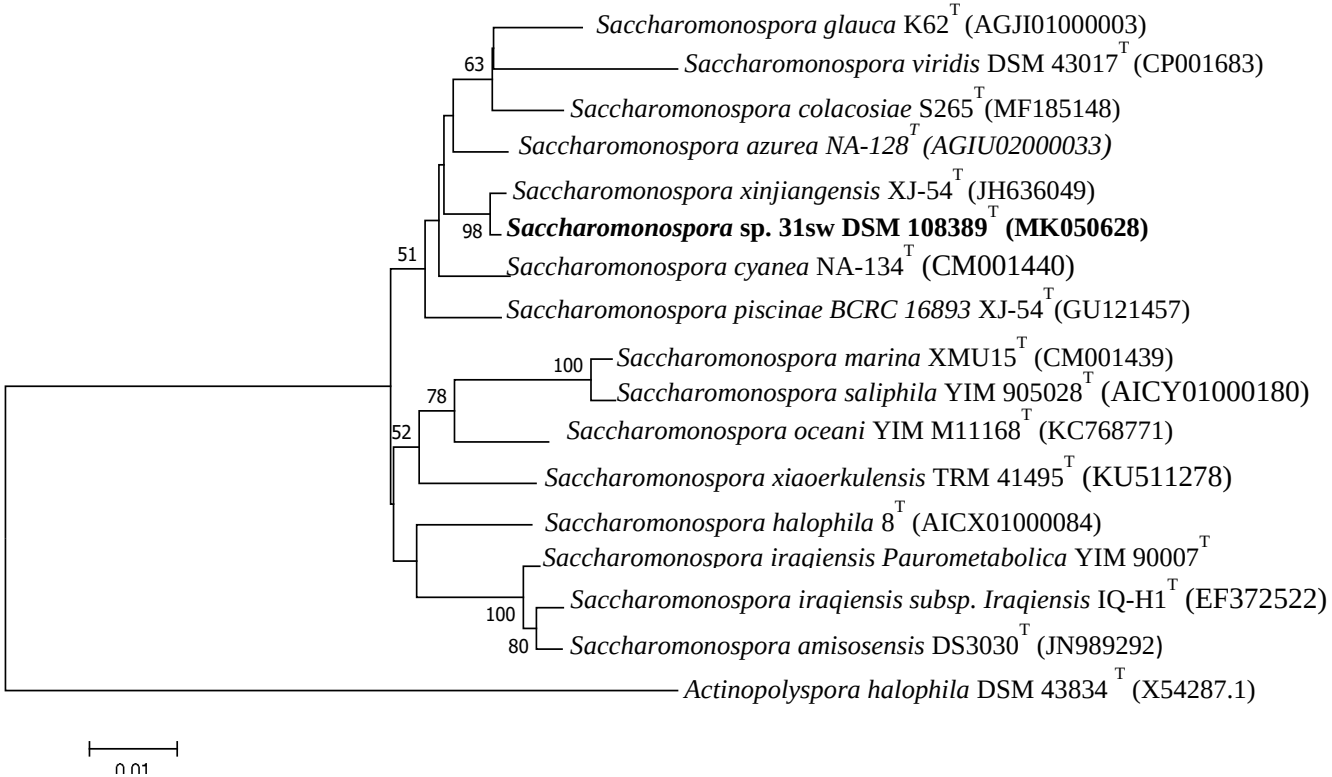

Figure 35. Neighbour-joining tree for strain 31sw based on 16S rRNA gene sequences (1492). It is showing relationships between strain 31sw and the type strains of closely related *Saccharomonospora* species. The evolutionary distances were determined using the Tamura-Nei method. Asterisks indicate branches of the tree that were also found using the maximum-likelihood and maximum-parsimony tree-making algorithms. ML specify nodes that were also recovered using the maximum-likelihood. Numbers at the nodes are percentage bootstrap values based on a Neighbour-joining analysis of 1,000 replicates, only values above 50% are shown. Bar 0.0050 substitutions per nucleotide position.

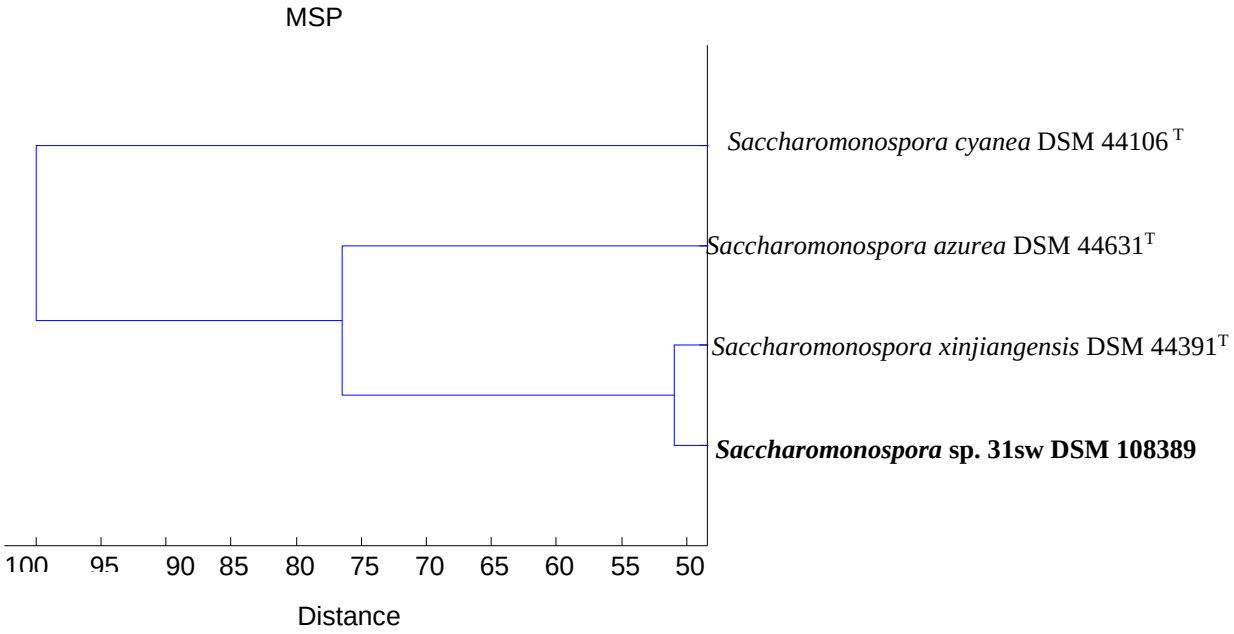

Figure 36. MALDI- TOF dendrogram of cell extract of strain 31sw. The dendrogram shows strain 31sw belongs to the genus *Saccharomonospora* and it remains in a different clade close to *Saccharomonospora xinjiangensis.*

4 Discussion

4.1 Isolation of novel Actinobacteria using integrated methods

The soil samples were collected from different regions of Iran with various textures in pH, salt, and humidity. The sand sample was collected from the Cuxhaven beach in Germany. Several studies reported that the distribution of rare Actinobacteria could be associated with environmental factors, such as soil type, pH, humus content, and the features of the humic acid[138]. For instance, *Microbispora* and *Streptosporangium* are most abundant in humus-rich acidic soils with low humic acid values (black coloured humic acid); whereas, *Saccharomonospora* are most plentiful in relatively humus-poor alkaline soils with higher values (brown humic acid). Species of *Dactylosporangium* and *Microtetraspora*, *Saccharomonospora*, and *Micromonospora* were frequently isolated from mountainous forest soils, level-land forest soils, and meadow soils, respectively[138,139]. Thus, biodiversity mining remains valuable to discover rare Actinobacteria with a high potential of producing novel bioactive metabolites.

Various isolation methods have been used for discovering several genera of Actinobacteria; and new methods have been utilized in recent years[139]. In this study, an integrated method was applied for the isolation of Actinobacteria. This integrated method involves combining different selective methods, such as pre-treatment of the sample (air-dried and serial dilution), nutritional selective medium 5336 (starch, casein, K_2HPO_4, $MgSO_4 \times 7H_2O$), and selective inhibition (adding antifungal and antibacterial agents to the medium). In previous studies, it has been reported that pre-treatment of soil samples can increase the rate of isolation of actinomycetes either by stimulating the growth of actinomycetes or by eliminating the huge number of Gram-negative bacterial and fungi[140,141]. It has also been stated that selective inhibition by adding antimicrobial agents to the enrichment medium has helped in the isolation of actinomycetes[142]. Previously it has also been stated that selective inhibition by adding antimicrobial agents to the enrichment medium caused to rise of isolation the actinomycetes[143,144].

In our investigation, with the application of multiple strategies, we could isolate a large number of Actinobacteria from different locations in Iran and Germany. From 48 isolates, around 67% belong to *Streptomyces*, and around 33% were non-

Streptomyces. Among the *Streptomyces* group, the strain 86D with 16S rRNA gene sequence similarity of 98.06% was selected for taxonomic analyses. The extract of production medium 5294 of strain 86D showed a moderate inhibition versus *Bacillus subtilis* and *Staphylococcus aureus.* Another isolate, strain 31sw, belongs to the rare Actinobacteria, which was isolated from a soil sample collected from Iran. The strain showed 99.63% gene sequence similarity to *Saccharomonospora xinjiangensis* species and was selected for further taxonomic evaluation. The crud extracts of *Saccharomonospora* 31sw in two different production media, 5294 and 5254, showed moderate inhibition against some microorganisms, such as *Bacillus subtilis*, *Micrococcus luteus*, and *Staphylococcus aureus*. However, the activity of the extract of 5254 was stronger than the extract of 5294. Two isolated strains M2^T and M3, belonged to the genus *Streptomonospora*, with 97.85% gene sequence similarity to the closest strain. The crude extracts of both strains showed strong activities against Gram-positive bacteria include *Bacillus subtilis*, *Staphylococcus aureus*, and *Micrococcus luteus* and Gram-negative bacterium *Legionella pneumophila*.

4.2 Description of *Streptomonospora litoralis* sp. nov., a halophilic actinomycete isolated from sand samples

During our investigation of rare Actinobacteria from beach sands and their secondary metabolites, two strains (M2^T and M3) were isolated from the sand of Cuxhaven, the North Sea, Germany (53° 52′ 39.5″ N, 8° 41′ 22.4″ E) on 20 July 2016. Comparison of the 16S rRNA sequences with EZbiocloud and NCBI database indicated that both strains M2^T and M3 belong to the genus *Streptomonospora*, which was described earlier with the type species of *Streptomonospora salina*[145]. The genus *Streptomonospora* belongs to the *Nocardiopsacea*[146] in the phylum Acidobacteria[147]. The level of DDH similarities between M2^T, *Streptomonospora halophila* DSM 45075^T, *Streptomonospora arabia* DSM 45083^T, and *Streptomonospora sediminis* DSM 45723^T were all below the extensively recognized 70% cut-off point (Wayne et al.)[148]. The level of DDH similarity between M2^T and M3 was 65/69%, which is close to the threshold, and we could not distinguish these strains as different species. In addition, the dendrogram based on MALDI-TOF mass spectra shows that the spectra of strains

M2^T and M3 differ from those of *Streptomonospora halophila* DSM 45075^T and other phylogenetically related actinomycetes. However, it was confirmed previously by Schumann and Maier that the resolution of the MALDI-TOF method is not sufficient for demonstrating strain-specific differences of the two isolates[103]. The dendrogram of RiboPrinter determined that the patterns of strains M2^T and M3 differ from one another and from the pattern of the closest related type strain *Streptomonospora halophila* DSM 45075^T. The RiboPrinter system has been shown to have a superior power for differentiation of bacteria at the level of species and even strains[77,149]. Enzyme activity data shows that both strains have negative results in producing beta-galactosidase, while this was positive in all three related strains. Hydrolyzing gelatin and trypsin production in M2^T and M3 was similar to *Streptomonospora sediminis* DSM 45723^T and *Streptomonospora arabica* DSM 45083^T. Cysteine aryl-amidase activity in strain M2^T was negative, but was positive in strain M3, making it one of the main distinguishing physiological characteristics between these strains and the three related type strains.

The polyphasic analysis supported the affiliation of strains M2^T and M3 with the genus *Streptomonospora*. However, the differences in biochemical, chemotaxonomical, and the level of DDH distinguished strains M2^T and M3 from closely related type strains. Based on these characteristics, the two strains are proposed to represent a novel species of the genus *Streptomonospora*. Strain M2^T is proposed as the type strain for this novel species, for which we propose the name *Streptomonospora litoralis* sp.

Streptomonospora M2^T is an aerobic, Gram-positive bacterium that grows on all ISP media. It shows various colours of substrate mycelium depending on the medium; on ISP2 (honey yellow), ISP3 (white), ISP4 (white), ISP5 (light ivory), ISP6 (golden yellow), ISP7 (ivory). The colour of aerial mycelia on all media is pure white, and diffusible pigments are produced on ISP2, ISP3, ISP5, and ISP7. Melanin is not produced on ISP6, ISP7, and SSM+T and SSM-T. At maturity on ISP3 medium, the aerial mycelium forms spore chains (wrinkled surface) and single non-motile spores (smooth surface). Strain M2^T grows on ISP2 medium with 0–15% NaCl (w/v), pH 4–9, at temperatures between 20 and 40°C; optimum

of growth as 7–10% NaCl, pH 7.2, at 28°C. Enzyme activities of strain M2^T were positive for alkaline phosphatase, esterase (C4), esterase lipase (C8), leucine aryl amidase, valine aryl amidase, acidic phosphatase, naphthol-AS-BI-phosphohydrolase, α-galactosidase, α-glucosidase, β-glucosidase, and gelatin. The strain does not have activity for lipase (C14), cystine arylamidase, trypsin, chymotrypsin, or urease. The diagnostic whole-cell sugars are galactose, glucose, and ribose. Predominant menaquinones (> 5%) include MK-10(H4), MK-10(H6), MK- 10(H8), MK-11(H6), and MK- 11(H8). The cell consists of polar lipids as phosphatidylglycerol, hydroxyl phosphatidylethanolamine, phosphatidylinositol, phosphatidylinositol mannosides, phosphatidylglycerol, and glycolipid. The profile of fatty acids (> 10%) is iso-$C_{16:0}$ (33.1%), anteiso- $C_{17:0}$ (24.4%), and 10 methyl $C_{18:0}$ (13.6%) The type strain M2^T is deposited with accession number of DSM 106425^T = NCCB 100650^T. The G+C content of genomic DNA of the type strain is 72.1 mol. The GenBank accession numbers of the 16S rRNA gene sequence and the genome sequence of M2^T are MG551552 and CP036455.1, respectively.

4.3 Isolation of two new thiopeptides from *Streptomonospora* sp. M2^T with distinctive activity

Two new compounds were isolated from *Streptomonospora* M2^T, named litoralimycins A (1) and B (2). These are novel derivatives of thiopeptide antibiotics. Thiopeptide (or thiazolyl peptides) have been isolated from various actinomycetes, mainly from soil actinomycetes and some from marine habitats[150]. They are highly modified sulfur-rich peptides of ribosomal origin. More than 100 chemical units of thiopeptides have been isolated in the last 50 years[151]. Their most typical feature is the central nitrogen-containing six-membered ring structure. With the oxidation state of this central ring, thiopeptides can be classified into five series[152]. The litoralimycins belong to the d series, which is the most numerous subgroups, due to their trisubstituted pyridine moiety[153]. Litoralimycin A (1) was strongly active against cell line MCF-7 relative to the other cell lines in the test assay, and the same inhibitory effect was reported for thiostrepton[154]. It was shown that this activity is based on its effect of decreasing transcriptional activity of the forkhead box M1 (FOXM1). FOXM1 is an oncogenic transcription factor that is upregulated in a varied range of cancers, and treatment with thiostrepton had an

effect on cell proliferation and cell-cycle progression in MCF-7 cells[154]. FOXM1 might be the shared molecular target[137]. Both Litoralimycin A (1) and B (2) showed weak activities against *Staphylococcus aureus*, *Micrococcus luteus*, and *Bacillus subtilis*, whereas litoralimycin A (1) was active against *Legionella pneumophila*. Thiopeptides have been known for more than 70 years and have rich biological activities, including inhibition of Gram-positive bacteria[155,156] and multidrug resistance *Mycobacterium tuberculosis*[157]. This is the first time that a new thiopeptide has been isolated from *Streptomonospora* spp., with a unique activity against the Gram-negative bacterium *Legionella pneumophila*.

4.4 Description of strain *Streptomyces* sp. 86D as a novel species isolated from an Iranian soil sample

Strain 86D was isolated from Lavasan/Tehran, Iran. Almost the complete 16S rRNA gene sequence (1496 bp) was deposited in the EZBioCloud server (https://www.ezbiocloud.net)[158], identifying the closest type strains as strain *Streptomyces violaceus* DSM 40082^T with 98.44% and *Streptomyces roseoviolaceus* DSM 40277^T with 98.44% gene sequence similarity. However, the phylogenetic tree based upon the neighbour-joining method and maximum parsimony analysis indicated *Streptomyces kalpinensis* TRM 46509^T as the closest related strain. Our comparison evaluation with the closest strains was completed according to the outcome of EZBioCloud.

Streptomyces forms the largest genus of Actinobacteria and the type genus of the family Streptomycetacea[159,160]. At least 8000 species of *Streptomyces* have been described[161]. Strain 86D can differentiate from its closest strains based upon physiological marks, such as alpha fucosidase, pyrrolidonyl arylamidase, and esculin (beta-glucosidase), NaCl tolerance, MALDI-TOF, and DNA-DNA hybridization. Therefore, we propose that strain 86D represents a novel species, for which we proposed the name *Streptomyces cyanogenus* sp.

Strain 86D grows well on all ISP media and GYM medium after 2 weeks of incubation at 30°C; aerial mycelium generates on ISP3 and ISP5 media (white colour). Strain 86D can tolerate up to 5% NaCl. The colony colour on different ISP

media is sand yellow, and on ISP3, besides sand yellow, a greenish colour was determined. Strain 86D produces brownish melanin on the SSM+T. The spore chain is long with smooth surfaces. Strain 86D utilizes all different single carbons as a source of carbon, including glucose, arabinose, sucrose, xylose, fructose, cellulose, inositol, mannose, rhamnose, and raffinose. Strain 86D shows positive activity for utilizing alpha fucosidase, pyrrolidonyl arylamidase, and esculin (β-glucosidase). The strain does not have activity for Lipase (C14), Chymotrypsin, β-galactosidase, nitrate reduction, and pyrazinamidase. The cell wall contains LL-diaminopimelic acid. The phospholipid system contains diphosphatidylglycerol (DPG), phosphatidylethanolamine (PE), phosphatidylinositol (PI), phosphatidyl-myo-inositol mannosides (PIMs), and the predominant menaquinones are MK-9 (H_8) and MK-9(H_6). The type strain 86D^T is deposited with the accession number of CIP111721^T = NCCB 100757^T. The GenBank accession number of the 16S rRNA gene sequence exists as MK120479.1.

4.5 Description of strain 31sw

Strain 31sw was isolated from a soil sample collected from Garmsar/Semnan/Iran (35.24.48N, 51, 55, 29.1 E). Almost the complete 16S rRNA gene sequence (1492 bp) of strain 31sw was compared based on pairwise nucleotide sequence alignment in the EzBioCloud server (https://www.ezbiocloud.net)[162]. The outcome indicated that the strain belongs to the genus *Saccharomonospora* and the closest related strains are *Saccharomonospora xinjiangensis* DSM 44391^T (99.65%), *Saccharomonospora azurea* DSM 44631^T (98.82%), and *Saccharomonospora cyanea* DSM 44106^T (98.48%). The MALDI-TOF evaluation also supported that strain 31sw remains in the *Saccharomonospora* genus, and the closest strains detected in the dendrogram were similar to the phylogenic tree based on 16S rRNA gene sequences. The similarity of DNA-DNA hybridization was determined by the high similarity score of strain 31sw with its closest strains *Saccharomonospora xinjiangensis* DSM 44391^T (60.5), *Saccharomonospora azurea* DSM 44631^T (72.9), and *Saccharomonospora cyanea* DSM 44106^T (41.3). Strain 31sw grew in the temperature range of 20–55°C with the optimum growth at 30°C; whereas the growth temperatures for the type strain of *Saccharomonospora xinjiangensis*, DSM 44391^T was reported as 45°C and 50°C. Strain 31sw produced aerial mycelium in

all ISP media, while the closest strain in our study *Saccharomonospora xinjiangensis* DSM 44391^T was only able to produce aerial mycelium in ISP5 and ISP7. Some tiny differences in physiological features were detected between strain31sw and related species. For instance, strain 31sw was positive for nitrate reduction activity, while this activity was not detected by *Saccharomonospora xinjiangensis* DSM 44391^T. On the contrary, trypsin utilization was positive for *Saccharomonospora xinjiangensis* DSM 44391^T but negative for 31sw. The chemotaxonomic analysis of strain 31sw showed that it belongs to the genus *Saccharomonospora*. The genome length of 4,713,420 of 31sw was applied for the online Average nucleotide identity (ANI) calculator in the EZBioCloud server (https://www.ezbiocloud.net/tools/ani)[163]. The value of ANI between 31sw and the strains *Saccharomonospora xinjiangensis* DSM 44391^T, *Saccharomonospora azurea* DSM 44631^T, and *Saccharomonospora cyanea* DSM 44106^T was 96.81%, 82.03%, 84.59%, respectively. The ANI score between strain 31sw and *Saccharomonospora xinjiangensis* DSM 44391^T was higher than the criterion for describing new species. Therefore, based on whole-genome sequencing, we cannot describe strain 31sw as a new species, but probably as a subspecies belonging to the *Saccharomonospora xinjiangensis* spp. The potential subspecies 31sw grows well on all ISP media and produces the white aerial mycelium in all different ISP media. Single spore forms on aerial hyphae, and the surfaces of spores are smooth. The strain grows in the temperature range of 20–55°C, with the optimum growth at 30°C. Strain 31sw grows in 0–2.5% NaCl, and the aerial mycelium was more branched in media supplemented with 2.5% NaCl. Glucose, sucrose, xylose, mannose, and fructose are utilized as carbon sources; however, arabinose, rhamnose, cellulose, raffinose, and inositol are not utilized. Strain 31sw is deposited in microbial collection with the accession number of DSM 108389=NCCB 100678. The GenBank accession numbers of the 16S rRNA gene sequence and the genome sequence of strain 31sw are MK050628.1 and NZ_CP038101.1, respectively.

5 Summary

During this study, many Actinobacteria were isolated from various areas in Iran and a neglected environment in Germany. Because of the isolation large number of Actinobacteria after initial screening, we could focus on just some strains with low 16S rRNA gene sequence similarity, some strains of rare Actinobacteria, and those Actinobacteria with remarkable biological activities. As a result, strains M2^{T} and M3, strain 86D, and strain 31sw were selected for polyphasic taxonomic evaluation. The crude extract of strain M2^{T} displayed high activity against Gram-positive bacteria, such as *Staphylococcus aureus* and *Micrococcus luteus*. Using upstream and downstream process development, we could isolate two new thiopeptide derivatives from strain M2^{T}. Strain M2^{T} showed 97.85% 16S rRNA gene sequence similarity to the closest type species of *Streptomonospora halophila.* The polyphasic evaluation suggested that strain M2^{T} belongs to the family *Nocardiopsacea* and probably represents a novel species within the genus *Streptomonospora.* The other strain 86D revealed moderate activity against *Bacillus subtilis* and *Staphylococcus aureus*, and by further analysis of the crude extract including fraction of extract by HPLC and LC-MS analysis, it was determined that its compounds were known. The 16S rRNA gene sequence analysis of strain 86D determined that it belongs to the genus *Streptomyces*. Further investigation, such as whole-genome sequencing and chemotaxonomy analysis, suggested that strain 86D represents a novel species within the genus *Streptomyces.* Based on the 16S rRNA, strain 31sw is related to the genus *Saccharomonospora* that belongs to rare Actinobacteria. Strain 31sw represents a potential subspecies within the species *Saccharomonospora xinjiangensis* DSM 44391$^{T.}$

6 References

1. Thirumurugan D, Cholarajan A, Raja SSS, Vijayakumar R. An introductory chapter: secondary metabolites. *Second metab—sources Appl*. 2018:1-21.
2. Shuikan AM, Hozzein WN, Alzharani MM, et al. Enhancement and Identification of Microbial Secondary Metabolites. In: Extremophilic Microbes and Metabolites-Diversity, Bioprespecting and Biotechnological Applications. IntechOpen; 2020.
3. Nicolaou KC, Rigol S. A brief history of antibiotics and select advances in their synthesis. *J Antibiot (Tokyo)*. 2018;71(2):153-184.
4. Gould K. Antibiotics: From prehistory to the present day. *J Antimicrob Chemother*. 2016;71(3):572-575. doi:10.1093/jac/dkv484
5. Hutchings M, Truman A, Wilkinson B. Antibiotics: past, present and future. *Curr Opin Microbiol*. 2019;51(Figure 1):72-80. doi:10.1016/j.mib.2019.10.008
6. Dias DA, Urban S, Roessner U. A historical overview of natural products in drug discovery. *Metabolites*. 2012;2(2):303-336. doi:10.3390/metabo2020303
7. Harvey AL, Edrada-Ebel R, Quinn RJ. The re-emergence of natural products for drug discovery in the genomics era. *Nat Rev Drug Discov*. 2015;14(2):111-129. doi:10.1038/nrd4510
8. Newman DJ, Cragg GM. Natural products as sources of new drugs from 1981 to 2014. *J Nat Prod*. 2016;79(3):629-661.
9. Keller NP. Fungal secondary metabolism: regulation, function and drug discovery. *Nat Rev Microbiol*. 2019;17(3):167-180. doi:10.1038/s41579-018-0121-1
10. Valli S, Suvathi SS, Aysha OS, Nirmala P, Vinoth KP, Reena A. Antimicrobial potential of Actinomycetes species isolated from marine environment. *Asian Pac J Trop Biomed*. 2012;2(6):469-473.
11. Baltz RH. Marcel Faber Roundtable: is our antibiotic pipeline unproductive because of starvation, constipation or lack of inspiration? *J Ind Microbiol Biotechnol*. 2006;33(7):507-513.
12. Müller R, Wink J. Future potential for anti-infectives from bacteria - How to

exploit biodiversity and genomic potential. *Int J Med Microbiol*. 2014;304(1):3-13. doi:10.1016/j.ijmm.2013.09.004

13. Ziemert N, Alanjary M, Weber T. The evolution of genome mining in microbes-a review. *Nat Prod Rep*. 2016;33(8):988-1005. doi:10.1039/c6np00025h
14. Bramhachari PV, Pinjari AB, Kariali E. Genomics of Actinobacteria With a Focus on Natural Product Biosynthetic Genes. *New Futur Dev Microb Biotechnol Bioeng*. 2018:325-335.
15. Aigle B, Lautru S, Spiteller D, et al. Genome mining of *Streptomyces ambofaciens*. *J Ind Microbiol Biotechnol*. 2014;41(2):251-263.
16. Singh BP, Rateb ME, Rodriguez-Couto S, Polizeli M, Li WJ. Editorial: Microbial Secondary Metabolites: Recent Developments and Technological Challenges. *Front Microbiol*. 2019;10:914. doi:10.3389/fmicb.2019.00914
17. Bush K. Investigational Agents for the Treatment of Gram-Negative Bacterial Infections: A Reality Check. *ACS Infect Dis*. 2015;1(11):509-511. doi:10.1021/acsinfecdis.5b00100
18. Baltz RH. Genetic manipulation of secondary metabolite biosynthesis for improved production in *Streptomyces* and other actinomycetes. *J Ind Microbiol Biotechnol*. 2016;43(2-3):343-370.
19. Zhu H, Sandiford SK, van Wezel GP. Triggers and cues that activate antibiotic production by actinomycetes. *J Ind Microbiol Biotechnol*. 2014;41(2):371-386.
20. Goering AW, McClure RA, Doroghazi JR, et al. Metabologenomics: Correlation of microbial gene clusters with metabolites drives discovery of a nonribosomal peptide with an unusual amino acid monomer. *ACS Cent Sci*. 2016;2(2):99-108.
21. Gross H, Stockwell VO, Henkels MD, Nowak-Thompson B, Loper JE, Gerwick WH. The genomisotopic approach: a systematic method to isolate products of orphan biosynthetic gene clusters. *Chem Biol*. 2007;14(1):53-63.
22. Laureti L, Song L, Huang S, et al. Identification of a bioactive 51-membered macrolide complex by activation of a silent polyketide synthase in *Streptomyces ambofaciens*. *Proc Natl Acad Sci*. 2011;108(15):6258-6263.
23. Lautru S, Deeth RJ, Bailey LM, Challis GL. Discovery of a new peptide

natural product by *Streptomyces coelicolor* genome mining. *Nat Chem Biol*. 2005;1(5):265-269.

24. Van Wezel GP, McDowall KJ. The regulation of the secondary metabolism of *Streptomyces*: new links and experimental advances. *Nat Prod Rep*. 2011;28(7):1311-1333.
25. Poole K. Bacterial stress responses as determinants of antimicrobial resistance. *J Antimicrob Chemother*. 2012;67(9):2069-2089.
26. Dashti Y, Grkovic T, Abdelmohsen UR, Hentschel U, Quinn RJ. Production of induced secondary metabolites by a co-culture of sponge-associated actinomycetes, *Actinokineospora* sp. EG49 and *Nocardiopsis* sp. RV163. *Mar Drugs*. 2014;12(5):3046-3059.
27. Wakefield J, Hassan HM, Jaspars M, Ebel R, Rateb ME. Dual induction of new microbial secondary metabolites by fungal bacterial co-cultivation. *Front Microbiol*. 2017;8:1284.
28. Tiwari K, Gupta RK. Rare actinomycetes: A potential storehouse for novel antibiotics. *Crit Rev Biotechnol*. 2012;32(2):108-132. doi:10.3109/07388551.2011.562482
29. Bull AT, Stach JEM, Ward AC, Goodfellow M. Marine actinobacteria: perspectives, challenges, future directions. *Antonie Van Leeuwenhoek*. 2005;87(1):65-79.
30. Mohammadipanah F, Wink J. Actinobacteria from arid and desert habitats: diversity and biological activity. *Front Microbiol*. 2016;6:1541.
31. Rateb ME, Ebel R, Jaspars M. Natural product diversity of actinobacteria in the Atacama Desert. *Antonie van Leeuwenhoek, Int J Gen Mol Microbiol*. 2018;111(8):1467-1477. doi:10.1007/s10482-018-1030-z
32. Becerril-Espinosa A, Freel KC, Jensen PR, Soria-Mercado IE. Marine Actinobacteria from the Gulf of California: Diversity, abundance and secondary metabolite biosynthetic potential. *Antonie van Leeuwenhoek, Int J Gen Mol Microbiol*. 2013;103(4):809-819. doi:10.1007/s10482-012-9863-3
33. Sun W, Zhang F, He L, Karthik L, Li Z. Actinomycetes from the South China Sea sponges: isolation, diversity, and potential for aromatic polyketides discovery. Front Microbiol 6: 1048–1062. *Go to Orig source. Go to PubMed*. 2015.

34. Horikoshi K, Antranikian G, Bull AT, Robb FT, Stetter KO. Extremophiles Handbook. Springer Science & Business Media; 2010.
35. Herold K, Xu Z, Gollmick FA, Gräfe U, Hertweck C. Biosynthesis of cervimycin C, an aromatic polyketide antibiotic bearing an unusual dimethylmalonyl moiety. *Org Biomol Chem*. 2004;2(17):2411-2414.
36. Derewacz DK, McNees CR, Scalmani G, et al. Structure and stereochemical determination of hypogeamicins from a cave-derived actinomycete. *J Nat Prod*. 2014;77(8):1759-1763.
37. Stankovic N, Radulovic V, Petkovic M, et al. *Streptomyces* sp. JS520 produces exceptionally high quantities of undecylprodigiosin with antibacterial, antioxidative, and UV-protective properties. *Appl Microbiol Biotechnol*. 2012;96(5):1217-1231.
38. Barka EA, Vatsa P, Sanchez L, et al. Taxonomy, physiology, and natural products of Actinobacteria. *Microbiol Mol Biol Rev*. 2016;80(1):1-43.
39. Nouioui I, Carro L, García-López M, et al. Genome-based taxonomic classification of the phylum Actinobacteria. *Front Microbiol*. 2018;9:2007.
40. Goodfellow M. Actinobacteria phyl. nov. Bergey's Manual of Systematics of Archaea and Bacteria. 2015 Apr 17:1-2.
41. Goodfellow M, Kämpfer P, Busse H-J, et al. Bergey's Manual® of Systematic Bacteriology: Volume Five The Actinobacteria, *Part A*. Springer; 2012.
42. Gao B, Gupta RS. Phylogenetic framework and molecular signatures for the main clades of the phylum Actinobacteria. *Microbiol Mol Biol Rev*. 2012;76(1):66-112.
43. McCormick JR, Flärdh K. Signals and regulators that govern *Streptomyces* development. *FEMS Microbiol Rev*. 2012;36(1):206-231.
44. Van der Meij A, Worsley SF, Hutchings MI, van Wezel GP. Chemical ecology of antibiotic production by actinomycetes. *FEMS Microbiol Rev*. 2017;41(3):392-416. doi:10.1093/femsre/fux005
45. Ahmed A, Earl J, Retchless A, et al. Comparative genomic analyses of 17 clinical isolates of *Gardnerella vaginalis* provide evidence of multiple genetically isolated clades consistent with subspeciation into genovars. *J Bacteriol*. 2012;194(15):3922-3937. doi:10.1128/JB.00056-12

46. Barka EA, Vatsa P, Sanchez L, et al. Taxonomy, Physiology, and Natural Products of Actinobacteria. *Microbiol Mol Biol Rev*. 2016;80(1):1-43. doi:10.1128/MMBR.00019-15
47. Shivlata L, Satyanarayana T. Thermophilic and alkaliphilic Actinobacteria: Biology and potential applications. *Front Microbiol*. 2015;6(SEP):1-29. doi:10.3389/fmicb.2015.01014
48. Vaijayanthi G, Vijayakumar R, Dhanasekaran D. Actinobacteria—a biofactory of novel enzymes. *Actinobacteria-basics Biotechnol Appl InTechOpen, London*. 2016:329-352.
49. Khanna M, Solanki R, Lal R. Selective isolation of rare actinomycetes producing novel antimicrobial compounds. *Int J Adv Biotechnol Res*. 2011;2(3):357-375.
50. Amin DH, Abdallah NA, Abolmaaty A, Tolba S, Wellington EMH. Microbiological and molecular insights on rare Actinobacteria harboring bioactive prospective. *Bull Natl Res Cent*. 2020;44(1). doi:10.1186/s42269-019-0266-8
51. Rangseekaew P, Pathom-Aree W. Cave actinobacteria as producers of bioactive metabolites. *Front Microbiol*. 2019;10(MAR). doi:10.3389/fmicb.2019.00387
52. Subramani R, Sipkema D. Marine Rare Actinomycetes: A Promising Source of Structurally Diverse and Unique Novel Natural Products. Vol 17.; 2019. doi:10.3390/md17050249
53. Amin DH. Rare Actinobacteria: A Possible Solution for Antimicrobial Drug Resistance in Egypt. *JOJ Nurs Heal Care*. 2018;6(4):4-6. doi:10.19080/jojnhc.2018.06.555695
54. Lam KS. Discovery of novel metabolites from marine actinomycetes. *Curr Opin Microbiol*. 2006;9(3):245-251. doi:10.1016/j.mib.2006.03.004
55. Tiwari K, Gupta RK. Rare actinomycetes: a potential storehouse for novel antibiotics. *Crit Rev Biotechnol*. 2012;32(2):108-132.
56. Kurtböke DI. Biodiscovery from rare actinomycetes: An eco-taxonomical perspective. *Appl Microbiol Biotechnol*. 2012;93(5):1843-1852. doi:10.1007/s00253-012-3898-2
57. Butler MS, Paterson DL. Antibiotics in the clinical pipeline in October

2019. *J Antibiot (Tokyo)*. 2020;73(6):329-364. doi:10.1038/s41429-020-0291-8

58. Xie CL, Liu Q, Xia JM, et al. Anti-allergic compounds from the deep-sea-derived actinomycete *Nesterenkonia flava* MCCC 1K00610. *Mar Drugs*. 2017;15(3):1-8. doi:10.3390/md15030071
59. Yoo E, Schulze CJ, Stokes BH, et al. The antimalarial natural product salinipostin A identifies essential α/β serine hydrolases involved in lipid metabolism in *P. falciparum* parasites. *Cell Chem Biol*. 2020;27(2):143-157.
60. Zhang Y, Adnani N, Braun DR, et al. Micromonohalimanes A and B: Antibacterial Halimane-Type Diterpenoids from a Marine *Micromonospora* Species. *J Nat Prod*. 2016;79(11):2968-2972. doi:10.1021/acs.jnatprod.6b00555
61. Wyche TP, Piotrowski JS, Hou Y, et al. Forazoline A: Marine-Derived Polyketide with Antifungal in Vivo Efficacy. *Angew Chemie - Int Ed*. 2014;53(43):11583-11586. doi:10.1002/anie.201405990
62. Vandamme PAR. Taxonomy and classification of bacteria. *Man Clin Microbiol*. 2015:252-269.
63. Kämpfer P, Glaeser SP. Prokaryotic taxonomy in the sequencing era - the polyphasic approach revisited. *Environ Microbiol*. 2012;14(2):291-317. doi:10.1111/j.1462-2920.2011.02615.x
64. Kersters K, De Vos P, Gillis M, Swings J, Vandamme P, Stackebrandt E. Introduction to the Proteobacteria. In: The Prokaryotes: A Handbook on the Biology of Bacteria. Vol 5. Springer; 2006:3-37.
65. Clarridge JE. Impact of 16S rRNA gene sequence analysis for identification of bacteria on clinical microbiology and infectious diseases. *Clin Microbiol Rev*. 2004;17(4):840-862. doi:10.1128/CMR.17.4.840-862.2004
66. Schleifer KH. Classification of Bacteria and Archaea: past, present and future. *Syst Appl Microbiol*. 2009;32(8):533-542.
67. Wink J, Mohammadipanah F, Hamedi J. *Biology and Biotechnology of Actinobacteria*. Springer; 2017.
68. Dastager SG, Li WJ, Dayanand A, et al. Seperation, identification and analysis of pigment (melanin) production in *Streptomyces*. *African J Biotechnol*. 2006;5(11):1131-1134. doi:10.5897/AJB05.361

69. Lechevalier MP, Lechevalier H. Chemical composition as a criterion in the classification of aerobic actinomycetes. *Int J Syst Evol Microbiol*. 1970;20(4):435-443.
70. Rosselló-Mora R, Amann R. The species concept for prokaryotes. *FEMS Microbiol Rev*. 2001;25(1):39-67. doi:10.1016/S0168-6445(00)00040-1
71. Mohammadian T, Alishahi M, Tabandeh MR, et al. Phylogenetic identification and in situ detection of individual microbial cells without cultivation. *Aquac Int J Eur Aquac Soc*. 2016;24(1):143-169. doi:10.1111/j.1439-0426.2012.01974.x
72. Stackebrandt E. Taxonomic parameters revisited: tarnished gold standards. *Microbiol Today*. 2006;33:152-155.
73. Tindall BJ, Rosselló-Móra R, Busse HJ, Ludwig W, Kämpfer P. Notes on the characterization of prokaryote strains for taxonomic purposes. *Int J Syst Evol Microbiol*. 2010;60(1):249-266. doi:10.1099/ijs.0.016949-0
74. De Lajudie PM, Andrews M, Ardley J, et al. Minimal standards for the description of new genera and species of rhizobia and agrobacteria. *Int J Syst Evol Microbiol*. 2019;69(7):1852-1863. doi:10.1099/ijsem.0.003426
75. Goris J, Konstantinidis KT, Klappenbach JA, Coenye T, Vandamme P, Tiedje JM. DNA-DNA hybridization values and their relationship to whole-genome sequence similarities. *Int J Syst Evol Microbiol*. 2007;57(1):81-91. doi:10.1099/ijs.0.64483-0
76. Rosselló-Móra R, Urdiain M, López-López A. DNA-DNA Hybridization. *Methods Microbiol*. 2011;38:325-347. doi:10.1016/B978-0-12-387730-7.00015-2
77. Schumann P, Pukall R. The discriminatory power of ribotyping as automatable technique for differentiation of bacteria. *Syst Appl Microbiol*. 2013;36(6):369-375.
78. Bentley SD, Chater KF, Cerdeño-Tárraga AM, et al. Complete genome sequence of the model actinomycete *Streptomyces coelicolor* A3(2). *Nature*. 2002;417(6885):141-147. doi:10.1038/417141a
79. Mardis ER. Next-generation sequencing platforms. *Annu Rev Anal Chem*. 2013;6:287-303.
80. Borriss R, Rueckert C, Blom J, Bezuidt O, Reva O, Klenk H-P. Whole

genome sequence comparisons in taxonomy. In: *Methods in Microbiology*. Vol 38. Elsevier; 2011:409-436.

81. Zhi XY, Li WJ, Stackebrandt E. An update of the structure and 16S rRNA gene sequence-based definition of higher ranks of the class Actinobacteria, with the proposal of two new suborders and four new families and emended descriptions of the existing higher taxa. *Int J Syst Evol Microbiol*. 2009;59(3):589-608. doi:10.1099/ijs.0.65780-0
82. Beutler JA, Alvarado AB, Schaufelberger DE, Andrews P, McCloud TG. Dereplication of phorbol bioactives: Lyngbya majuscula and croton cuneatus. *J Nat Prod*. 1990;53(4):867-874. doi:10.1021/np50070a014
83. Hubert J, Nuzillard JM, Renault JH. Dereplication strategies in natural product research: How many tools and methodologies behind the same concept? *Phytochem Rev*. 2017;16(1):55-95. doi:10.1007/s11101-015-9448-7
84. Ghisalberti EL. Detection and Isolation of Bioactive Natural Products. CRC Press, Boca Raton; 1993.
85. Wagner HK, Wolff PM. New Natural Products and Plant Drugs with Pharmacological, Biological Or Therapeutical Activity: Proceedings of the First International Congress on Medicinal Plant Research, Section A, Held at the University of Munich, Germany, September 6–10, 1976. Springer Science & Business Media; 2012.
86. Wolfender J-L, Marti G, Ferreira Queiroz E. Advances in Techniques for Profiling Crude Extracts and for the Rapid Identificationof Natural Products: Dereplication, Quality Control and Metabolomics. *Curr Org Chem*. 2010;14(16):1808-1832. doi:10.2174/138527210792927645
87. Hanson T, Brooks TM, Da Fonseca GAB, et al. Warfare in biodiversity hotspots. *Conserv Biol*. 2009;23(3):578-587.
88. Kiani M, Mohammadi S, Babaei A, et al. Iran supports a great share of biodiversity and floristic endemism for Fritillaria spp.(Liliaceae): A review. *Plant Divers*. 2017;39(5):245-262.
89. Mohammadipanah F, Atasayar E, Heidarian S, Wink J. *Glycomyces sediminimaris* sp. Nov., a new species of actinobacteria isolated from marine sediment. *Int J Syst Evol Microbiol*. 2018;68(7):2357-2363.

doi:10.1099/ijsem.0.002847

90. Nikou MM, Ramezani M, Harirchi S, et al. *Salinifilum* gen. nov., with description of *Salinifilum proteinilyticum* sp. nov., an extremely halophilic actinomycete isolated from Meighan wetland, Iran, and reclassification of *Saccharopolyspora aidingensis* as *Salinifilum aidingensis comb*. nov. and Sacc. *Int J Syst Evol Microbiol*. 2017;67(10):4221-4227.
91. Babadi ZK, Sudarman E, Ebrahimipour GH, Primahana G, Stadler M, Wink J. Structurally diverse metabolites from the rare actinobacterium *Saccharothrix xinjiangensis*. *J Antibiot (Tokyo)*. 2020;73(1):48-55.
92. Suter MA. Isolierung und Charakterisierung von Melanin-negativen Mutanten aus *Streptomyces glaucescens*. 1978.
93. Hayakawa M, Otoguro M, Takeuchi T, Yamazaki T, Iimura Y. Application of a method incorporating differential centrifugation for selective isolation of motile actinomycetes in soil and plant litter. *Antonie van Leeuwenhoek, Int J Gen Mol Microbiol*. 2000;78(2):171-185. doi:10.1023/A:1026579426265
94. Charousová I, Steinmetz H, Medo J, Javoreková S, Wink J. Characterization of Antimycins – Producing *Streptomycete* Strain VY46 Isolated from Slovak Soil. *Brazilian Arch Biol Technol*. 2016;59(0):1-8. doi:10.1590/1678-4324-2016160274
95. Wink J. Biological Active Rakicidins A, B and E produced by the Marine *Micromonospora* sp. Isolate Guam1582. *Adv Biotechnol Microbiol*. 2016;1(2). doi:10.19080/aibm.2016.01.555558
96. Mohr KI, Stechling M, Wink J, Wilharm E, Stadler M. Comparison of myxobacterial diversity and evaluation of isolation success in two niches: Kiritimati Island and German compost. *Microbiologyopen*. 2016;5(2):268-278. doi:10.1002/mbo3.325
97. Chun J, Lee JH, Jung Y, et al. EzTaxon: A web-based tool for the identification of prokaryotes based on 16S ribosomal RNA gene sequences. *Int J Syst Evol Microbiol*. 2007;57(10):2259-2261. doi:10.1099/ijs.0.64915-0
98. Kumar S, Stecher G, Li M, Knyaz C, Tamura K. MEGA X: Molecular evolutionary genetics analysis across computing platforms. *Mol Biol Evol*.

2018;35(6):1547-1549. doi:10.1093/molbev/msy096

99. Thompson JD, Higgins DG, Gibson TJ. CLUSTAL W: Improving the sensitivity of progressive multiple sequence alignment through sequence weighting, position-specific gap penalties and weight matrix choice. *Nucleic Acids Res*. 1994;22(22):4673-4680. doi:10.1093/nar/22.22.4673
100. Saitou N, Nei M. The neighbor-joining method: a new method for reconstructing phylogenetic trees. *Mol Biol Evol*. 1987;4(4):406-425. doi:10.1093/oxfordjournals.molbev.a040454
101. Felsenstein J. Evolutionary trees from DNA sequences: A maximum likelihood approach. *J Mol Evol*. 1981;17(6):368-376. doi:10.1007/BF01734359
102. Felsenstein J. Confidence limits on phylogenies: a justification. *Evolution (N Y)*. 1985;39:783-791.
103. Schumann P, Maier T. MALDI-TOF mass spectrometry applied to classification and identification of bacteria. In: *Methods in Microbiology*. Vol 41. Elsevier; 2014:275-306.
104. Wink J, Schumann P, Atasayar E, et al. '*Streptomyces caelicus*', an antibiotic-producing species of the genus *Streptomyces*, and *Streptomyces canchipurensis* Li et al. 2015 are later heterotypic synonyms of *Streptomyces muensis* Ningthoujam et al. 2014. *Int J Syst Evol Microbiol*. 2017;67(3):548-556. doi:10.1099/ijsem.0.001612
105. Schumann P, Pukall R. *Leucobacter weissii* sp. Nov., an isolate from activated sludge once described as first representative of the peptidoglycan variation B2δ, and emended description of the genus *Leucobacter*. *Int J Syst Evol Microbiol*. 2017;67(12):5244-52351. doi:10.1099/ijsem.0.002454
106. Kieser T, Bibb MJ, Buttner MJ, Chater KF, Hopwood DA, John Innes F. Practical *Streptomyces* Genetics.; 2000.
107. Ziemke F, Höfle MG, Lalucat J, Rossellö-Mora R. Reclassification of *Shewanella putrefaciens* Owen's genomic group II as *Shewanella baltica* sp. nov. *Int J Syst Evol Microbiol*. 1998;48(1):179-186.
108. Glaeser SP, Falsen E, Martin K, Kämpfer P. *Alicyclobacillus consociatus* sp. nov., isolated from a human clinical specimen. *Int J Syst Evol Microbiol*. 2013;63(PART10):3623-3627. doi:10.1099/ijs.0.048173-0

109. Shirling EBT, Gottlieb D. Methods for characterization of *Streptomyces* species. *Int J Syst Bacteriol*. 1966;16(3):313-340.
110. Charousová I, Javoreková S, Wink J. Isolation and characterization of *Streptomyces rishiriensis* (vy31) with antibiotic activity against various pathogenic microorganisms. *J Microbiol Biotechnol Food Sci*. 2020;2020:23-27.
111. Wink J. Polyphasic taxonomy and antibiotic formation in some closely related genera of the family Pseudonocardiaceae. *Recent Res Dev Antibiot*. 2002;2:97-140.
112. Landwehr W, Kämpfer P, Glaeser SP, et al. Taxonomic analyses of members of the *Sreptomyces cinnabarinus* cluster, description of *Streptomyces cinnabarigriseus* sp. Nov. and *Streptomyces davaonensis* sp. nov. *Int J Syst Evol Microbiol*. 2018;68(1):382-393. doi:10.1099/ijsem.0.002519
113. Kutzner HJ. The family Streptomycetaceae. *The prokaryotes*. 1981.
114. Humble MW, King A, Phillips I. API ZYM: a simple rapid system for the detection of bacterial enzymes. *J Clin Pathol*. 1977;30(3):275-277.
115. Soto A, Zapardiel J, Soriano F. Evaluation of API Coryne system for identifying coryneform bacteria. *J Clin Pathol*. 1994;47(8):756-759. doi:10.1136/jcp.47.8.756
116. Panschin I, Huang S, Meier-Kolthoff JP, et al. Comparing polysaccharide decomposition between the type strains *Gramella echinicola* KMM 6050T (DSM 19838T) and *Gramella portivictoriae* UST040801-001T (DSM 23547T), and emended description of *Gramella echinicola* Nedashkovskaya et al. 2005 emend. Shahina et. *Stand Genomic Sci*. 2016;11(1):1-16. doi:10.1186/s40793-016-0163-9
117. Hasegawa T, Takizawa M, Tanida S. A rapid analysis for chemical grouping of aerobic actinomycetes. *J Gen Appl Microbiol*. 1983;29(4):319-322. doi:10.2323/jgam.29.319
118. Kröger FA, Nachtrieb NH. The chemistry of imperfect crystals. *PhT*. 1964;17(10):66.
119. Card GL. Metabolism of phosphatidylglycerol, phosphatidylethanolamine, and cardiolipin of *Bacillus stearothermophilus*. *J Bacteriol*.

1973;114(3):1125-1137. doi:10.1128/jb.114.3.1125-1137.1973

120. Sasser M. Identification of bacteria by gas chromatography of cellular fatty acids. 1990.
121. Baumann S, Herrmann J, Raju R, et al. Cystobactamids: myxobacterial topoisomerase inhibitors exhibiting potent antibacterial activity. *Angew Chemie Int Ed*. 2014;53(52):14605-14609.
122. Landwehr W, Karwehl S, Schupp PJ, Schumann P, Wink J. Biological active rakicidins A, B and E produced by the marine *Micromonospora* sp. isolate Guam1582. *Adv Biotechnol Microbiol*. 2016;1(2):1-5.
123. Mosmann T. Rapid colorimetric assay for cellular growth and survival: application to proliferation and cytotoxicity assays. *J Immunol Methods*. 1983;65(1-2):55-63.
124. Mulwa LS, Jansen R, Praditya DF, et al. Lanyamycin, a macrolide antibiotic from *Sorangium cellulosum*, strain Soce 481 (Myxobacteria). *Beilstein J Org Chem*. 2018;14(1):1554-1562.
125. Yun B-S, Fujita K, Furihata K, Seto H. Absolute stereochemistry and solution conformation of promothiocins. *Tetrahedron*. 2001;57(48):9683-9687.
126. Viehrig K, Surup F, Harmrolfs K, Jansen R, Kunze B, Müller R. Concerted action of P450 plus helper protein to form the amino-hydroxy-piperidone moiety of the potent protease inhibitor crocapeptin. *J Am Chem Soc*. 2013;135(45):16885-16894.
127. Tamura K, Nei M. Estimation of the number of nucleotide substitutions in the control region of mitochondrial DNA in humans and chimpanzees. *Mol Biol Evol*. 1993;10(3):512-526. doi:10.1093/oxfordjournals.molbev.a040023
128. Blin K, Shaw S, Steinke K, et al. antiSMASH 5.0: updates to the secondary metabolite genome mining pipeline. *Nucleic Acids Res*. 2019;47(W1):W81-W87.
129. Krügel H, Krubasik P, Weber K, Saluz HP, Sandmann G. Functional analysis of genes from *Streptomyces griseus* involved in the synthesis of isorenieratene, a carotenoid with aromatic end groups, revealed a novel type of carotenoid desaturase. *Biochim Biophys Acta (BBA)-Molecular Cell Biol Lipids*. 1999;1439(1):57-64.

130. Jiang J, He X, Cane DE. Biosynthesis of the earthy odorant geosmin by a bifunctional *Streptomyces coelicolor* enzyme. *Nat Chem Biol*. 2007;3(11):711.
131. Prabhu J, Schauwecker F, Grammel N, Keller U, Bernhard M. Functional expression of the ectoine hydroxylase gene (thpD) from *Streptomyces chrysomallus* in *Halomonas elongata*. *Appl Environ Microbiol*. 2004;70(5):3130-3132.
132. Kodani S, Hudson ME, Durrant MC, Buttner MJ, Nodwell JR, Willey JM. The SapB morphogen is a lantibiotic-like peptide derived from the product of the developmental gene ramS in *Streptomyces coelicolor*. *Proc Natl Acad Sci*. 2004;101(31):11448-11453.
133. Dimise EJ, Widboom PF, Bruner SD. Structure elucidation and biosynthesis of fuscachelins, peptide siderophores from the moderate thermophile *Thermobifida fusca*. *Proc Natl Acad Sci U S A*. 2008;105(40):15311-15316. doi:10.1073/pnas.0805451105
134. Malcolmson SJ, Young TS, Ruby JG, Skewes-Cox P, Walsh CT. The posttranslational modification cascade to the thiopeptide berninamycin generates linear forms and altered macrocyclic scaffolds. *Proc Natl Acad Sci*. 2013;110(21):8483-8488.
135. Engelhardt K, Degnes KF, Kemmler M, et al. Production of a new thiopeptide antibiotic, TP-1161, by a marine *Nocardiopsis* species. *Appl Environ Microbiol*. 2010;76(15):4969-4976. doi:10.1128/AEM.00741-10
136. Du Y, Qiu Y, Meng X, Feng J, Tao J, Liu W. A Heterotrimeric Dehydrogenase Complex Functions with 2 Distinct YcaO Proteins to Install 5 Azole Heterocycles into 35-Membered Sulfomycin Thiopeptides. *J Am Chem Soc*. 2020;142(18):8454-8463.
137. Khodamoradi S, Stadler M, Wink J, Surup F. Litoralimycins A and B, New Cytotoxic Thiopeptides from *Streptomonospora* sp. M2. *Mar Drugs*. 2020;18(6):280.
138. Hayakawa H, Ishizawa K, Yamazaki T, Nonomura H. Distribution of antibiotic-producing *Microbispora* strains in soils with different pHs. *Actinomycetes*. 1995;6(3):75-79.
139. Hayakawa M. Studies on the Isolation and Distribution of Rare

Actinomycetes in Soil. *Actinomycetologica*. 2008;22(1):12-19. doi:10.3209/saj.saj220103

140. Hong K, Gao AH, Xie QY, et al. Actinomycetes for marine drug discovery isolated from mangrove soils and plants in China. *Mar Drugs*. 2009;7(1):24-44. doi:10.3390/md7010024
141. Matsukawa E, Nakagawa Y, Iimura Y, Hayakawa M. A New Enrichment Method for the Selective Isolation of *Streptomycetes* from the Root Surfaces of Herbaceous Plants. *Actinomycetologica*. 2007;21(2):66-69. doi:10.3209/saj.saj210202
142. Küster E, Williams ST. Selection of media for isolation of *Streptomycetes*. *Nature*. 1964;202(4935):928-929.
143. Hayakawa M, Sadakata T, Kajiura T, Nonomura H. New methods for the highly selective isolation of *Micromonospora* and *Microbispora* from soil. *J Ferment Bioeng*. 1991;72(5):320-326.
144. Hayakawa M, Nonomura H. Humic acid-vitamin agar, a new medium for the selective isolation of soil actinomycetes. *J Ferment Technol*. 1987;65(5):501-509.
145. Cui X-L, Mao P-H, Zeng M, et al. *Streptimonospora salina* gen. nov., sp. nov., a new member of the family Nocardiopsaceae. *Int J Syst Evol Microbiol*. 2001;51(2):357-363.
146. Rainey FA, Ward-Rainey N, Kroppenstedt RM, Stackebrandt E. The genus *Nocardiopsis* represents a phylogenetically coherent taxon and a distinct actinomycete lineage: proposal of Nocardiopsaceae fam. nov. *Int J Syst Evol Microbiol*. 1996;46(4):1088-1092.
147. Thrash JC, Coates JD. Phylum XVII. Acidobacteria phyl. nov. In: *Bergey's Manual® of Systematic Bacteriology*. Springer; 2010:725-735.
148. Wayne LG, Brenner DJ, Colwell RR, et al. Report of the ad hoc committee on reconciliation of approaches to bacterial systematics. *Int J Syst Evol Microbiol*. 1987;37(4):463-464.
149. Bruce J. Automated system rapidly identifies and characterizes microorganisms in food. *Food Technol*. 1996;50(1):77-81.
150. Bagley MC, Dale JW, Merritt EA, Xiong X. Thiopeptide antibiotics. *Chem Rev*. 2005;105(2):685-714. doi:10.1021/cr0300441

151. Shen X, Mustafa M, Chen Y, Cao Y, Gao J. Natural thiopeptides as a privileged scaffold for drug discovery and therapeutic development. *Med Chem Res*. 2019;28(8):1063-1098. doi:10.1007/s00044-019-02361-1
152. Just-Baringo X, Albericio F, Álvarez M. Thiopeptide Antibiotics: Retrospective and Recent Advances. Vol 12.; 2014. doi:10.3390/md12010317
153. Malcolmson SJ, Young TS, Ruby JG, Skewes-Cox P, Walsh CT. The posttranslational modification cascade to the thiopeptide berninamycin generates linear forms and altered macrocyclic scaffolds. *Proc Natl Acad Sci U S A*. 2013;110(21):8483-8488. doi:10.1073/pnas.1307111110
154. Hegde NS, Sanders DA, Rodriguez R, Balasubramanian S. The transcription factor FOXM1 is a cellular target of the natural product thiostrepton. *Nat Chem*. 2011;3(9):725-731.
155. Miyairi N, MLYOSHI T, AOKI H, et al. Studies on thiopeptin antibiotics. *J Antibiot (Tokyo)*. 1970;23(3):113-119.
156. Ciufolini MA, Shen YC. Studies toward Thiostrepton Antibiotics: Assembly of the Central Pyridine− Thiazole Cluster of Micrococcins. *J Org Chem*. 1997;62(12):3804-3805.
157. Singh SB, Xu L, Meinke PT, et al. Thiazomycin, nocathiacin and analogs show strong activity against clinical strains of drug-resistant *Mycobacterium tuberculosis*. *J Antibiot (Tokyo)*. 2017;70(5):671-674. doi:10.1038/ja.2016.165
158. Yoon S-H, Ha S-M, Kwon S, et al. Introducing EzBioCloud: a taxonomically united database of 16S rRNA gene sequences and whole-genome assemblies. *Int J Syst Evol Microbiol*. 2017;67(5):1613.
159. Ray L, Suar M, Pattnaik AK, Raina V. *Streptomyces chilikensis* sp. nov., a halophilic *Streptomycete* isolated from brackish water sediment. *Int J Syst Evol Microbiol*. 2013;63(8):2757-2764.
160. Lodders N, Kämpfer P. Streptomycetaceae: phylogeny, ecology and pathogenicity. *eLS*. 2007.
161. Sharma M, Dangi P, Choudhary M. Actinomycetes : Source , Identification , and Their Applications Actinomycetes : Source , Identification , and Their Applications. 2019;(February).

162. Yoon SH, Ha SM, Kwon S, et al. Introducing EzBioCloud: A taxonomically united database of 16S rRNA gene sequences and whole-genome assemblies. *Int J Syst Evol Microbiol*. 2017;67(5):1613-1617. doi:10.1099/ijsem.0.001755

163. Yoon S-H, Ha S, Lim J, Kwon S, Chun J. A large-scale evaluation of algorithms to calculate average nucleotide identity. *Antonie Van Leeuwenhoek*. 2017;110(10):1281-1286.

164. Van der Meij A, Worsley SF, Hutchings MI, van Wezel GP. Chemical ecology of antibiotic production by actinomycetes. *FEMS Microbiol Rev*. 2017;41(3):392-416.

7 Supplementary

Table S 1. Table of morphological characteristics of genus *Streptomonospora* on ISP media. All media were adjusted to pH 7.2 and supplemented with NaCl 7-10%; the strains were cultivated on these media at 28°C for 14 days before being observed. Diffusible pigments were produced on most of the media tested. 1, *S.* M2^{T}, 2, *S.* M3, 3, *S. halophila* DSM45075^{T}, 4, *S. sediminis* DSM 45723^{T}, 5, *S. arabica* DSM 45083^{T}, 6, *S. alba* DSM 44589^{T}, 7, *S. algeriensis* DSM 45604^{T} 8, *S. amylolytica* DSM 45171^{T}, 9, *S. flavalba* DSM 45155^{T}, 10, *S. halotolerans* CGMCC 4.7218^{T}, 11, *S. nanhaiensis* KCTC 2914^{T}, 12, *S. salina* DSM 44593^{T}, 13, *S. tuzyakensis* DSM 45930^{T}. All data are from this study. Med, Medium ,– No pigment.

Med	Features	**1**	**2**	**3**	**4**	**5**	**6**	**7**	**8**	**9**	**10**	**11**	**12**	**13**
Isp2	Substrate mycelium	Honey yellow	Maize yellow	Honey yellow	light ivory	Maize yellow	Sand yellow	Maize yellow	Sand yellow	Honey yellow	Single yellow	Beige	Maize yellow	Golden yellow
	Aerial mycelium	pure white	Signal white	signal white	No	No	Cream white	Grey white	No	No	Single white	No	Pure white	Cream
	Soluble pigments	lemon yellow		No	No	No	No	No	Sand yellow	No	Sand yellow	NO	Maize yellow	No
	Substrate mycelium	White	Brown beige	Ivory	Light ivory	Sand yellow	White	Sand yellow	Sand yellow	Ivory	Ivory	No	Beige	Single yellow

ISP3	Aerial mycelium	pure white	pure white	pure white	No	Pure white	Cream white	Grey white	Grey white	Pure white	Single white	No	Pure white	Cream
	Soluble pigments	Ivory	Sand yellow	No	Ivory	Sand yellow	No	Sand yellow	Beige	Sandy yellow	Ivory	No	Sand yellow	Sand yellow
ISP4	Substrate mycelium	white	Light ivory	Light ivory	light ivory	Light ivory	light ivory	Ivory	Ivory	Ochre yellow	Light ivory	Sand yellow	Light ivory	Honey yellow
	Aerial mycelium	No	No	signal white	Pure white	No	Cream white	Grey white	Grey white	No	No	No	Oyster white	Cream
	Soluble pigments	No	No	No	No	No	No	Sand yellow	Light ivory	Light ivory	Light ivory	No	Ivory	Sand yellow
ISP5	Substrate mycelium	Light ivory	Sand yellow	Ivory	Ivory	Ivory	Ivory	Ivory	Oyster white	Sandy yellow	Ivory	Sand yellow	Ivory	Ochre yellow
	Aerial mycelium	Pure white	Pure white	signal white	Pure white	Pure white	Cream white	Grey white	Grey white	Pure white	Single white	No	Pure white	Cream
	Soluble pigments	Light ivory	No	no	Light ivory	Light ivory	No	Ivory	Light ivory	Ivory	Light ivory	No	Ivory	Ivory

	Substrate mycelium	Golden yellow	Maize yellow	Maize yellow	Ivory	Sand yellow	Golden yellow	Maize yellow	Honey yellow	Maize yellow	Gold yellow	Beige	Honey yellow	Maize yellow
ISP 6	Aerial mycelium	Pure white	signal white	No	No	No	Grey white	Grey white	No	Pure white	No	No	Grey white	Cream
	Soluble pigments	No	No	No	No	Sand yellow	No	Gold yellow	No	Honey yellow	Gold yellow	No	No	Golden yellow
	Substrate mycelium	Ivory	Beige brown	Golden yellow	Ivory	Brown yellow	Light ivory	Sand yellow	Ivory	Maize yellow	Bright orange	Sand yellow	Maize yellow	Maize yellow
ISP7	Aerial mycelium	Pure white	Signal white	cream	Pure white	Grey white	Grey white	Grey white	Grey white	Pure white	Single white	Pure white	Pure white	Cream
	Soluble pigments	Light ivory	Beige	sand yellow	Light ivory	Beige	No	Sand yellow	Light ivory	Ivory	Beige	No	Single yellow	Single yellow
	Substrate mycelium	Ochre yellow	Pale brown	Brown beige	Curry	Clay Brown	Ochre yellow	Sand yellow	Ivory	Brawn beige	Khaki Grey	Khaki green	Brawn beige	Golden yellow
SSM +T	Aerial mycelium	Pure white	cream	pure white	Pure white	Pure white	Grey white	Grey white	No	Pure white	no	No	Pure white	Cream

	Soluble pigments	Light ivory	Brown beige	Ivory	Ivory	Olive brown	No	Beige	Sand yellow	Beige	Sand yellow	No	Sand yellow	Golden yellow
SSM-T	Substrate mycelium	Ochre yellow	Sand yellow	Olive yellow	Curry	Green beige	Ochre yellow	Sand yellow	Ivory	Maize yellow	Khaki grey	Green brawn	Curry	Golden yellow
	Aerial mycelium	Pure white	Cream	signal white	Pure white	Pure white	Grey white	Grey white	No	Pure white	No	No	Pure white	Cream
	soluble pigments	Light ivory	No	No	Light ivory	Ivory	No	Beige	Ivory	Ivory	Light ivory	No	Light ivory	Honey yellow

Table S 2. API ZYM and API Coryne test results of M2^T and all members of genus *Streptomonospora*. Data are from this study, for all strains phosphatases alkaline, esterase lipase (C8), leucine aryl amidase, valine aryl amidase, phosphatase acid, naphthol-AS-BI-phosphohydrolase, phosphatase acid, alpha glucosidase, beta glucosidase and chymotrypsin were positive while all members were negative for pyrazinamidase, xylose fermentation, beta glucuronides, mannitol, maltose, ribose fermentation, lactose fermentation ,glucose fermentation and sucrose fermentation . 1, *S.* M2^T, 2, *S.* M3, 3, *S. halophila* DSM45075^T, 4, *S. sediminis* DSM 45723^T, 5, *S. arabica* DSM 45083^T, 6, *S. alba* DSM 44589^T, 7, *S. algeriensis* DSM 45604^T, 8, *S. amylolytica* DSM 45171^T, 9, *S. flavalba* DSM 45155^T, 10, *S. halotolerans* CGMCC 4.7218^T, 11, *S. nanhaiensis* KCTC 29145^T, 12, *S. salina* DSM 44593^T, 13, *S. tuzyakensis* DSM 45930^T. + Positive, - negative, w Weak, v Variable.

	1	2	3	4	5	6	7	8	9	10	11	12	13
Tests													
Api ZYM:													
Phosphatases alkaline	+	+	+	+	+	+	+	+	+	+	+	+	+
Esterase (C4)	+	+	+	+	+	+	+	+	+	+	+	+	+
Esterase lipase (C8)	+	+	+	+	+	+	-	+	+	+	+	+	+
Lipase (C14)	-	-	+	-	-	+	+	-	-	+	+	+	+
Leucine arylamidase	+	+	+	+	+	+	+	+	+	+	+	+	+
Valine arylamidase	+	+	+	+	+	+	+	+	+	+	+	+	+
Cystine arylamidase	-	+	+	+	+	+	+	+	+	+	+	+	+
Trypsin	-	+	-	-	-	+	-	-	+	-	-	+	+
Chymotrypsin	-	+	+	+	+	+	+	+	+	-	-	+	+
Phosphatase acid	+	+	+	+	+	+	+	+	+	+	+	+	+

Naphthol-AS-BI-phosphohydrolase	+	+	+	+	+	+	+	+	+	+	+	+	+
α- galactosidase	+	+	+	+	+	+	+	+	+	+	+	-	-
β -galactosidase	-	-	+	+	+	+	+	+	+	-	-	+	-
β- glucuronidase	-	-	-	-	-	-	-	-	+	-	-	+	-
α -glucosidase	+	+	+	+	+	+	+	+	+	+	+	+	+
β - glucosidase	+	+	-	+	+	+	-	+	+	+	+	+	+
N-acetyl-β-glucoseamidase	+	+	-	+	+	+	+	+	+	+	+	-	+
α -mannosidase	-	-	-	-	+	-	-	-	-	-	-	-	-
α - fucosidase	-	-	-	-	-	-	-	-	-	-	-	-	-

Table S 3. Carbon utilization in strain M2^T and all members of genus *Streptomonospora.* 1, *S.* M2^T, 2, *S.* M3, 3, *S. halophila* DSM 45075^T, 4, *S. sediminis* DSM 45723^T, 5, *S. arabica* DSM 45083^T, 6, *S. alba* DSM 44589 ^{T}, 7, *S. algeriensis* DSM 45604^T, 8, *S. amylolytica* DSM 45171^T, 9, *S. flavalba* DSM 45155^T, 10, *S. halotolerans* CGMCC 4.7218^T, 11, *S. nanhaiensis* KCTC 29145^T, 12, *S. salina* DSM 44593^T, 13, *S. tuzyakensis* DSM 45930^T. + positive result; - negative result; (+) weakly positive result.

Carbon utilization		1	2	3	4	5	6	7	8	9	10	11	12	13
Glucose		+	+	+	+	+	+	+	+	+	+	+	+	+
Arabinose		+	+	+	+	+	+	+	+	+	+	+	+	-
Sucrose		-	-	-	+	-	+	-	+	+	+	+	-	+
Xylose		-	+	+	+	+	-	+	+	+	+	+	+	+
Inositol		-	-	-	+	-	+	-	+	+	-	(+)	-	-
Mannose		(+)	-	+	+	+	+	-	-	+	+	+	-	+
Fructose		+	+	+	+	+	+	+	-	+	+	+	+	+
Rhamnose		+	+	+	-	+	(+)	+	+	+	+	+	+	+
Raffinose		-	-	-	+	+	(+)	-	-	+	-	(+)	-	-
Cellulose		-	-	-	-	+	(+)	0	+	+	0	(+)	-	-

Table S 4. Some physiological and chemical properties of genus *Streptomonospora.*1, *S.* M2^T, 2, *S.* M3, 3, *S. halophila* DSM45075^T, 4, *S. sediminis* DSM 4572^T, 5, *S. arabica* DSM 45083^T, 6, *S. alba* DSM 44589^T, 7, *S. algeriensis* DSM 45604^T, 8, *S. amylolytica* DSM 45171^T, 9, *S. flavalba* DSM 45155^T, 10, *S. halotolerans* CGMCC 4.7218^T, 11, *S. nanhaiensis* KCTC 29145^T, 12, *S. salina* DSM 44593^T, 13, *S. tuzyakensis* DSM 45930^T, nd: not detected.

Characteristic	1	2	3	4	5	6	7	8	9	10	11	12	13
single spore surface	smooth	smooth	Wrinkled /smooth	Wrinkled	smooth/ Wrinkled	nd	nd	nd	nd	Wrinkled	Smooth	Wrinkled	smooth
NaCl concentration for growth (%, w/v)	0-15	0-15	5-20	0-20	0-15	5-25	0-7.5	5-20	5-20	0-10	0-20	5-20	4-20
(Optimum)	7-10	7-10	10	0-7	5	10	0-5	10	10	nd	0-7	15	10
Growth temperature °C	20-37	20-37	20-45	15-45	10-40	20-45	20-45	20-45	20-45	20-37	10-50	nd	28-37
(Optimum) °C	30	28-30	28-30	28	28-30	28	25-35	37	37	28	37	28	37
Whole-cell sugars	Gal, Glu, Rib,	Gal, Glu,	Gal	Gal, Glu, Rib	Glu, Gal	Gal, Ara	Gal, Glu, Rib,	Gal	Gal	Gal, Glu, Rib	Glu, Gal	Glu, GAL,	Gal, Glu, Rib

		Rib,					Man					Rib, Ara, XYL, Man	
Predominant menaquinones (> 10%)	MK-10(H4), MK-10(H6), MK-10(H8), MK-11(H6)	MK-10(H4), MK-10(H6), MK-10(H8), MK-11(H6)	MK-10(H8) , MK-10(H6), MK-11(H8)	MK-10(H6), MK-11(H4,6,8)	MK-10(H4), MK-10(H6)	MK-10(H8) , MK-10(H6)	MK-10(H4), MK-11(H4)	MK-10(H6,8), MK-9(H8)	MK-10(H6,8), MK-9(H8)	MK-10(H4) MK-10(H6)	MK-10(H4,6), MK-11(H4,6)	MK-10(H8), MK-10(H6), MK-10(H4)	MK-10(H6,8)
Diagnostic phospholipids	DPG, PG, PC, PE , PI, GL, PL	DPG, PG, PC, PE, PI, GL,PL	DPG, PG, PC, PIM, PI, PL	DPG, PC, PG, PI, PIM, PGL, GL, PL	PC, PIM, DPG, PME, PG, PI	PG, PE, PI, DPG, MPE, PS,PC, PL	PME, DPG, PG, PC, PIM	DPG, PG, PC, PIM, PI	DPG, PG, PC, PIM, PI	PG, PE, PI, DPG, PIM, GL, PC, PL	DPG, PC, PG, PI, PIM, PGL, GL, PL	PG, PI, PC, 2MPE, PL	DPG, PG, PC
Major fatty acid (> 10%)	i-C16 : 0 , ai-C17 : 0, 10-methyl	i-C16 : 0 , ai-C17 : 0, 10-methyl	i-C16 : 0 , ai-C17 : 0, 10-methyl	i-C160, C16:0	iso-C16 : 0, 10-methyl	ai-C17 : 0 , i-C16 : 0	ai-c15:00, i-C16 : 0	ai-C17i:0 , C16:0	ai-C17i:0, C16:0	MK-10 (H2,4,6, 8)	i-C16	ai-C17: 0 (26.0 %), i-C16 : 0 (25.1 %)	ai-C17: 0, 10-methyl C18: 0,

	C18 : 0	C18 : 0	C17 : 0, 10-methyl C18 : 0		C18 :0 , ai:C17 : 0, iso-C17 : 0, iso-C18 :0								i-C16:0
DNA G+C (mol%)	72.1	72.1	72.1	70.7	72.3	74.4	71.1	71.2	72.5	71.8	74.4	72.9	71.1

Table S 5. Statistic data of Genome strain M2^{T} get from IMGM database.

Attribute	Value	Percentage%
DNA, total number of bases	5814190	100%
DNA coding number of bases	4883388	83.9
DNA G+C number of bases	4193912	72.1
DNA scaffolds	2	100
CRISPR Count	3	
Genes total number	5218	100
Protein coding genes	5107	97.8
Regulatory and miscellaneous features	15	0.2
RNA genes	96	1.8
rRNA genes	15	0.2
5S rRNA	5	0.1
16S rRNA	5	0.1
23S rRNA	5	0.1
tRNA genes	58	1.1
Other RNA genes	23	0.4
Function unknown	5171	74.5
Protein coding genes with function prediction	3539	67.8
coding genes without function prediction	1568	30.0
Protein coding genes with enzymes	1087	6.0
Protein coding genes coding signal peptides	315	
Protein coding genes with COGs3	3569	68.4
Protein coding genes with KOGs3	988	18.8
Protein coding genes with Pfam[3]	3890	74.5
Protein coding genes with TIGRfam[3]	1122	21.5
Protein coding genes with SMART	1042	19.9
Protein coding genes with SUPERFam	4047	78.0
COG clusters	1679	47.0

Pfam clusters	2026	52.0
TIGRfam clusters	992	82.3

Table S 6. Number of genes identified in strains $M2^T$ associated with functional categories in COG.

Function	Code	Value	Percentage %
Amino acid transport and metabolism	[E]	331	7.6
Carbohydrate transport and metabolism	[G]	337	7.8
Cell cycle control, cell division, chromosome partitioning	[D]	47	1.0
Cell motility	[N]	13	0.3
Cell wall/membrane/envelope biogenesis	[M]	178	4.1
Chromatin structure and dynamics	[B]	1	0.02
Coenzyme transport and metabolism	[H]	242	5.6
Cytoskeleton	[Z]	1	0.02
Defense mechanisms	[V]	131	3.04
Energy production and conversion	[C]	248	5.7
Extracellular structures	[W]	12	0.28
Function unknown	[S]	206	4.7
General function prediction only	[R]	537	12.4
Inorganic ion transport and metabolism	[P]	219	5.0
Intracellular trafficking, secretion, and vesicular transport	[U]	36	0.84
Lipid transport and metabolism	[I]	226	5.2

Mobilome: prophages, transposons	[X]	45	1.0
Nucleotide transport and metabolism	[F]	88	2.0
Posttranslational modification, protein turnover, chaperones	[O]	159	3.6
RNA processing and modification	[A]	1	0.02
Replication, recombination and repair	[L]	123	2.6
Secondary metabolites biosynthesis, transport and catabolism	[Q]	215	4.9
Signal transduction mechanisms	[T]	229	5.3
Transcription	[K]	447	11.0
Translation, ribosomal structure and biogenesis	[J]	206	4.7
Not in COG	[NA]	1649	31.6

Region	Type	From	To	Most similar known cluster		Similarity
Region 1	terpene	423,490	438,281	geosmin	Terpene	100%
Region 2	ectoine	565,443	574,647	ectoine	Other	100%
Region 3	NRPS	880,824	934,147	A54145	NRP	5%
Region 4	thiopeptide , bacteriocin	1,419,328	1,455,671	radamycin / globimycin	RiPP	94%
Region 5	terpene	1,908,147	1,934,887	isorenieratene	Terpene	100%
Region 6	NRPS	3,239,084	3,306,974	fuscachelin A / fuscachelin B / fuscachelin C	NRP	88%
Region 7	T1PKS	3,470,426	3,531,958	meridamycin	NRP + Polyketide	60%
Region 8	T1PKS , T3PKS	3,545,304	3,647,129	aculeximycin	Polyketide	44%
Region 9	ectoine	3,655,290	3,665,664	kosinostatin	NRP + Polyketide	13%
Region 10	NRPS-like	4,271,276	4,314,656	SapB	RiPP:Lanthipeptide	100%
Region 11	lanthipeptide	5,041,547	5,066,613			
Region 12	T1PKS	5,566,535	5,614,151			

Figure S 1. List of predicted secondary metabolite gene clusters for strain M2^T identified by analysis of the M2^T genome sequence with the bioinformatic tool antiSMASH 5.0

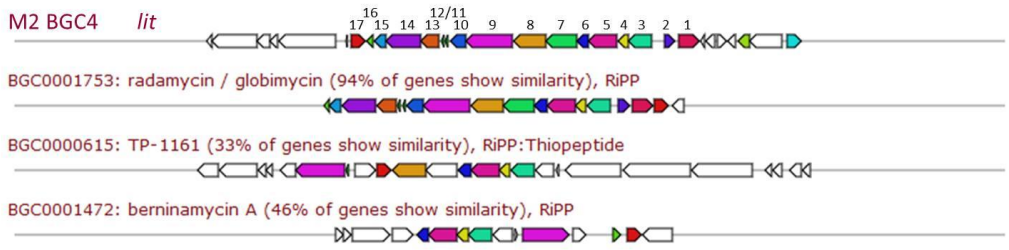

Figure S 2. BGC4 from strain M2^T in comparison to other known thiopeptide gene clusters. BGC4 from strain M2^T in comparison to other known thiopeptide gene clusters. The predicted M2^T biosynthetic genes are numbered as listed in Table S1. Homologous genes are indicated by the same arrow color. RiPP = ribosomally synthesized and post-translationally modified peptide.

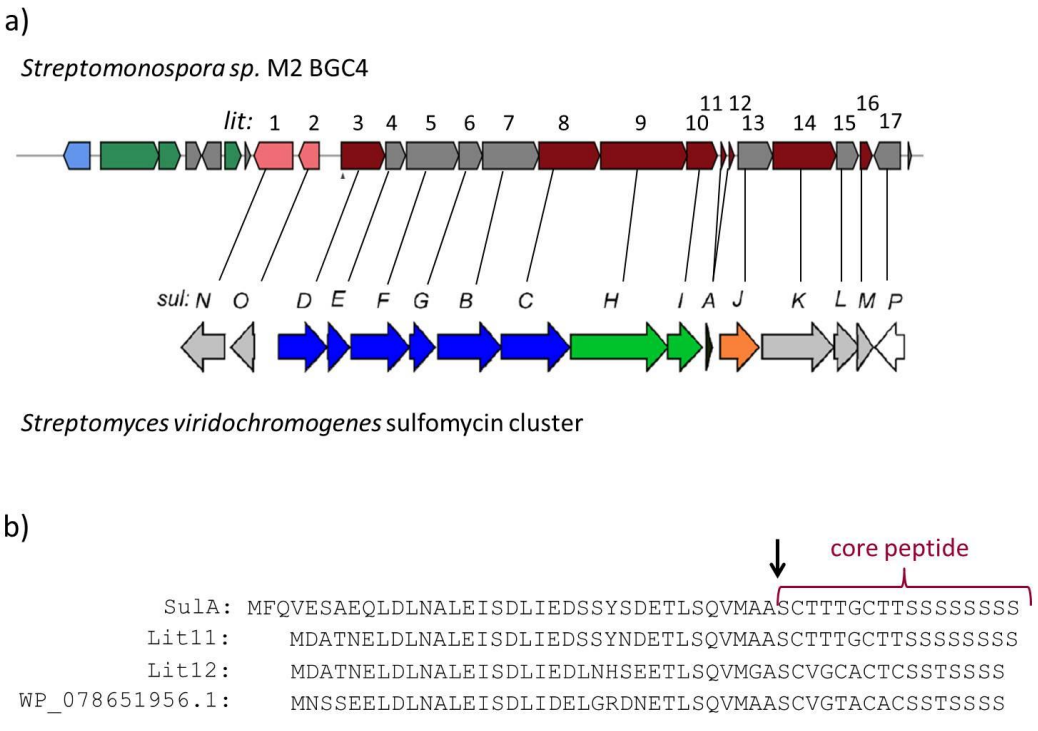

Figure S 3. a) Schematic presentation of BGC4 from strain *Streptomonospora* sp. M2^T (upper part) and the sulfomycin cluster from *Streptomyces viridochromogenes*.. b) Alignment of amino acid sequences from different precursor peptides from thiopeptide producers. SulA: sulfomycin producer *S. viridochromogenes*; Lit11/12: litoralimycin producer *S.* sp. M2^T, WP_078651956.1: globimycin/radamycin producer *S. globisporus* subsp. *globisporus*. Red brace indicates core peptide sequence; black arrow indicated pre-peptide cleavage position.

Table S 7. M2^T BGC4 genes and their deduced functions. ORF, open reading frame; †ID/SM, % identity/similarity of amino acid sequences. *S. alba, Streptomonospora alba; S. auratus, Streptomyces auratus; S. incarnatus, Streptomyces incarnatus; S.* sp. PA3, *Streptomonospora* sp. PA3; *S. virido., Streptomyces viridochromogenes* ATCC 29776*; M. nebraskense, Mycobacterium nebraskense; N. gilva, Nocardiopsis gilva; N. halotolerans, Nocardiopsis halotolerans; N. sinuspersic, Nocardiopsis sinuspersic.*

Gene-No.	**ORF**	**Predicted function**	**ID/SM†**	**Matched strain**	**Accession number**	**Sulfomycin-related homolog**	**ID/SM†**	**Matched strain**	**Accession number**
6160	*orf1*	ABC transporter ATP-binding protein	83/87	*S. alba*	WP_040270763				
6155	*orf2*	two-component sensor histidine kinase	62/70	*S.* sp. PA3	WP_156002281				
6150	*orf3*	response regulator transcription factor	84/90	*S. alba*	WP_040270764				
6145	*orf4*	hypothetical protein	61/73	*S. alba*	WP_040270745				
6140	*orf5*	hypothetical protein	70/81	*N. halotolerans*	WP_017571558				
6135	*orf6*	MarR family transcriptional regulator	77/84	*N. sinuspersic*	WP_077690797				
6130	*orf7*	RidA family protein	87/94	*N. gilva*	WP_051060844				
6125	*lit1*	cytochrome P450	88/93	*S. auratus*	WP_040899041	SulN	87/93	*S. virido.*	QJC58222
6120	*lit2*	class I SAM-dependent methyltransferase	81/89	*S. auratus*	WP_106430513	SulO	81/90	*S. virido.*	QJC58216
6115	*lit3*	YcaO-like family protein	84/90	*S. auratus*	WP_040899039	SuD	84/90	*S. virido.*	QJC58217

6110	*lit4*	cyclodehydratase	84/89	*S. auratus*	WP_006605028	SulE	83/89	*S. virido.*	QJC58220
6105	*lit5*	TpaE	82/89	*S. incarnatus*	AKJ11409	SulF	82/89	*S. virido.*	QJC58219
6100	*lit6*	TpaF	80/86	*S. incarnatus*	AKJ11410	SulG	81/86	*S. virido.*	QJC58218
6095	*lit7*	hypothetical protein	73/82	*S. auratus*	WP_144044220	SulB	72/80	*S. virido.*	QJC58223
6090	*lit8*	YcaO-like family protein	82/86	*S. auratus*	WP_051007002	SulC	80/87	*S. virido.*	QJC58224
6085	*lit9*	lantibiotic dehydratase	86/91	*S. auratus*	WP_106430410	SulH	85/91	*S. virido.*	QJC58225
6080	*lit10*	hypothetical protein	81/87	*S. auratus*	WP_078568713	SulI	79/85	*S. virido.*	QJC58226
6075	*lit11*	thiocillin/thiostrepton family thiazolyl peptide	82/91	*S. auratus*	WP_051006902	SulA	81/94	*S. virido.*	QJC58227
6070	*lit12*	thiocillin/thiostrepton family thiazolyl peptide	76/85	*S. auratus*	WP_051006902	SulA	68/88	*S. virido.*	QJC58227
6065	*lit13*	hypothetical protein	57/88	*S. incarnatus*	AKJ11416	SulJ	75/87	*S. virido.*	QJC58228
6060	*lit14*	radical SAM protein	91/95	*S. incarnatus*	AKJ11417	SulK	91/95	*S. virido.*	QJC58229
6055	*lit15*	hypothetical protein	82/89	*S. incarnatus*	AKJ11418	SulL	80/89	*S. virido.*	QJC58230
6050	*lit16*	hypothetical protein	90/95	*S. auratus*	WP_006605017	SulM	88/94	*S. virido.*	QJC58231
6045	*lit17*	23S rRNA methyltransferase	83/90	*S. incarnatus*	AKJ11419	SulP	83/89	*S. virido*	QJC58232
6040	*orf8*	IS481 family transposase	77/87	*M. nebraskense*	WP_047324341				

Table S 8. Table of API ZYM and API coryne test results of strain 86D and closest strains. 1, *Streptomyces* sp. 86D^T, 2, *Streptomyces spiralis* NBRC 14215^T, 3, *Streptomyces violaceus* NRRL B-2867^T, 4, *Streptomyces roseoviolaceus* DSM 40277^T. + positive, - negative, (+) weakly positive.

Api ZYM	1	2	3	4
Phosphatase alkaline	+	+	+	+
Esterase (C4)	+	(+)	(+)	+
Esterase Lipase (C8)	+	(+)	+	+
Lipase (C14)	-	-	(+)	-
Leucin arylamidase	+	+	+	+
Valine arylamidase	+	+	+	+
Cystine arylamidase	(+)	(+)	-	+
Trypsin	(+)	-	-	+
Chymotrypsin	-	-	+	+
Phosphatase acid	+	+	+	+
Naphthol-AS-BI-phosphohydrolase	+	+	+	+
alpha galactosidase	(+)	+	-	+
beta galactosidase	+	(+)	+	+
beta glucuronidase	-	-	-	-
alpha glucosidase	+	+	+	+
beta glucosidase	+	-	+	+
N-acetyl-beta-glucoseamidase	+	+	+	+
alpha mannosidase	+	+	+	+
alpha fucosidase	(+)	-	-	-
Api Coryne				
Nitrate reduction	-	-	-	-
Pyraziamidase	-	-	-	-
Pyrrolidonyl arylamidase	+	-	-	-
Alkaline phosphatase	+	+	-	+
beta glucuronidase	-	-	-	-
beta galactosidase	+	-	+	+
alpha glucosidase	+	+	+	+
N-acetyl-beta glucoseamidase	-	+	(+)	+

Esculin (beta glucosidase)	+	-	-	-
Urease	(+)	(+)	+	-
Gelatin (hydrolysis)	+	+	+	+
Glucose fermentation	-	-	-	-
Ribose fermentation	-	-	-	-
Xylose fermentation	-	-	-	-
Mannitol fermentation	-	-	-	-
Maltose fermentation	-	-	-	-
Lactose fermentation	-	-	-	-
Sucrose fermentation	-	-	-	-
Glycogen fermentation	-	-	-	-

Table S 9. Morphology of strain 31sw in comparison with three closest type strains on ISP media. All media were adjusted to pH 7.2 and they were cultivated on these media at 28°C for 14 days before being observed. 1, strain 31sw, 2, *Saccharomonospora cyanea* DSM 44106^{T}, 3, *Saccharomonospora xinjiangensis* DSM 44391^{T}, 4, *Saccharomonospora azurea* DSM 44631^{T}. N: Negative.

Medium		**1**	**2**	**3**	**4**
	Substrate mycelium	Sand yellow	Sand yellow	Sand yellow	Grey beige
Isp2	Aerial mycelium	Cream	Signal white	N	N
	Soluble pigments	N	Ochre yellow	N	N
	Substrate mycelium	Ivory	Sand yellow	Ivory	Chrome green
ISP3	Aerial mycelium	Signal white	White	N	Signal white
	Soluble pigments	N	Light ivory	N	N
	Substrate mycelium	Ivory	Light ivory	Ivory	Oyster white
ISP4	Aerial mycelium	Signal white	Light green	N	Signal white
	Soluble pigments	N	Pebble grey	N	N
	Substrate mycelium	Light ivory	Light ivory	Ivory	Black brown
ISP5	Aerial mycelium	Traffic grey	N	Signal white	Signal white
	Soluble pigments	Light ivory	Pebble grey	N	N
	Substrate mycelium	Sand yellow	Beige		Sand yellow
ISP 6	Aerial mycelium	Cream	N	N	N
	Soluble pigments	N	Brown beige	N	N
	Substrate mycelium	Light ivory	Ivory	Ivory	Khaki grey
ISP7	Aerial mycelium	Traffic grey	White	Signal White	Telegrey4

	Soluble pigments	Light ivory	Stone grey	N	N
	Substrate mycelium	Sand yellow	Ochre yellow	Ivory	Graphite black
SSM+T	Aerial mycelium	Traffic white	Signal white	N	Signal white
	Soluble pigments	N	Green Brawn	N	N
	Substrate mycelium	Sand yellow	Ivory	Ivory	Sand yellow
SSM-T	Aerial mycelium	Traffic white	N	N	Signal white
	Soluble pigments	N	Stone grey	N	N

Table S 10. Table of physiological charachteristic of strain 31sw in comparison with three closest type species. 1. strain 31sw, 2, *Saccharomonospora cyanea* DSM 44106 ^{T}, 3, *Saccharomonospora xinjiangensis* DSM 44391^{T}, 4, *Saccharomonospora azurea* DSM 44631^{T}. + positive, (+) weakly positive, - negative.

Api ZYM	**1**	**2**	**3**	**4**
Phosphatase alkaline	+	+	+	+
Esterase (C4)	+	(+)	+	(+)
Esterase Lipase (C8)	+	+	+	+
Lipase (C14)	+	(+)	+	(+)
Leucin arylamidase	+	+	+	+
Valine arylamidase	+	+	+	+
Cystine arylamidase	+	+	+	(+)
Trypsin	-	-	+	-
Chymotrypsin	(+)	-	(+)	(+)
Phosphatase acid	+	+	+	+
Naphthol-AS-BI-phosphohydrolase	+	+	+	+
alpha galactosidase	-	+	-	+
beta galactosidase	-	+	-	(+)
beta glucuronidase	-	-	-	+

alpha glucosidase	+	+	+	+
beta glucosidase	+	+	+	+
N- acetyl-beta-glucoseamidase	+	+	+	(+)
alpha mannosidase	-	-	-	-
alpha fucosidase	-	-	-	-
Api Coryne				
nitrate reduction	+	-	-	-
Pyraziamidase	-	-	-	-
Pyrrolidonyl arylamidase	-	-	-	+
Alkaline phosphatase	+	+	+	+
beta glucuronidase	-	-	-	-
beta galactosidase	-	+	-	-
alpha glucosidase	+	+	+	+
N-acetyl-beta glucoseamidase	+	+	+	-
Esculin (beta glucosidase)	-	+	-	-
Urease	+	-	+	+
Gelatin (hydrolysis)	+	+	+	+
Glucose fermentation	-	-	-	-
Ribose fermentation	-	-	-	-
Xylose fermentation	-	-	-	-
Mannitol fermentation	-	-	-	-
Maltose fermentation	-	-	-	-
Lactose fermentation	-	-	-	-
Sucrose fermentation	-	-	-	-
Glycogen fermentation	-	-	-	-

Table S 11. Table list of isolates based on 16S rRNA gene sequences similarity in EZ biocloud database.

Name of isolates	Closest type strain based on 16S rRNA	Similarity %	Completeness of the sequence %
31SY	*Streptomyces radiopugnans*	97.4	100
86D	*Streptomyces violaceus*	98.02	100
M. semeg 20	*Mycolicibacterium arabiense*	98.34	100
31sw	*Saccharomonospora xinjiangensis*	99.63	100
18w	*Streptomyces amphotericinicus*	98	100
33D	*Streptomyces radiopugnans*	97.4	100
M2	*Streptomonospora halophila*	98.04	100
M3	*Streptomonospora halophila*	98.04	100
86C	*Actinomadura luteofluorescens*	99.01	100
1BOS	*Streptomyces rochei*	99.89	63.4
2BOS	*Streptomyces phaeoluteigriseus*	100	63
5BOS	*Streptomyces galilaeus*	100	61.5
3BOS	*Streptomyces neyagawaensis*	100	61.2
4BOS	*Streptomyces violaceochromogenes*	100	62.1
7POS	*Streptomyces galilaeus*	100	63.1
8POS	*Streptomyces avidinii*	100	63.5
9pos	*Streptomyces roseolus*	99.77	61.5
10POS	*Streptomyces virginiae*	100	63.2
11POS	*Streptomyces avidinii*	100	63.2
125OS	*Streptomyces setonii*	100	61.6

IIIOS	*Streptomyces djakartensis*	99.76	29.3
VIIIOS	*Streptomyces radiopugnans*	99.33	63.6
IXpos	*Streptomyces ambofaciens*	99.78	62
X5os	*Streptomyces phaeoluteigriseus*	99.56	63.1
XIOS	*Streptomyces turgidiscabies*	99.32	61.4
XIIos	*Micromonospora gifhornensis*	99.89	65.6
Mol-2	*Streptomyces spiroverticillatus*	98.96	65.8
MOL-3	*Pararhizobium giardinii*	100	67.9
zar-1	*Paracoccus fontiphilus*	99.12	66.1
zar-4	*Planomonospora algeriensis*	99.89	64.5
zar-5	*Streptomyces phaeoluteigriseus*	99.89	64.5
5hb	*Streptomyces phaeoluteigriseus*	98.53	68.8
5Q	*Streptomyces cinereoruber*	97.79	66.2
5yp	*Streptomyces pseudovenezuelae*	98.27	68.8
31sb	*Micromonospora tulbaghiae*	100	100
41so	*Micromonospora tulbaghiae*	100	100
5br	*Streptomyces phaeoluteigriseus*	98.53	68.7
8b	*Streptomyces plumbiresistens*	97.84	60.3
8E	*Streptomyces galilaeus*	98.53	50.4
8g	*Streptomyces galilaeus*	98.53	52.4
8I	*Streptomyces zinciresistens*	98.27	62.2
8II	*Streptomyces galilaeus*	98.53	63.9
8III	*Streptomyces albidochromogenes*	98.96	62

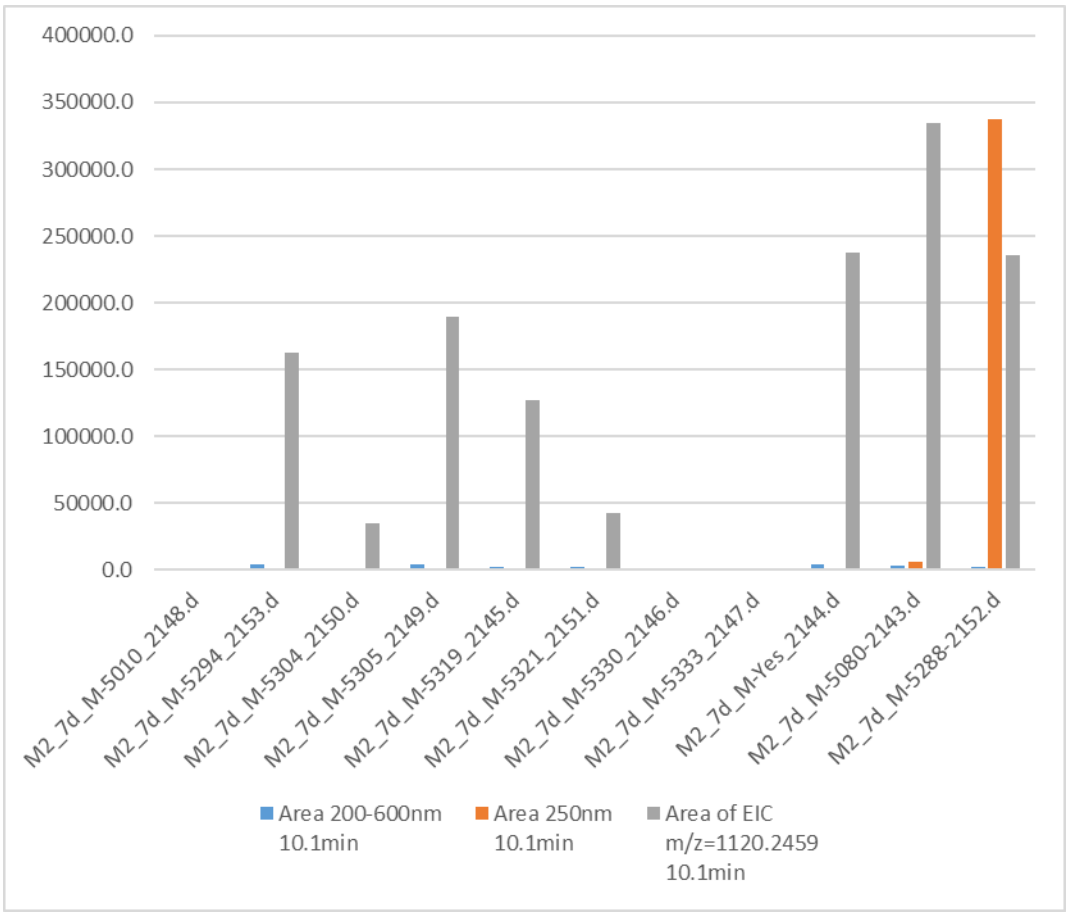

Figure S 4. Optimization of production media for strain M2^{T}.

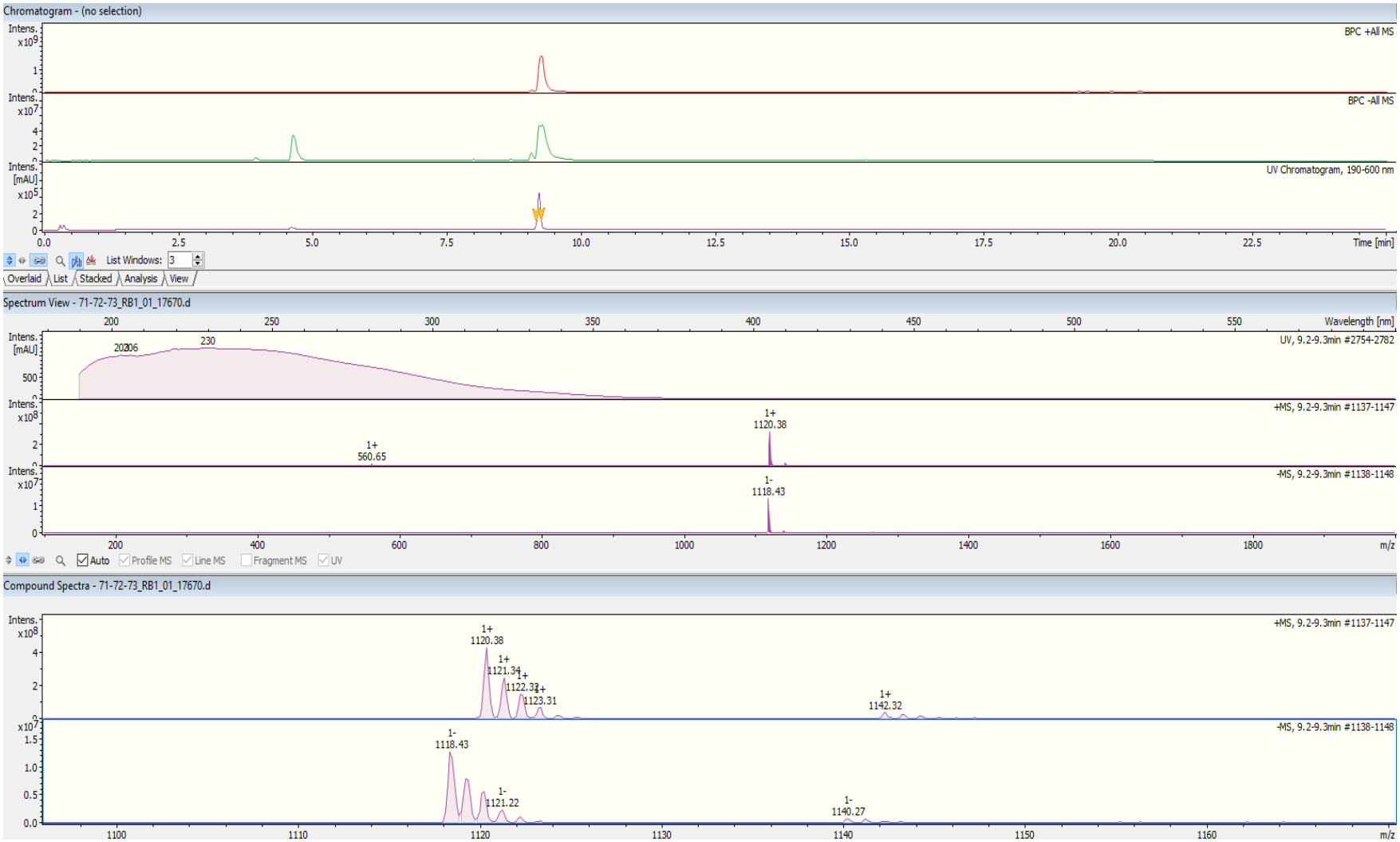

Figure S 5. HPLC-ESIMS spectrum of litoralimycin A (1).

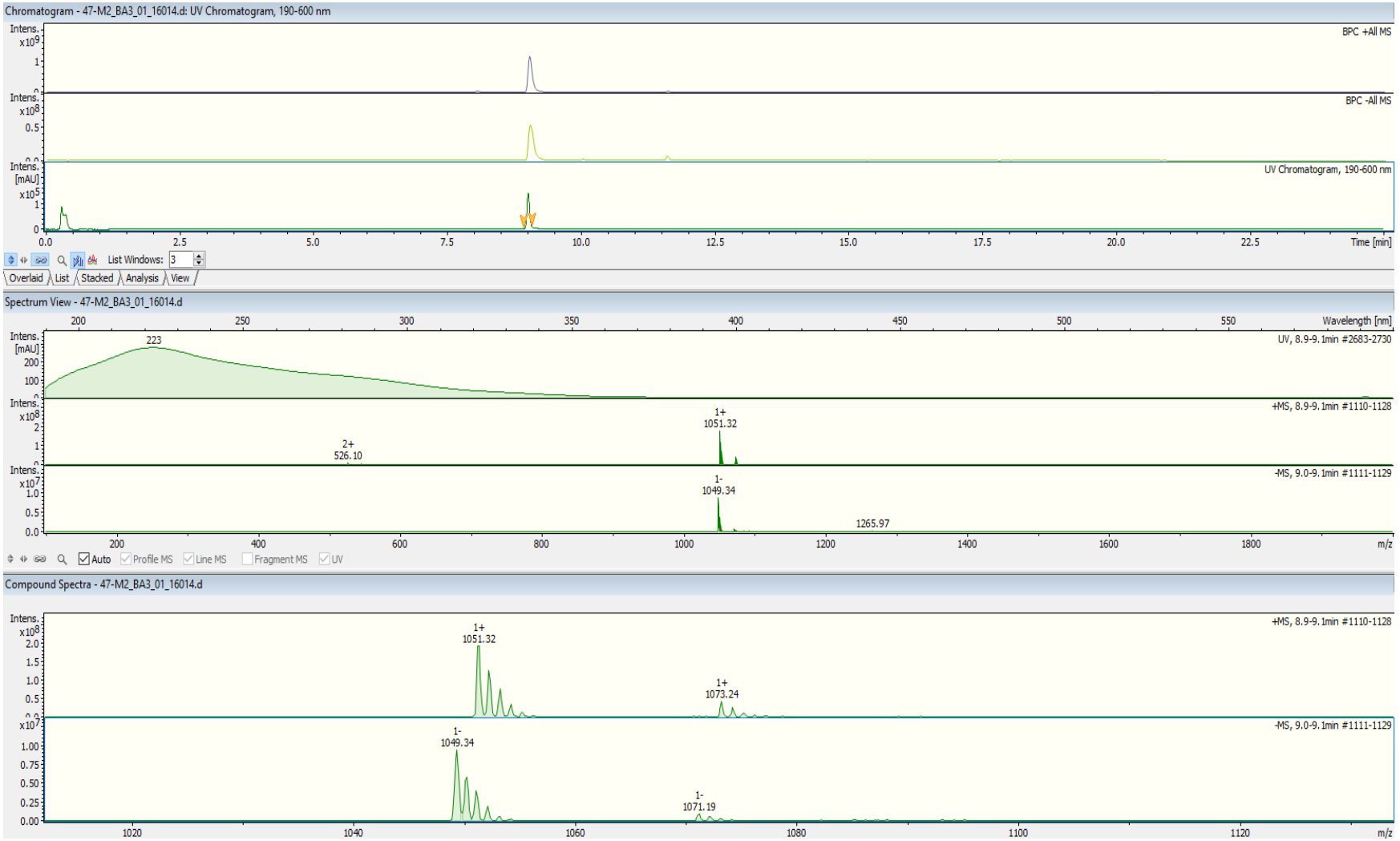

Figure S 6. HPLC-ESIMS spectrum of litoralimycin B (**2**)

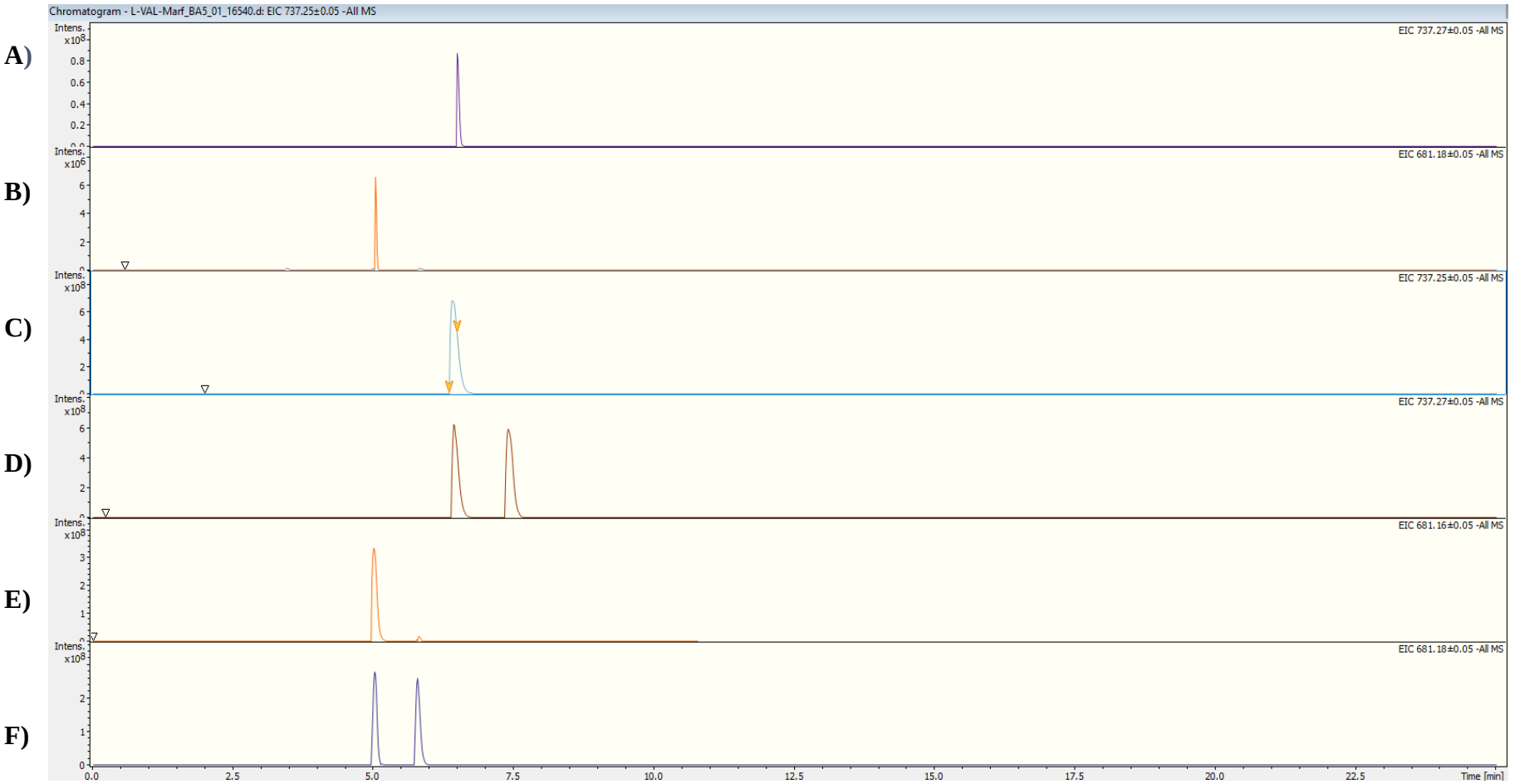

Figure S 7. Marfey derivatization for determination of type and configuration of amino acids in litoralimycin A (**1). A)** Detection of L-valin after ozonolysis, hydrolysis and derivatization with FDAA; B) Detection of L-Alanine after ozonolysis, hydrolysis and derivatization with FDAA; C) FDAA derivative of L-valin standard; D) FDAA derivative of DL-Valin standard; E) FDAA derivative of L-Alanine standard; F) FDAA derivative of DL-Alanine standard.

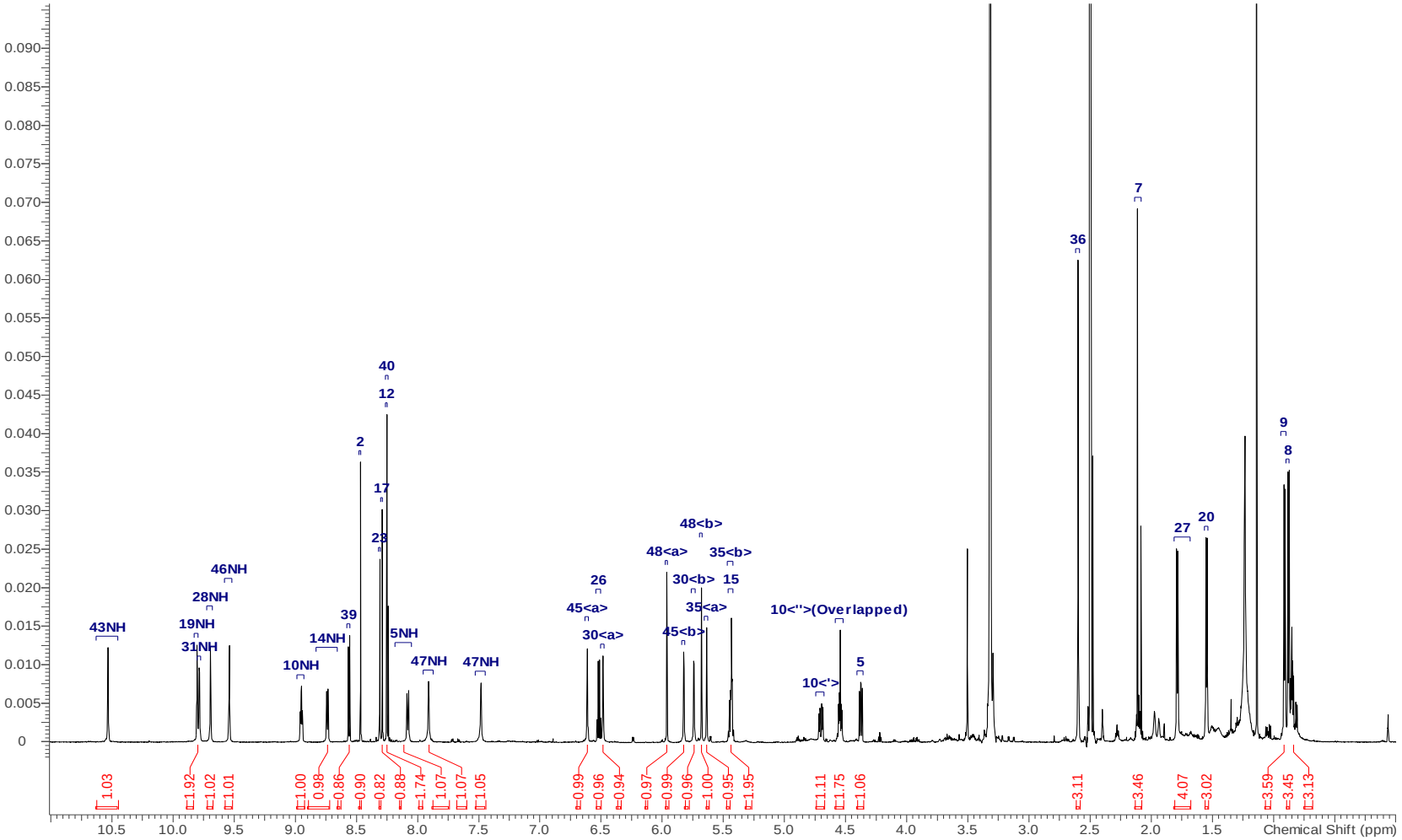

Figure S 8. ^{1}H NMR spectrum (700 MHz, DMSO-d_6) of litoralimycin A (**1**).

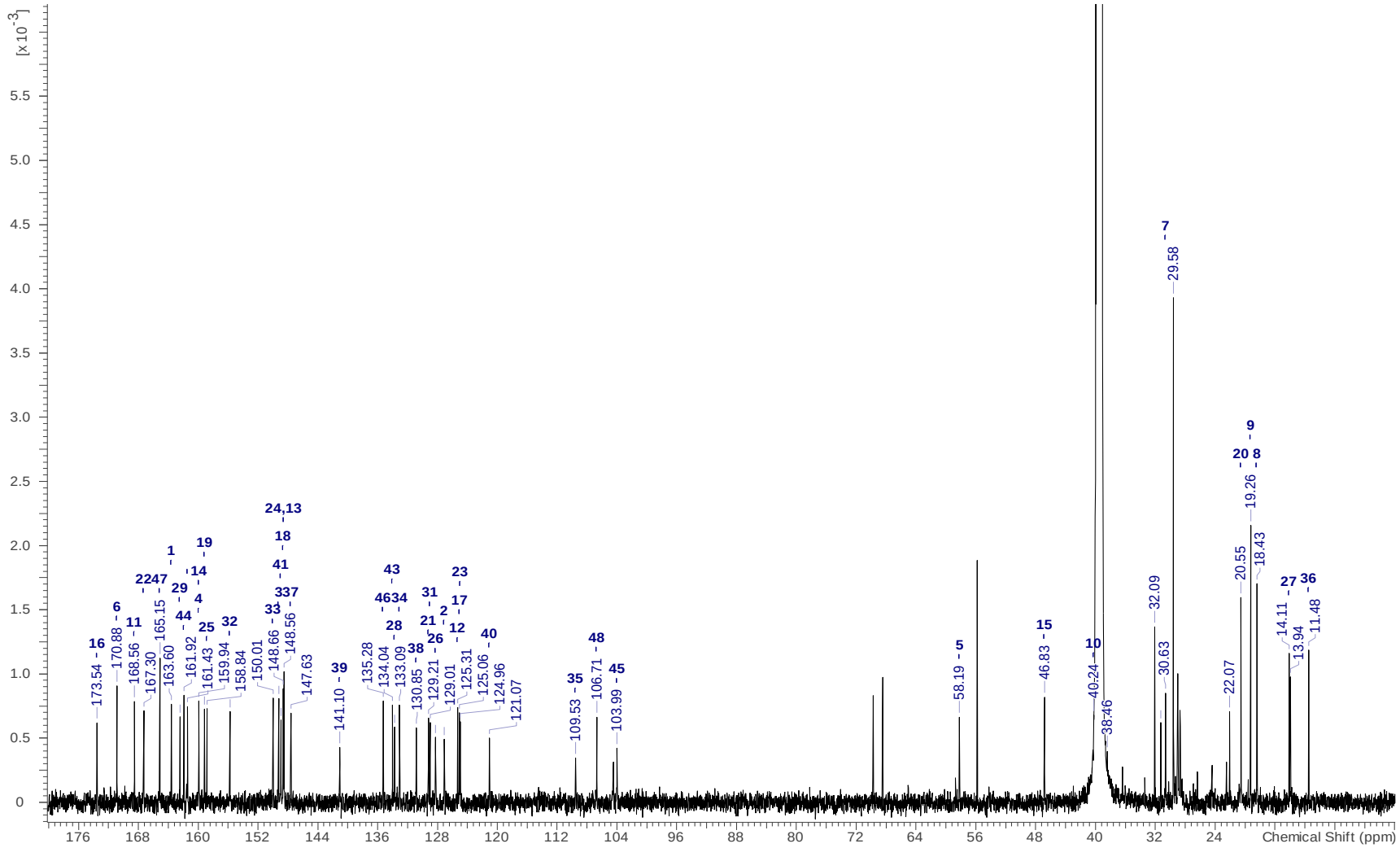

Figure S 9. ^{13}C NMR spectrum (175 MHz, DMSO-d_6) of litoralimycin A (**1**).

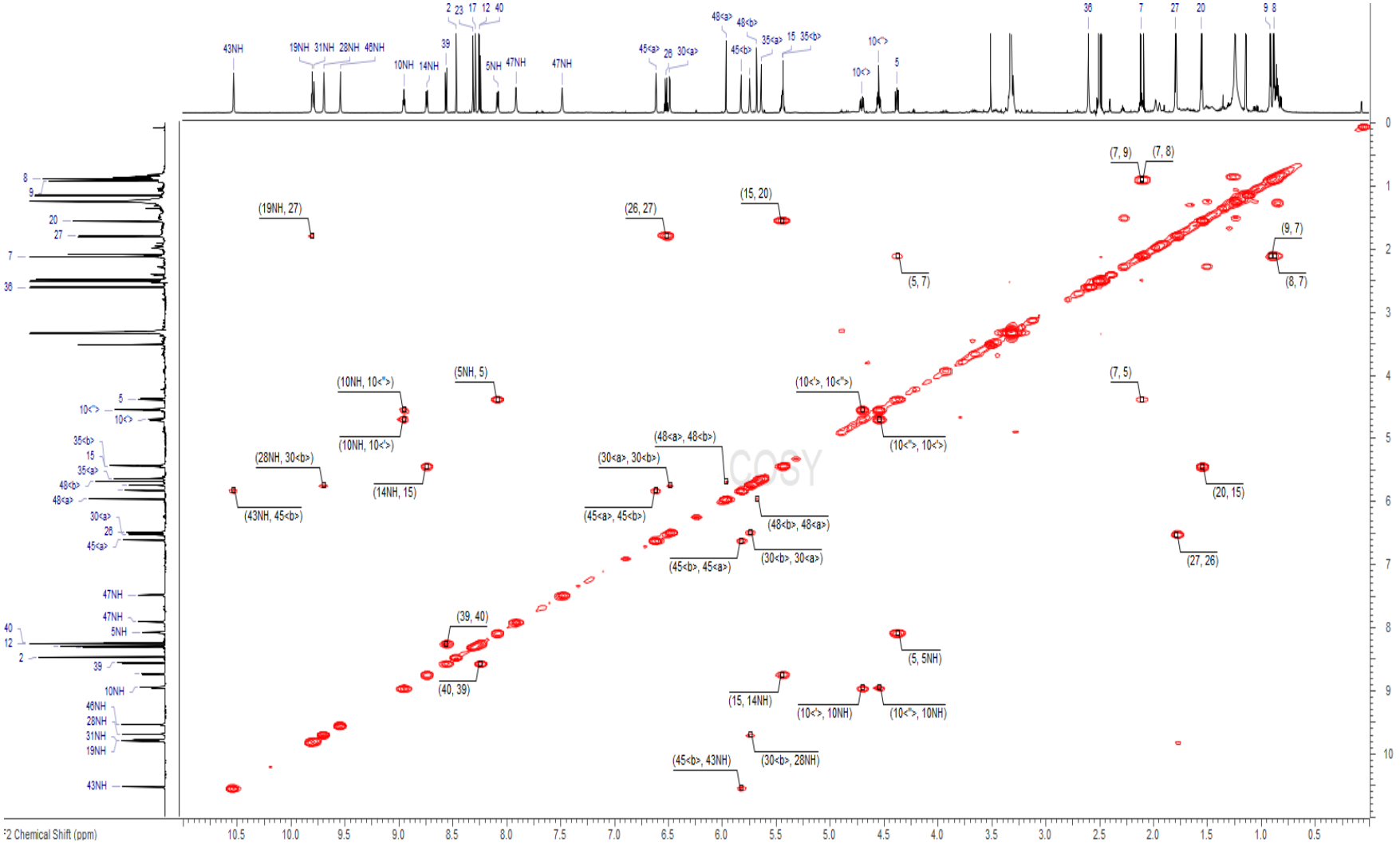

Figure S 10. COSY NMR spectrum (700 MHz, DMSO-d_6) of litoralimycin A (**1**).

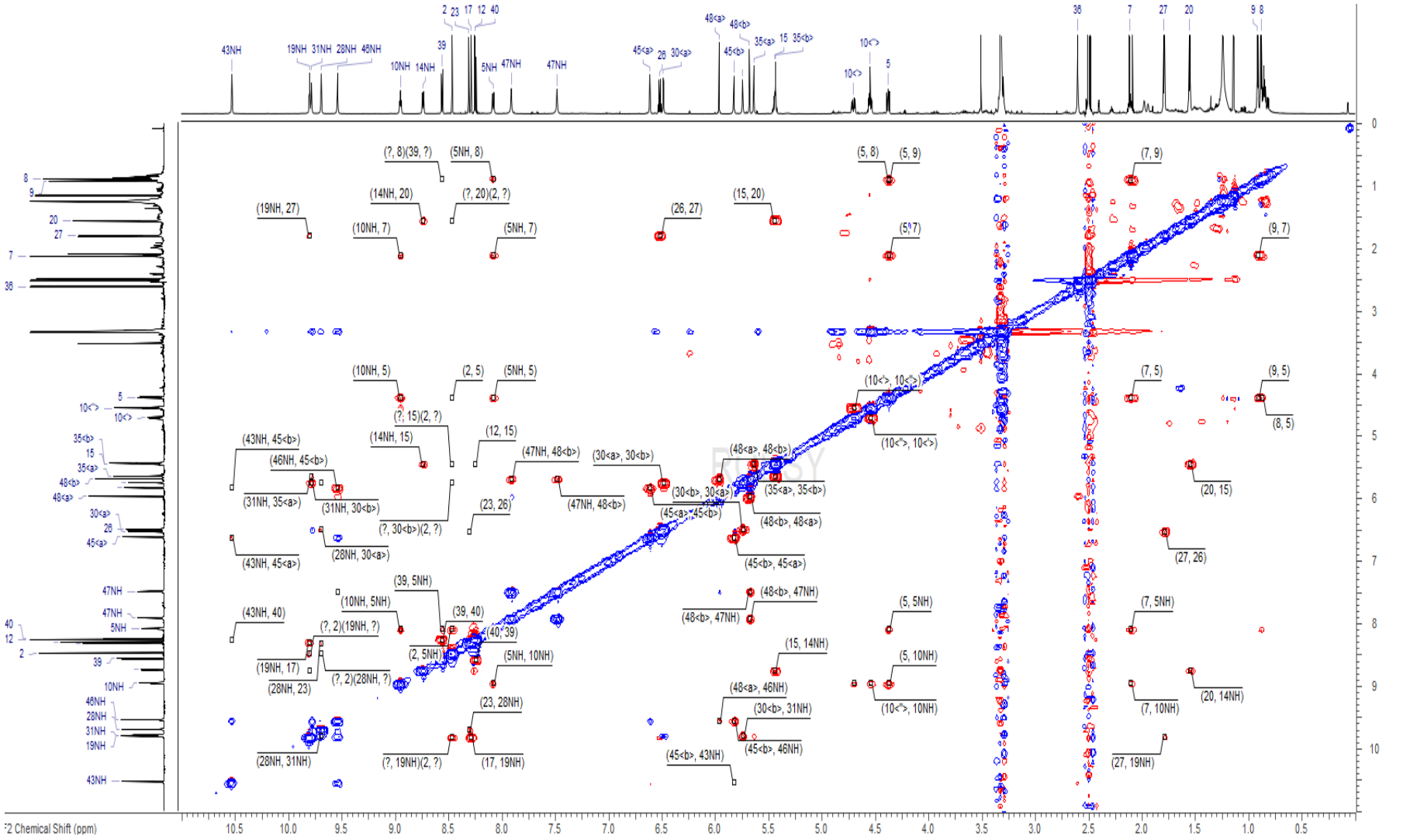

Figure S 11. ROESY NMR spectrum (700 MHz, DMSO-d_6) of litoralimycin A (**1**).

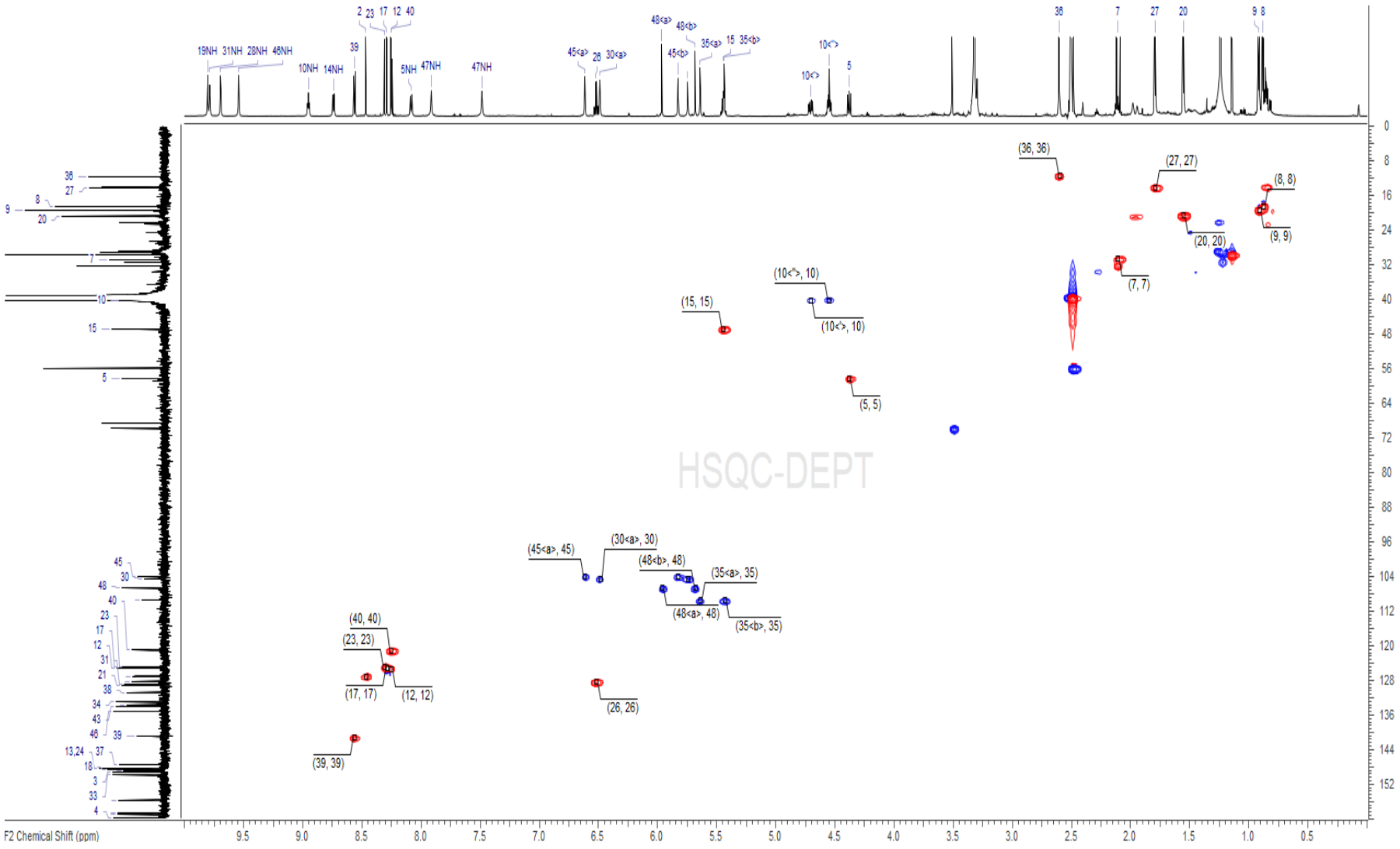

Figure S 12. HSQC NMR spectrum (700 MHz, DMSO-d_6) of litoralimycin A (**1**).

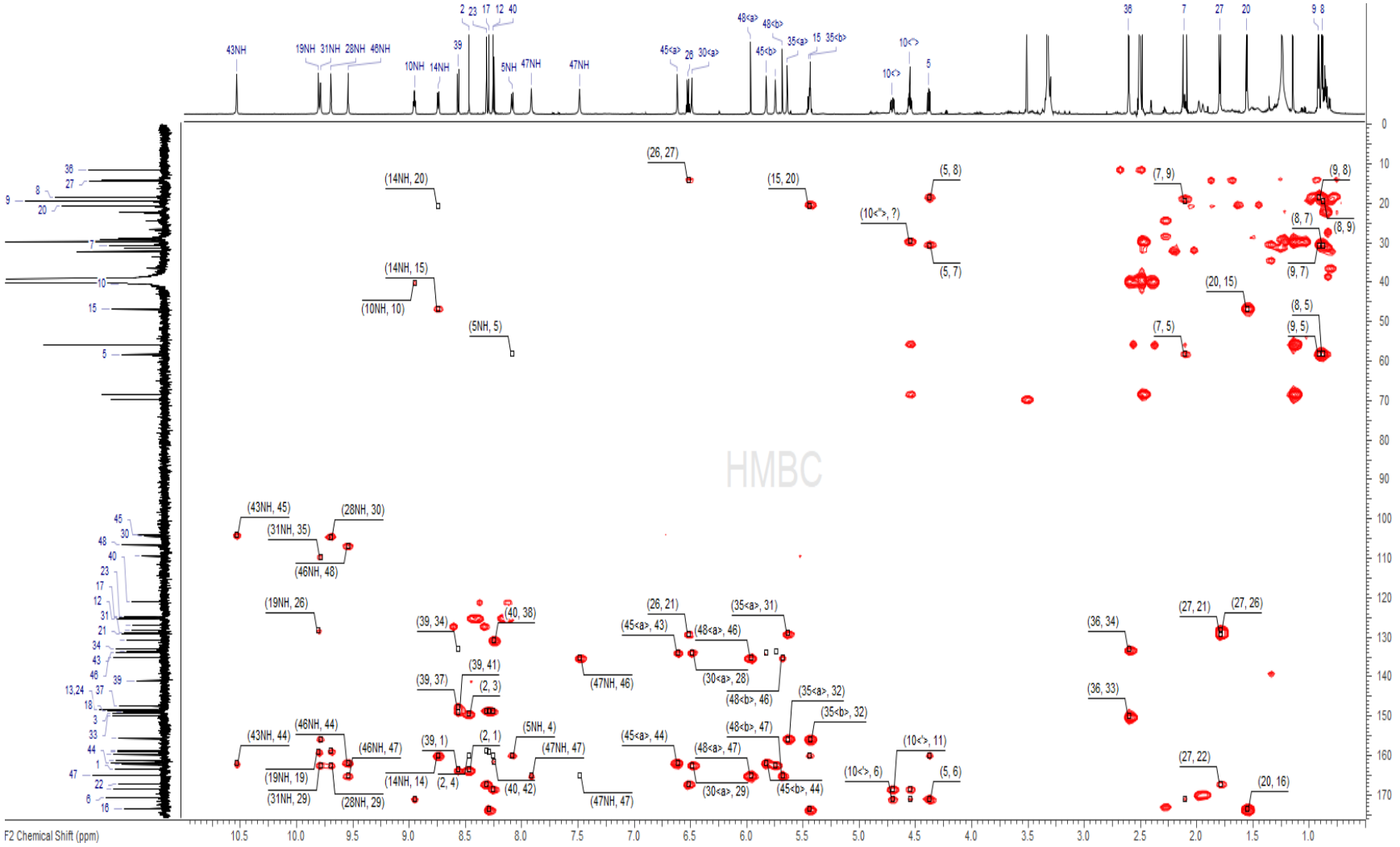

Figure S 13. HMBC NMR spectrum (700 MHz, DMSO-d_6) of litoralimycin A (**1**).

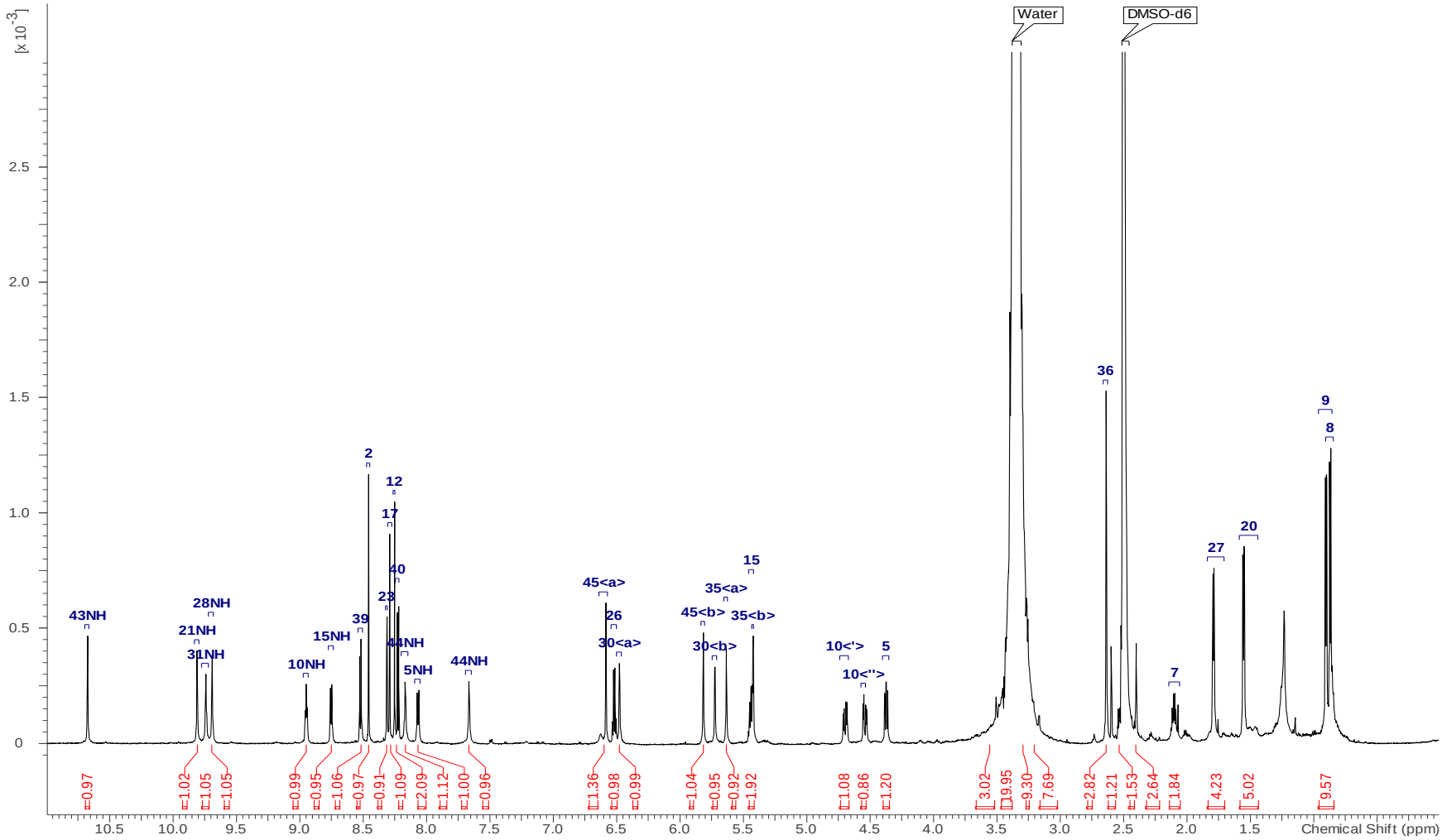

Figure S 14. ^{1}H NMR spectrum (700 MHz, DMSO-d_6) of litoralimycin B (**2**).

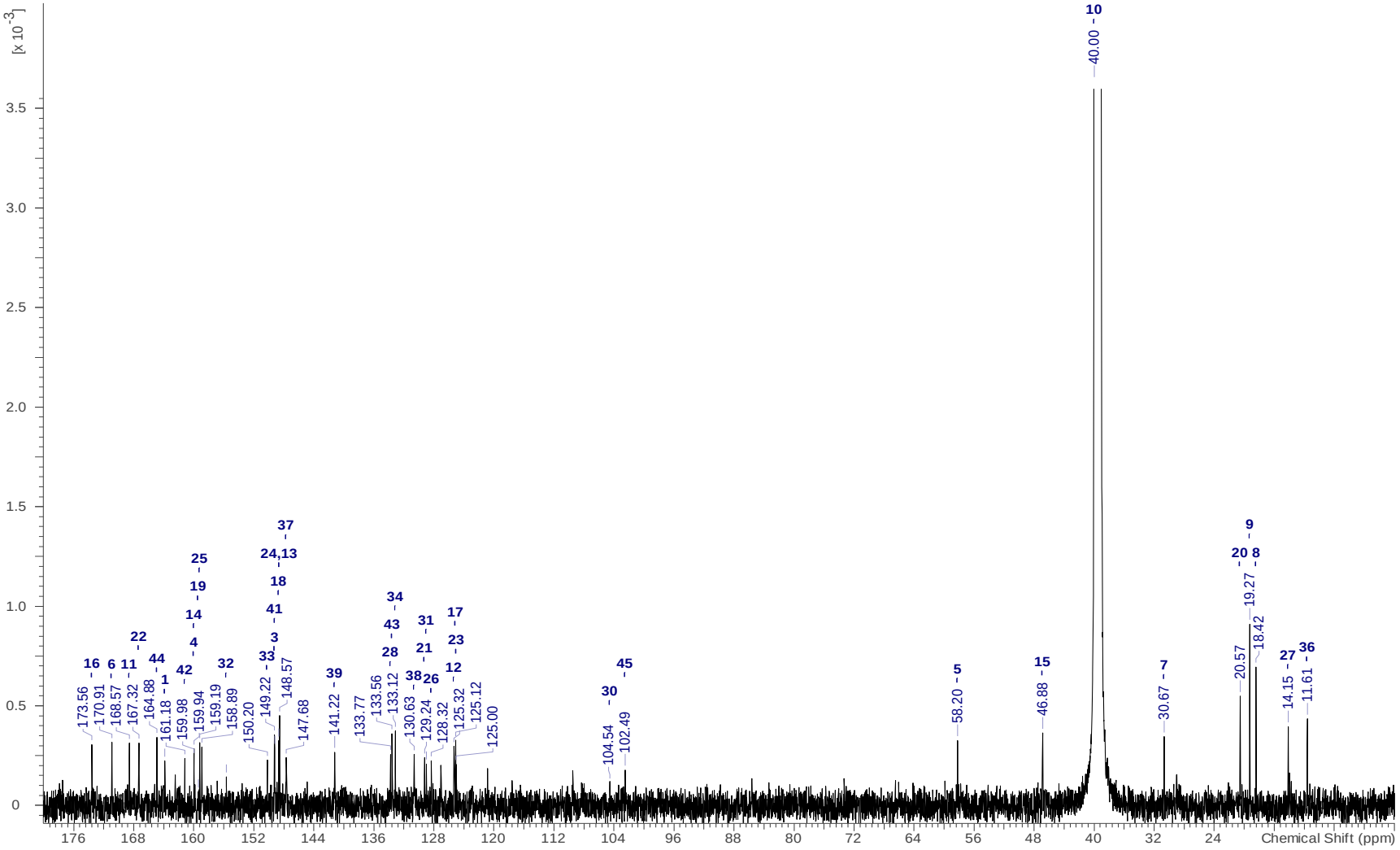

Figure S 15. ^{13}C NMR spectrum (175 MHz, DMSO-d_6) of litoralimycin B (**2**).

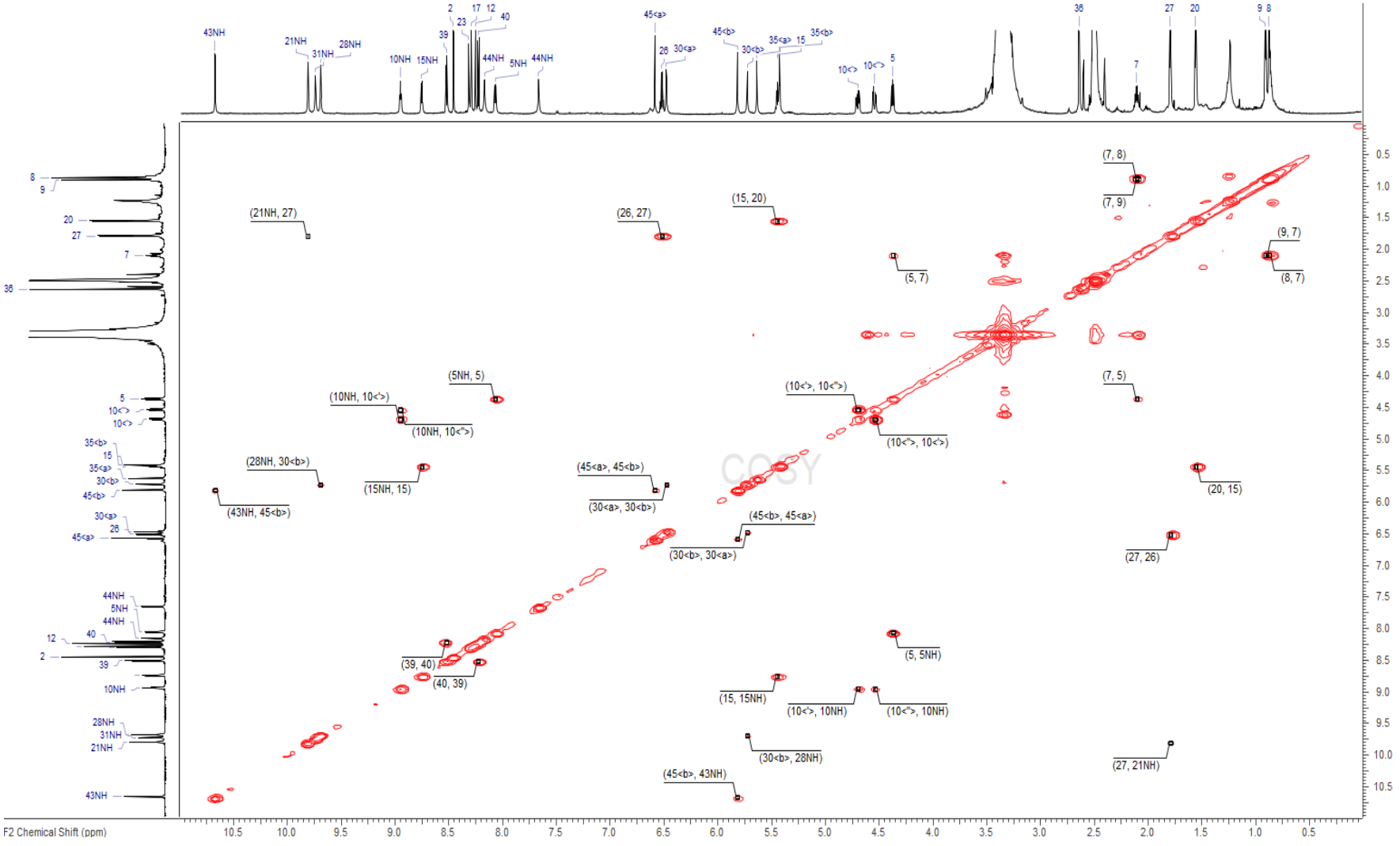

Figure S 16. COSY NMR spectrum (700 MHz, DMSO-d_6) of litoralimycin B (**2**).

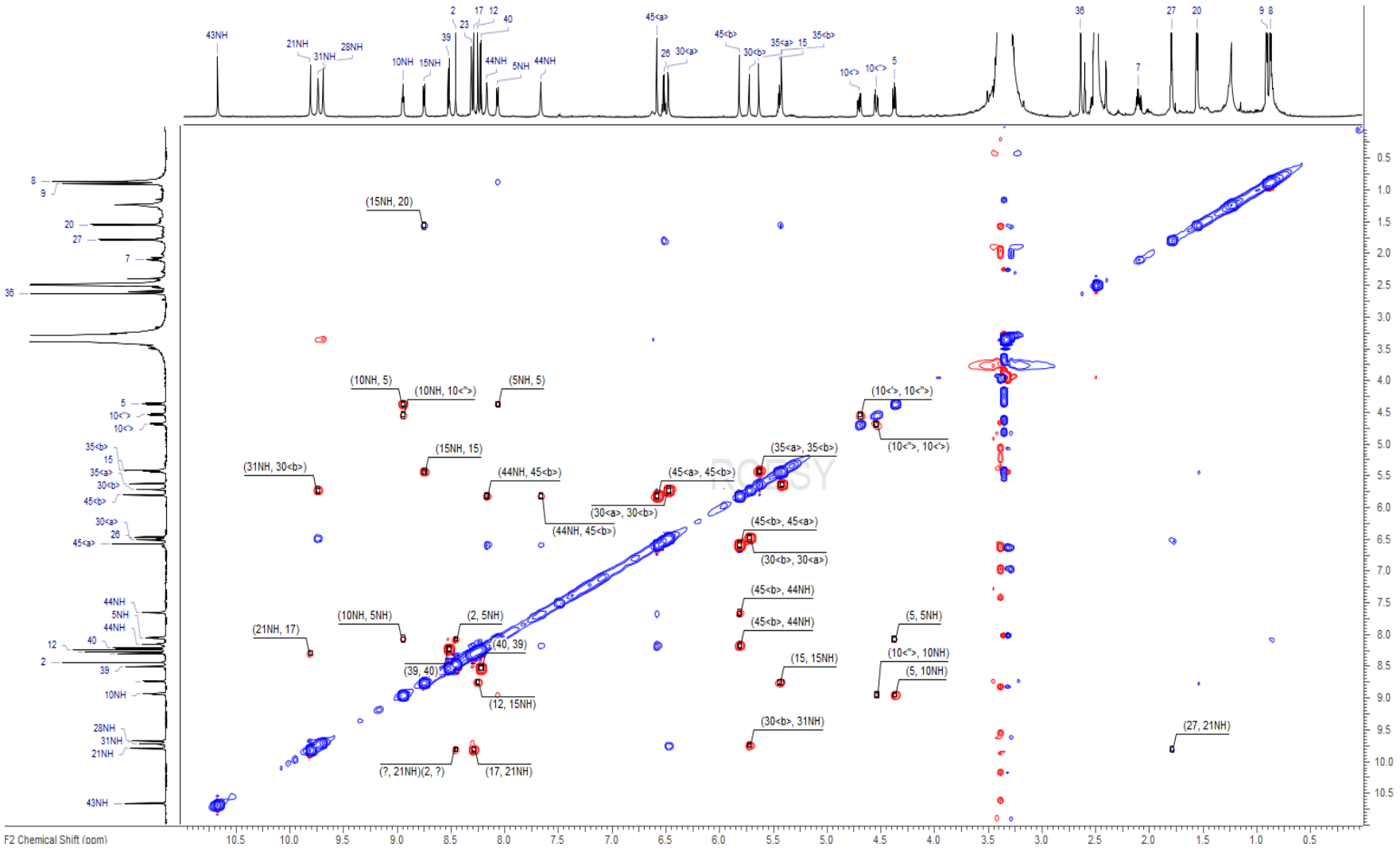

Figure S 17. ROESY NMR spectrum (700 MHz, DMSO-d_6) of litoralimycin B (**2**).

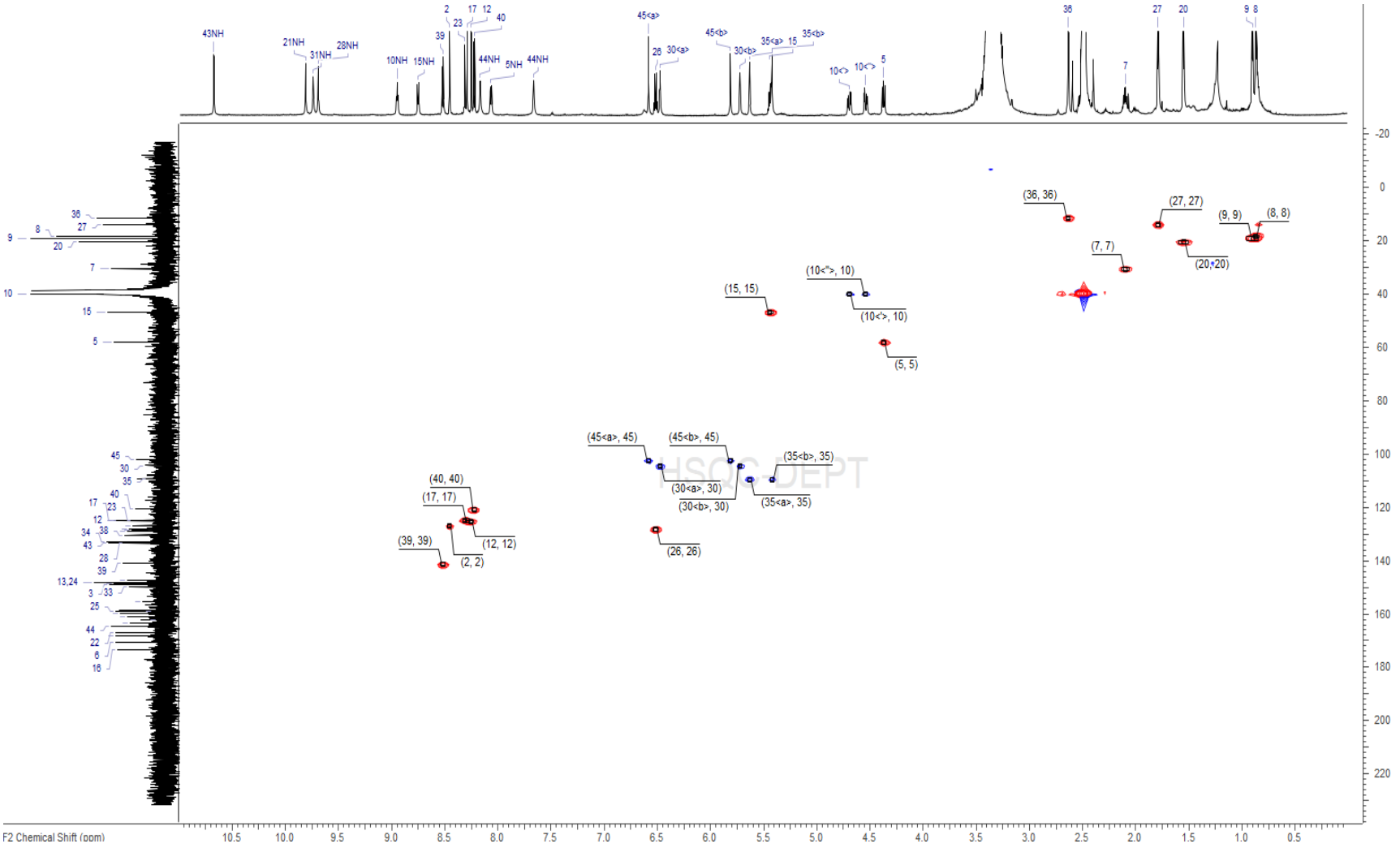

Figure S 18. HSQC NMR spectrum (700 MHz, DMSO-d_6) of litoralimycin B (**2**).

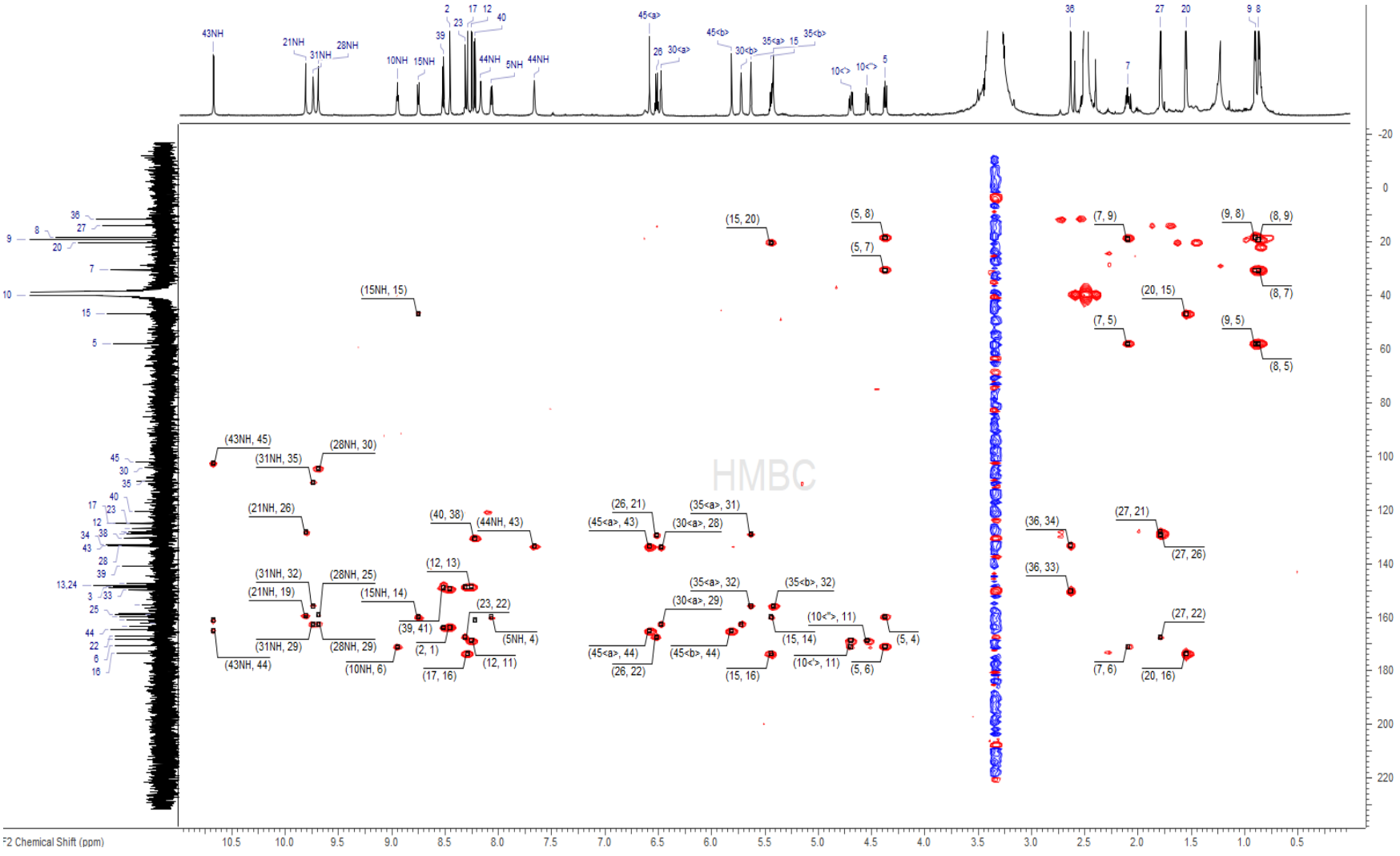

Figure S 19. HMBC NMR spectrum (700 MHz, DMSO-d_6) of litoralimycin B (**2**).

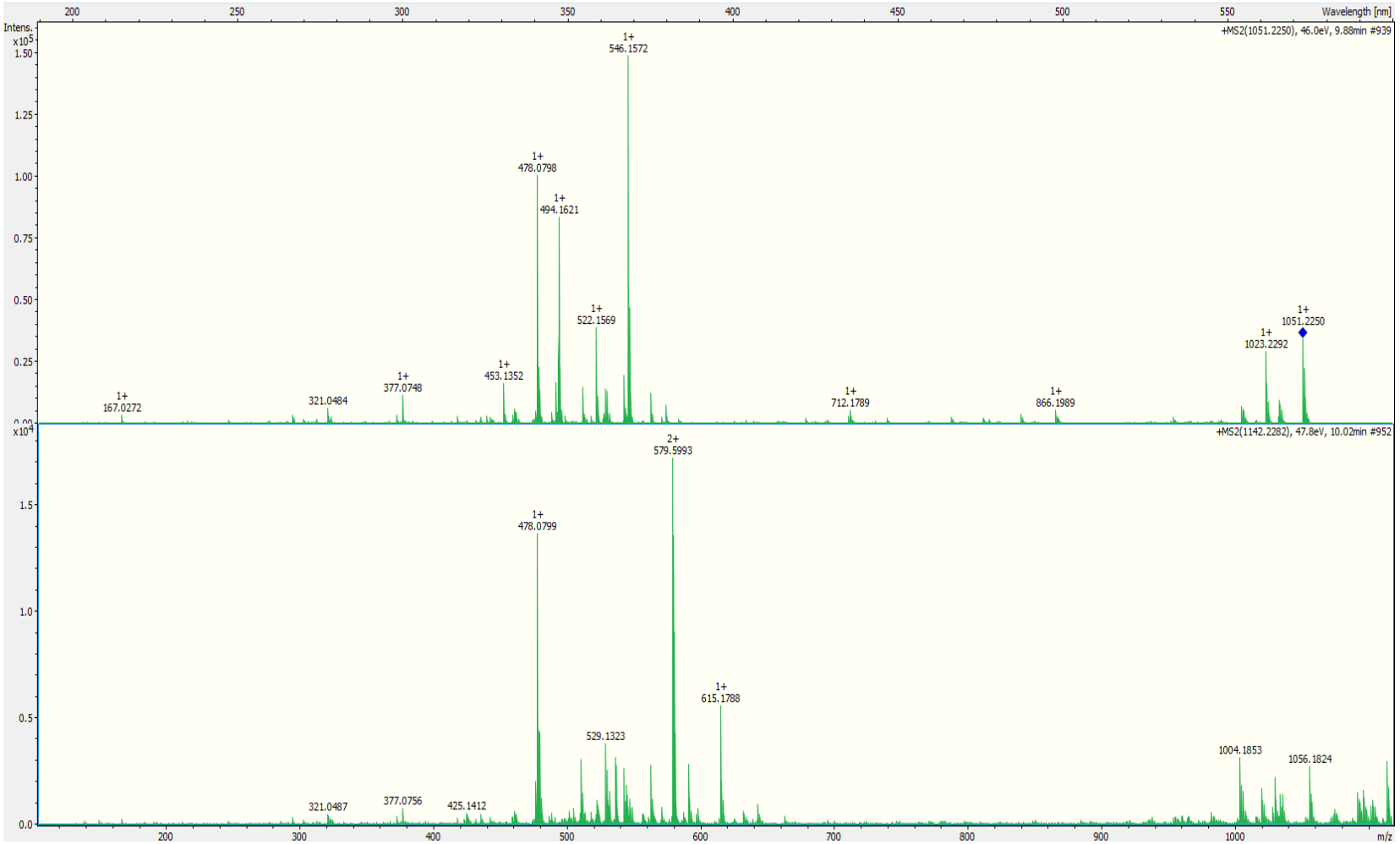

Figure S 20. MS/MS data for **1**(lower part) and **2** (upper part) with fragmentation $[M+Na]^+$ ions at m/z 1142.2282 and 1051.2250, respectively.